DEVELOPMENT OF STATE DEPENDENT FACTORIZED OPTIMAL CONTROL METHODS WITH APPLICATION TO SPACECRAFT COULOMB FORMATIONS

A THESIS SUBMITTED TO
THE GRADUATE SCHOOL OF NATURAL AND APPLIED SCIENCES
OF
MIDDLE EAST TECHNICAL UNIVERSITY

BY

MOHAMMAD MEHDI GOMROKI

IN PARTIAL FULFILLMENT OF THE REQUIREMENTS
FOR
THE DEGREE OF DOCTOR OF PHILOSOPHY
IN
AEROSPACE ENGINEERING

DECEMBER 2017

Approval of the thesis:

DEVELOPMENT OF STATE DEPENDENT FACTORIZED OPTIMAL CONTROL METHODS WITH APPLICATION TO SPACECRAFT COULOMB FORMATIONS

Submitted by **MOHAMMAD MEHDI GOMROKI** in partial fulfillment of the requirements for the degree of **Doctor of Philosophy in Aerospace Engineering Department, Middle East Technical University** by,

Prof. Dr. Gülbin Dural Ünver _____
Dean, Graduate School of **Natural and Applied Sciences**

Prof. Dr. Ozan Tekinalp _____
Head of Department, **Aerospace Engineering**

Prof. Dr. Ozan Tekinalp _____
Supervisor, **Aerospace Engineering Dept., METU**

Assist. Prof. Dr. Francesco Topputo _____
Co-Supervisor, **Aerospace Science and Technology Dept., POLIMI**

Examining Committee Members:

Assist. Prof. Dr. Ali Türker Kutay _____
Aerospace Engineering Dept., METU

Prof. Dr. Ozan Tekinalp _____
Aerospace Engineering Dept., METU

Prof. Dr. M. Kemal Özgören _____
Mechanical Engineering Dept., METU

Prof. Dr. Metin U. Salamcı _____
Mechanical Engineering Dept., Gazi University

Assist. Prof. Dr. Nazım Kemal Üre _____
Aeronautical Engineering Dept., ITU

Date: _____

I hereby declare that all information in this document has been obtained and presented in accordance with academic rules and ethical conduct. I also declare that, as required by these rules and conduct, I have fully cited and referenced all material and results that are not original to this work.

Name, Last name: MOHAMMAD MEHDI, GOMROKI

Signature:

ABSTRACT

DEVELOPMENT OF STATE DEPENDENT FACTORIZED OPTIMAL CONTROL METHODS WITH APPLICATION TO SPACECRAFT COULOMB FORMATIONS

Gomroki, Mohammad Mehdi
Ph.D., Department of Aerospace Engineering
Supervisor: Prof. Dr. Ozan Tekinalp
Co-Supervisor: Assist. Prof. Dr. Francesco Topputo

December 2017, 119 pages

Among spacecraft formation control techniques, Coulomb tether to control the relative distance is proposed in the literature. A Coulomb tether is similar to physical tether that uses coulomb forces to keep spacecraft at close proximity. It is indicated that a coulomb tether provides an almost a propellantless formation control. The charges loaded to the bodies, can create attractive and repulsive forces between these bodies. Since the forces are relative, coulomb forces cannot change the total linear or angular momentum of the formation. In this thesis, state dependent factorized optimal control methods are applied to control the formation attitude and relative position of the spacecraft Coulomb formation at Earth-moon libration points, Earth circular orbits, and deep space utilizing coulomb forces as well as thrusters. Nonlinear equations of motion of a two-craft Coulomb formation are properly manipulated to obtain a suitable State Dependent Coefficient (SDC) formulation for orbit radial, along-track, and orbit-normal configurations at Earth-Moon libration points, and Earth circular orbits. Moreover, the nonlinear equations of motion and their SDC factorized form of a three-craft Coulomb formation at deep space are discussed.

Nonlinear feedback control of radially aligned spacecraft Coulomb formation through numerical simulations are presented in the current work. Moreover, the

nonlinear optimal control is realized using the Approximating Sequence of Riccati Equations (ASRE) and State Dependent Coefficient Direct (SDC-Direct) methods. The SDC-Direct method is an approached developed and implemented in the current thesis. The present work introduces the SDC-Direct method to solve constrained nonlinear optimal control problems using state dependent coefficient factorization and Chebyshev polynomials. A recursive approximation technique known as Approximating Sequence of Riccati Equations is used to replace the nonlinear problem by a sequence of linear-quadratic and time-varying approximating problems. The state variables are approximated and expanded in Chebyshev polynomials. Then, the control variables are written as a function of state variables and their derivatives. The constrained nonlinear optimal control problem is then converted to a quadratic programming problem, and a constrained optimization problem is solved. Different final state conditions (unspecified, partly specified, and fully specified) are handled, and the effectiveness of the approaches in reconfiguring the formation and comparison of them is demonstrated through numerical simulations.

Keywords: spacecraft formation; Coulomb tether; nonlinear optimal control; Chebyshev polynomials; optimization

ÖZ

Durum Değişkenine Bağlı Çarpanlara Ayrılmış Optimal Kontrol Yöntemlerinin Geliştirilmesi ve Uzay Aracı Coulomb Kol Uçuşuna Uygulanması

Gomroki, Mohammad Mehdi
Doktora, Havacılık ve Uzay Mühendisliği Bölümü
Tez Yöneticisi: Prof. Dr. Ozan Tekinalp
Eş Tez Yöneticisi: Yrd. Doç. Dr. Francesco Topputo

Aralık 2017, 119 sayfa

Uzay aracı kol uçuşu kontrol teknikleri arasında, mesafeyi kontrol etmek için Coulomb tether literatürde önerilmiştir. Coulomb tether, uzay aracını yakın da tutmak için coulomb kuvvetleri kullanan fiziksel tether'a benzemektedir. Bir Coulomb tether'in neredeyse itici olmayan bir kol uçuşu kontrolü sağladığı belirtilir. cisimlere yüklenen yükler, bu cisimler arasında çekici ve itici güçler yaratabilir. Kuvvetler görece olduğundan, coulomb kuvveti kol uçuşunda toplam doğrusal veya açısal momentumunu değiştiremez. Bu tez çalışmasında, Dünya-Ay librasyon noktalarındaki, Dünya dairesel yörüngelerinde derin uzayda Coulomb kol uçuşu göreli yönelimi ve pozisyon kontrol etmek için duruma bağlı faktörleştirilmiş optimal kontrol yöntemleri uygulamaktadır. İki araçlı bir Coulomb kol uçuşu doğrusal olmayan denklemleri, Dünya-Ay librasyon noktalarında ve Dünya dairesel yörüngelerinde yörünge radyal, yörünge yol boyunca ve yörünge normali için uygun bir Durum Bağımlı Katsayı (SDC) formülasyonu elde etmek için düzgün şekilde manipüle edilir. Dahası, doğrusal olmayan hareket denklemleri ve derin uzaydaki üç çaraçlı bir Coulomb kol uçuşunun SDC'ye göre biçimlendirilmiş formu tartışılmıştır.

Radyal olarak hizalanmış uzay aracının doğrusal olmayan geri besleme kontrolü Coulomb kol uçuşları sayısal simulasyonlar vasıtasıyla mevcut çalışmada

sunulmaktadır. Ayrıca doğrusal olmayan optimum kontrol, Approximating Sequence of Riccati Equations (ASRE) ve Duruma Bağlı Katsayı Doğrudan (SDC-Doğrudan) yöntemleri kullanılarak gerçekleştirilir. SDC-Direct yöntemi, bu tezde geliştirilen ve uygulanan bir yaklaşımdır. Bu çalışmada, bağımlı katsayı çarpanlara ayırma ve Chebyshev polinomları kullanılarak kısıtlı doğrusal olmayan optimal kontrol problemlerinin çözümü için SDC-Doğrudan yöntem tanıtılmaktadır. Doğrusal olmayan problemi doğrusal-kuadratik ve zamanla değişen yaklaşık problemlerin bir dizisi ile değiştirmek için, Riccati Denklemlerinin Yaklaşan Sırası olarak bilinen tekrarlayan bir yaklaşım tekniği kullanılır. Durum değişkenleri, Chebyshev polinomların kullanılarak genişletilir. Ardından, kontrol değişkenleri, durum değişkenleri ve türevlerinin bir fonksiyonu olarak yazılır. Sınırlandırılmış doğrusal olmayan optimal kontrol problemi daha sonra bir kuadratik programlama problemine dönüştürülür ve kısıtlı bir optimizasyon problemi çözülür. Farklı son durum koşulları (belirtilmemiş, kısmen belirtilmiş ve tam olarak belirtilmiş) ele alınmış ve bunların yeniden biçimlendirilmesinde ve karşılaştırılmasında yaklaşımların etkinliği sayısal benzetimlerle gösterilmiştir.

Anahtar kelimeler: uzay aracı kol uçuşu, Coulomb bağı, doğrusal olmayan optimal kontrol, Chebyshev polinomları, eniyileme

To My Wife

ACKNOWLEDGMENTS

I would like to thank my supervisor Prof. Ozan Tekinalp and my co-supervisor Dr. Francesco Topputo for their invaluable supervision, guidance and criticism and especially their extreme support during the entire study period from both human and scientific standpoint.

I am grateful to Prof. Gerard Gomez of the University of Barcelona who was the coordinator of the Astrodynamics Network AstroNet-II project funded by Marie-Curie Research Training Network. I had the chance to be an FP7 Marie Curie Early Stage Researcher at the AstroNet-II project (project number PITN-GA-2011-289240) and had obtained many experiences by attending training schools and doing my internships. The valuable cooperation of Prof. Franco Bernelli-Zazzera during the visiting period at the Polytechnic University of Milan has been really appreciated.

I also thank examining committee members, Prof. Metin U. Salamcı, Prof. M. Kemal Özgören, Dr. Ali Türker Kutay, and Dr. Nazım Kemal Üre for their valuable comments and contributions.

Special thanks go to my family for being a continuous and endless source of happiness. Finally yet importantly, a particular acknowledgment goes to my lovely wife, Malihe, for her patience, supportive in the difficult moments, and the simple reason of being part of my life.

TABLE OF CONTENTS

ABSTRACT v
ÖZ vii
ACKNOWLEDGMENTS x
TABLE OF CONTENTS xi
LIST OF TABLES xiv
LIST OF FIGURES xvi
CHAPTER 1 1
1 INTRODUCTION 1
1.1 Introduction and Literature Survey 1
1.2 Work Outline 4
CHAPTER 2 7
2 TWO-CRAFT EQUATIONS OF MOTION AND SDC FACTORIZATIONS AT EARTH CIRCULAR ORBITS 7
2.1 Orbit-Radial Configuration 7
2.2 Along-Track Configuration 15
2.3 Orbit-Normal Configuration 17
CHAPTER 3 21
3 TWO-CRAFT EQUATIONS OF MOTION AND SDC FACTORIZATIONS AT LIBRATION POINTS 21
3.1 Earth-Moon Collinear Libration Points 21
3.1.1 Orbit-Radial Configuration 21
3.1.2 Along-Track Configuration 29
3.1.3 Orbit-Normal Configuration 32
3.2 Orbit-Radial Configuration at Earth-Moon Triangular Libration Points 34
CHATER 4 41

4 THREE-CRAFT EQUATIONS OF MOTION AND SDC FACTORIZATIONS AT DEEP SPACE 41
4.1 Planar Three Bodies Dynamic 41
4.2 SDC Factorization Form 44
CHAPTER 5 49
5 STATE DEPENDENT FACTORIZED OPTIMAL CONTROL METHODS 49
5.1 Review of Optimal Solutions to Unconstrained Nonlinear Optimal Control Problems 49
5.1.1 Statement of Unconstrained Nonlinear Optimal Control Problem 49
5.1.2 Approximating Sequence of Riccati Equations Method 50
5.2 State Dependent Coefficient Direct Method 53
5.2.1 Statement of Constrained Nonlinear Optimal Control Problem 54
5.2.2 Converting Constrained Nonlinear Optimal Control Problems to Quadratic Programming Problems Using Chebyshev Polynomials 54
5.2.3 Number of Inputs Less than Number of States 63
CHAPTER 6 67
6 APPLICATION OF STATE DEPENDENT RICCATI EQUATION METHOD TO SPACECRAFT COULOMB FORMATIONS 67
6.1 State Dependent Riccati Equation Method 67
6.2 Numerical Simulations 68
6.2.1 Orbit-Radial Two-craft Coulomb Formation at Earth Circular Orbits 69
6.2.2 Orbit-Radial Two-craft Coulomb Formation at Collinear Libration Points 72
6.2.3 Orbit-Radial Two-craft Coulomb Formation at Triangular Libration Points 74

6.2.4 Three-craft Coulomb Formation at Deep Space 76
CHAPTER 7 83
7 APPLICATION OF STATE DEPENDENT FACTORIZED OPTIMAL CONTROL METHODS TO SPACECRAFT COULOMB FORMATIONS 83
7.1 Numerical Simulations 83
7.1.1 Orbit-Radial Two-craft Coulomb Formation at Earth Circular Orbits 83
7.1.2 Orbit-Radial Two-craft Coulomb Formation at Collinear Libration Points 89
7.1.3 Orbit-Radial Two-craft Coulomb Formation at Triangular Libration Points 93
CHAPTER 8 97
8 APPLICATION OF STATE DEPENDENT FACTORIZED OPTIMAL CONTROL METHODS TO VAN DER POL OSCILLATOR AND LOW-THRUST RENDEZVOUS PROBLEMS 97
8.1 Problem 1: Van der Pol Oscillator 97
8.1.1 Soft Constrained Problem 99
8.1.2 Hard Constrained Problem 103
8.2 Problem 2: Low-Thrust Rendezvous 105
8.2.1 Soft Constrained Problem 106
8.2.2 Hard Constrained Problem 110
CHAPTER 9 113
9 CONCLUSION AND FUTURE WORKS 113
REFERENCES 115
CURRICULUM VITAE 119

LIST OF TABLES

TABLES

Table 1. Simulation parameters for two-craft implementations. 68

Table 2. Simulation parameters for three-craft implementations. 69

Table 3. ASRE-Approach1 iterations for two-craft Earth circular orbit Case1. 84

Table 4. ASRE-Approach2 iterations for two-craft Earth circular orbit Case1. 84

Table 5. SDC-Direct iterations for two-craft Earth circular orbit Case1. 85

Table 6. SDC-Direct iterations for two-craft Earth circular orbit Case2. 87

Table 7. ASRE-Approach1 iterations for two-craft collinear libration point. 89

Table 8. ASRE-Approach2 iterations for two-craft collinear libration point. 90

Table 9. SDC-Direct iterations for two-craft collinear libration point. 91

Table 10. ASRE-Approach1 iterations for two-craft triangular libration point. 93

Table 11. ASRE-Approach2 iterations for two-craft triangular libration point. 93

Table 12. SDC-Direct iterations for two-craft triangular libration point. 94

Table 13. SDC-Direct method iterations for Problem1-SCP-Case1. 99

Table 14. SDC-Direct method iterations for Problem1-SCP-Case2. 101

Table 15. SDC-Direct method iterations for Problem1-SCP-Case3. 102

Table 16. SDC-Direct method iterations for Problem1-HCP. 104

Table 17. SDC-Direct method iterations for Problem2-SCP-Case1. 106

Table 18. SDC-Direct method iterations for Problem2-SCP-Case2. 108

Table 19. SDC-Direct method iterations for Problem2-SCP-Case3..... 109

Table 20. SDC-Direct method iterations for Problem2-HCP-Case1. 110

Table 21. SDC-Direct method iterations for Problem2-HCP-Case2. 112

LIST OF FIGURES

FIGURES

Figure 1. Representing formation configuration for two-craft Earth circular orbits. 8

Figure 2. Euler angle representations. 8

Figure 3. Formation configuration at Earth-moon collinear libration point. 22

Figure 4. Formation configuration at Earth-moon triangular libration point. 35

Figure 5. Three-craft Coulomb formation [12]. 41

Figure 6. Collinear invariant shape Coulomb formation [12]. 41

Figure 7. The rotating B frame 42

Figure 8. Separation distance, yaw angle, and pitch angle stabilizations using SDRE method for two-craft Earth circular orbit. 70

Figure 9. Coulomb force and the forces generated by the thrusters in the yaw and pitch direction using SDRE method for two-craft Earth circular orbit. 71

Figure 10. Charge product using SDRE method for two-craft Earth circular orbit. 71

Figure 11. Separation distance, yaw angle, and pitch angle stabilizations using SDRE method for two-craft collinear libration point. 72

Figure 12. Coulomb force and the forces generated by the thrusters in the yaw and pitch direction using SDRE method for two-craft collinear libration point. 73

Figure 13. Charge product using SDRE method for two-craft collinear libration point. 73

Figure 14. Separation distance, yaw angle, and pitch angle stabilizations using SDRE method for two-craft triangular libration point. 74

Figure 15. Coulomb force and the forces generated by the thrusters in the yaw and pitch direction using SDRE method for two-craft triangular libration point. 75

Figure 16. Charge product using SDRE method for two-craft triangular libration point. 75

Figure 17. Position history of Craft1 for Case1. 76

Figure 18. Position history of Craft2 for Case1. 77

Figure 19. Position history of Craft2 for Case1. 77

Figure 20. Control inputs for Case 1. 78

Figure 21. Formation angular velocity for Case 1. 78

Figure 22. Position history of Craft1 for Case2. 79

Figure 23. Position history of Craft2 for Case2. 80

Figure 24. Position history of Craft2 for Case2. 80

Figure 25. Control inputs for Case 2. 81

Figure 26. Formation angular velocity for Case 2. 81

Figure 27. Approximate trajectory solutions using SDC Factorized optimal methods for two-craft Earth circular orbit Case1. 84

Figure 28. Approximate control solutions using SDC Factorized optimal methods for two-craft Earth circular orbit Case1. 85

Figure 29. Charge product using SDC Factorized optimal methods for two-craft Earth circular orbit Case1. 86

Figure 30. Approximate trajectory solutions using SDC Direct method for two-craft Earth circular orbit Case1 and Case2. 88

Figure 31. Approximate control solutions using SDC Direct method for two-craft Earth circular orbit Case1 and Case2. 88

Figure 32. Charge product using SDC Direct method for two-craft Earth circular orbit Case1 and Case2. 89

Figure 33. Approximate trajectory solutions using SDC Factorized optimal methods for two-craft collinear libration point. 91

Figure 34. Approximate control solutions using SDC Factorized optimal methods for two-craft collinear libration point. 92

Figure 35. Charge product using SDC Factorized optimal methods for two-craft collinear libration point. 92

Figure 36. Approximate trajectory solutions using SDC Factorized optimal methods for two-craft triangular libration point. 94

Figure 37. Approximate control solutions using SDC Factorized optimal methods for two-craft triangular libration point. 95

Figure 38. Charge product using SDC Factorized optimal methods for two-craft triangular libration point. 95

Figure 39. Problem1-SCP-Case1 (N = 12): Approximate trajectory and control solutions. 100

Figure 40. Problem1-SCP-Case1 (N = 12): Approximate trajectory and control solutions. 101

Figure 41. Problem1-SCP-Cases 1 and 3 (N =12): Approximate trajectory and control solutions. 103

Figure 42. Problem1-HCP (N = 12): Approximate trajectory and control solutions. 104

Figure 43. Problem2-SCP-Cases 1 and 2 (N = 12): Approximate trajectory and control solutions. 107

Figure 44. Problem2-SCP-Cases 1 and 2 (N = 12): Approximate trajectory and control solutions. 110

Figure 45. Problem2-HCP-Cases 1 and 2 (N = 12): Approximate trajectory and control solutions with SDC Direct method. 111

CHAPTER 1

INTRODUCTION

1.1 Introduction and Literature Survey

Spacecraft flying in formation for carrying out interferometry missions, sharing resources, or patching together sensor data to obtain a higher resolution observation has been envisaged in the past. Among formation flying techniques, tethers were also proposed. A Coulomb tether is similar to physical tether that uses coulomb forces to keep spacecraft at close proximity [1]. This approach produces almost a propellant less formation control [2]. Such formations with the charges loaded to the bodies, create attraction and repulsion between these bodies. Natural charging of the spacecraft is observed at even geostationary altitudes [3]. However, such coulomb forces cannot change the inertial translational and rotational momentum of the spacecraft [4]. The separation distance between two spacecraft is controllable by using electrostatic forces that can utilize both attractive and repulsive forces between spacecraft [5, 6]. Such charged Coulomb formations are unstable, and require feedback control to be stabilized [1].

The dynamic analysis and optimal reconfiguration of two-craft Coulomb formations at Earth circular orbits is presented and discussed in the literature [7]. The orbit radial dynamic analysis of a two-spacecraft Coulomb formation at Earth-Moon collinear and triangular libration points was previously addressed [8]. In addition, reference [9] investigates the orbit radial stabilization of a two-craft Coulomb formation about circular orbits and Earth–Moon collinear libration points in the presence of solar perturbation effects using the Lyapunov feedback control method.

In the current thesis, the nonlinear feedback control of two-craft Coulomb formations at Earth circular orbits and Earth-moon libration points using State-Dependent Riccati Equations (SDRE) method are presented and discussed. In addition, the State Dependent Coefficient (SDC) factorized optimal control methods are developed and applied to these applications.

Furthermore, three-craft Coulomb formations are presented and studied in the literature. The similarity between the gravitational and electrostatic spinning 3-body problem to determine invariant shape solutions are addressed in the literature, and it is shown that multiple invariant shape solutions might be possible for a single set of craft charges [10]. In reference [11], the collinear equilibrium three-craft-formation charge feedback control problem is studied. In that work, a Lyapunov-based nonlinear control algorithm is developed to stabilize the formation to the desired shape and size.

It is shown that for any desired collinear invariant shape geometry, there exists a real charge solution. For a given set of charges, three collinear invariant shape solutions are possible [12]. Through linear stability and shape analysis of spinning three-craft Coulomb formations, with specific formation geometries, it is shown that the in-plane motion may be marginally stable for the three-craft invariant shape formations in circular trajectories [12]. Nonlinear feedback control of three-craft Coulomb formation using the SDRE control method is studied in the current thesis.

It should be noticed that in the current work, the nonlinear equations of motion for the two-craft and three-craft configurations are written in the SDC factorized form suitable for the SDRE, Approximating Sequence of Riccati Equations (ASRE), and developed SDC-Direct methods.

The SDRE method [13-16] is employed due to its simplicity and effectiveness in many applications [17-21]. This method treats the original infinite-horizon, nonlinear optimal control problem as an infinite-horizon pointwise linear-quadratic regulator (LQR). A number of LQR problems are solved sequentially at each time instant. This is done by using state-dependent matrices that are pointwise evaluated at each time step. The SDRE method may also be used to solve finite-horizon optimal

control [16]; one such approach chooses the state-dependent matrices as functions of the time-to-go [22].

Çimen and Banks [23, 24] introduced a method known as Approximating Sequence of Riccati Equations (ASRE) which uses State Dependent Coefficient (SDC) factorization and iterative Time-Varying Linear Quadratic Regulator (TV-LQR) approximations to solve Unconstrained Nonlinear Optimal Control (UNOC) problem with unspecified final states. The ASRE approach is applied to many problems like maneuvering of two-craft Coulomb formations at Earth circular orbits and Earth-moon collinear libration points [25, 26]. Topputo and Bernelli [27, 28] solved UNOC problems with unspecified, partly specified, and fully specified final states by using ASRE method differing in the way the time dependent linear quadratic regulator problems are solved. Rather than integrating the Riccati equation in [23, 24], the approach represented in [27, 28] integrates the Hamiltonian matrix equation to obtain state transition sub-matrices which enables easy handling of boundary conditons.

Many numerical methods have been used to solve nonlinear optimal control problems in the literature using direct and indirect methods [29]. Indirect methods stem from the calculus of variations [30]; direct methods use nonlinear programming optimization methods [31]. One of the approaches for handling the direct methods is based on parameterization. For the parameterization method, three different approaches are implemented in the literature: parameterization of the state variables [32], parameterization of the control variables [33], and parameterization of both states and controls [34]. In the current thesis, the state variable parameterization approach is implemented to approximate the states using Chebyshev polynomials. Then, the state derivatives are derived from the state variables. To this end, the control variables are obtained as a function of state variables and their derivatives. The SDC approaches in [23, 24, 27, 28] involve unconstrained nonlinear optimal control problems. However, Constrained Nonlinear Optimal Control (CNOC) problems are more fit to applications [35-37]. A solution to CNOC problems using Chebyshev polynomials which uses quasilinearization is presented in [35]. Elnagar and Kazemi [36] proposed a method to generate optimal trajectories with linear and

nonlinear constrained dynamic systems. Their approach is based on the utilization of Chebyshev polynomials to parameterize the system and transform the optimal control problem to a nonlinear programming problem. Also in [37], a generic Bolza optimal control problem with state and control constraints is solved using a direct transcription method.

In the present work, replacing the original dynamic system by Time-Varying Linear Quadratic Regulator (TV-LQR) problems using iterative ASRE method and parameterizing the states by finite-length Chebyshev polynomials is proposed to convert the constrained nonlinear optimal control problem into a constrained quadratic programming problem. Jaddu and Majdalawi [38] solved nonlinear optimal control problems using SDC factorization and Chebyshev polynomials. Their approach is similar to that in the current thesis with three differences. First, there are no constraints on states and controls in their work, the resulting quadratic programming problem has linear equality constraints only, and is more easily solved. Second, further Chebyshev techniques are used in that paper to form an analytical approximation to the performance index, whereas in the current thesis numerical integration is used. Third, there are no specified terminal states, while our approach deals with three different final state conditions: hard constrained (final state fully specified), soft constrained (final state not specified), and mixed constrained problems (final state partly specified).

1.2 Work Outline

The remaining part of the thesis is organized as follows. The nonlinear equations of motion for three configurations (orbit radial, along track, and orbit normal) of a two-spacecraft Coulomb formation at Earth circular orbits are derived and converted to the SDC factorized form in Chap. 2. The nonlinear equations of motion and their SDC factorization of two-craft Coulomb formation at Earth-moon libration points is derived and discussed in Chap. 3. Moreover, Chap. 4 presents the nonlinear equations of three-craft Coulomb formation that are converted to SDC factorized form. In Chap. 5, the ASRE approaches are presented and development of the SDC-Direct method for solving constrained nonlinear optimal control problems using

state-dependent factorization and Chebyshev polynomials is given and discussed. The SDRE method and its application to Coulomb formation flying through numerical simulations is given in Chap. 6. In addition, Chap. 7 shows the numerical implementations of the ASRE approaches and SDC-Direct method with application to Coulomb tethered satellite formations. Application of SDC-Direct method to two more problems is presented in Chap. 8 to compare the results of the developed method with those given in the literature. Concluding remarks are given in Chap. 9.

CHAPTER 2

TWO-CRAFT EQUATIONS OF MOTION AND SDC FACTORIZATIONS AT EARTH CIRCULAR ORBITS

2.1 Orbit-Radial Configuration

The problem of describing the relative motion of a two-craft Coulomb formation is considered in this section. It is assumed that the formation center of mass is rotating in an Earth circular orbit. Such equations are called Clohessy-Wiltshire equations or Hill's equations [39]. As shown in Figure 1, the center of mass of the formation which is coincident with the points $\mathcal{N}$ and $\mathcal{B}$ is in a circular orbit of radius R_C with a constant orbital rate $\Omega = \sqrt{GM_e / R_C^3}$, where G is the universal gravitational constant and M_e is the Earth's mass. Three reference frames are defined here. First, an Earth centered inertial frame $\mathcal{E}: \{\hat{e}_1, \hat{e}_2, \hat{e}_3\}$. Second, a fixed reference frame $\mathcal{N}: \{\hat{n}_1, \hat{n}_2, \hat{n}_3\}$ with (x, y, z) coordinates which rotates with a constant orbital rate $\boldsymbol{\Omega}$ with respect to the inertial coordinate system. The reference frame $\mathcal{N}$ is sometimes called Hill's frame. The $\hat{n}_1$ axis is in the orbit radial direction, the $\hat{n}_2$ axis is aligned with the along-track direction, and the $\hat{n}_3$ axis is completing the right-handed coordinate frame which is directed out of the orbital plane. The basis vectors of the $\mathcal{E}$ frame are in the same direction of the $\mathcal{N}$ frame. Third, a body-fixed reference frame $\mathcal{B}: \{\hat{b}_1, \hat{b}_2, \hat{b}_3\}$ which rotates with respect to $\mathcal{N}$ frame. The angular velocity vector of $\mathcal{N}$ with respect to $\mathcal{E}$ is defined as

$$\boldsymbol{\Omega} = \boldsymbol{\Omega}^{\mathcal{N}/\mathcal{E}} = \Omega\, \hat{n}_3 = \Omega\, \hat{e}_3 \tag{2.1}$$

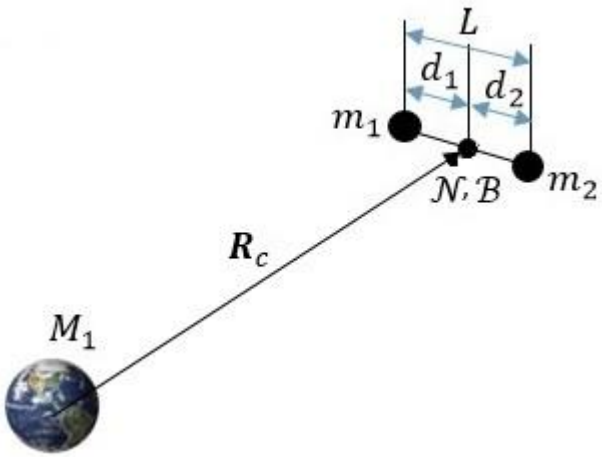

Figure 1. Representing formation configuration for two-craft Earth circular orbits.

The two-craft Coulomb formation is assumed to behave like a rigid body. The relative attitude between the $\mathcal{N}$ and $\mathcal{B}$ frames is defined using the 3-2-1 sequence of Euler angle rotations. As illustrated in Figure 2, the Euler angles, $\psi, \theta, and\ \varphi$, are yaw, pitch, and roll angles, respectively from Hill orbit frame to the formation body-fixed frame.

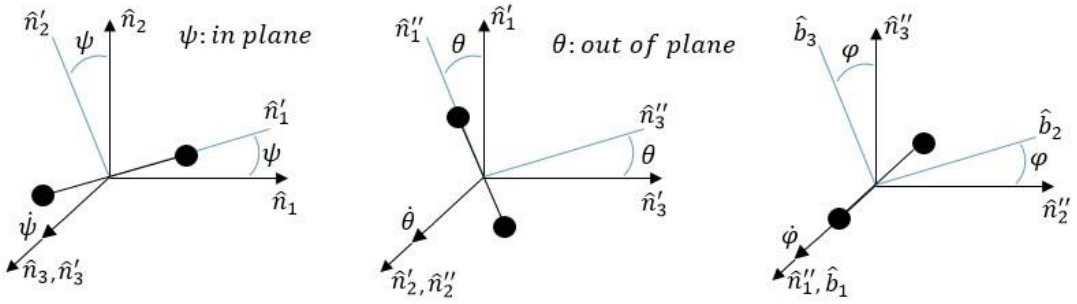

Figure 2. Euler angle representations.

The 3,2,1 sequence used in this manuscript is given by

$$\mathcal{N} \longrightarrow \mathcal{N}' : C_3(\psi)$$

$$\mathcal{N}' \longrightarrow \mathcal{N}'' : C_2(\theta)$$

$$\mathcal{N}'' \longrightarrow \mathcal{B} : C_1(\varphi)$$

where $\mathcal{N}'$ and $\mathcal{N}''$ are two intermediate reference frames with basis vectors $\{\hat{n}_1', \hat{n}_2', \hat{n}_3'\}$ and $\{\hat{n}_1'', \hat{n}_2'', \hat{n}_3''\}$, respectively. The C_3, C_2, and C_1 terms are rotation matrices that are obtained as [40]

$$C_3(\psi) = \begin{bmatrix} cos\,\psi & sin\,\psi & 0 \\ -sin\,\psi & cos\,\psi & 0 \\ 0 & 0 & 1 \end{bmatrix} \tag{2.2}$$

$$C_2(\theta) = \begin{bmatrix} cos\,\theta & 0 & -sin\,\theta \\ 0 & 1 & 0 \\ sin\,\theta & 0 & cos\,\theta \end{bmatrix} \tag{2.3}$$

$$C_1(\varphi) = \begin{bmatrix} 1 & 0 & 0 \\ 0 & cos\,\varphi & sin\,\varphi \\ 0 & -sin\,\varphi & cos\,\varphi \end{bmatrix} \tag{2.4}$$

Now, the direction cosine matrix of $\mathcal{B}$ with respect to $\mathcal{N}$ or the rotation matrix from $\mathcal{N}$ to $\mathcal{B}$ is given as

$$C^{\mathcal{B}/\mathcal{N}} = C_1(\varphi)\, C_2(\theta)\, C_3(\psi) = \begin{bmatrix} cos\,\theta\, cos\,\psi & cos\,\theta\, sin\,\psi & -sin\,\theta \\ sin\,\varphi\, sin\,\theta\, cos\,\psi - cos\,\varphi\, sin\,\psi & sin\,\varphi\, sin\,\theta\, sin\,\psi + cos\,\varphi\, cos\,\psi & sin\,\varphi\, cos\,\theta \\ cos\,\varphi\, sin\,\theta\, cos\,\psi + sin\,\varphi\, sin\,\psi & cos\,\varphi\, sin\,\theta\, sin\,\psi - sin\,\varphi\, cos\,\psi & cos\,\varphi\, cos\,\theta \end{bmatrix} \tag{2.5}$$

The satellites are assumed to be point masses, so the third Euler angle is meaningless. The direction cosine matrix will be obtained as

$$C^{\mathcal{B}/\mathcal{N}} = \begin{bmatrix} cos\,\theta\, cos\,\psi & cos\,\theta\, sin\,\psi & -sin\,\theta \\ -sin\,\psi & cos\,\psi & 0 \\ sin\,\theta\, cos\,\psi & sin\,\theta\, sin\,\psi & cos\,\theta \end{bmatrix} \tag{2.6}$$

Based on the information given in Figure 1, the relative distance of the two-craft formation is shown by L and the masses m_1 and m_2 are located at the distances d_1 and d_2 respectively with respect to the formation center of mass. Since the origin of the Hill frame and formation center of mass are coincident to each other, the center of mass is at the origin of $\mathcal{N}$ and $\mathcal{B}$ frames such that

$$m_1\boldsymbol{d}_1 + m_2\boldsymbol{d}_2 = \boldsymbol{0} \tag{2.7}$$

For the orbit-radial configuration, the relative distance vector of the two-craft is aligned with the orbit-radial direction. By analyzing the geometry of the formation, one may obtain

$$\boldsymbol{L} = L\,\hat{b}_1 \tag{2.8}$$

$$\boldsymbol{L} = \boldsymbol{d}_1 - \boldsymbol{d}_2 \tag{2.9}$$

Substituting Eqs. (2.8) and (2.9) into Eq. (2.7) gives

$$m_1\boldsymbol{d}_1 + m_2\boldsymbol{d}_2 = \boldsymbol{0} \rightarrow m_1(\boldsymbol{L} + \boldsymbol{d}_2) + m_2\boldsymbol{d}_2 = \boldsymbol{0} \rightarrow \boldsymbol{d}_2 = -\frac{m_1}{m_1+m_2} L\,\hat{b}_1 \quad (2.10)$$

and

$$\boldsymbol{d}_1 = \frac{m_2}{m_1+m_2} L\,\hat{b}_1 \quad (2.11)$$

The vector $\boldsymbol{d}_1$ may be written in the Hill orbit frame in a matrix vector notation as

$$[d_1]_{\mathcal{N}} = \begin{bmatrix} x_1 \\ y_1 \\ z_1 \end{bmatrix} = \left[C^{\mathcal{B}/\mathcal{N}}\right]^T [d_1]_{\mathcal{B}} = \left[C^{\mathcal{B}/\mathcal{N}}\right]^T \begin{bmatrix} \frac{m_2}{m_1+m_2} L \\ 0 \\ 0 \end{bmatrix} = \frac{m_2 L}{m_1+m_2} \begin{bmatrix} cos\,\theta\, cos\,\psi \\ cos\,\theta\, sin\,\psi \\ -sin\,\theta \end{bmatrix} \quad (2.12)$$

Similarly, the position vector of the mass m_2 in the $\mathcal{N}$ frame can be written as

$$[d_2]_{\mathcal{N}} = \begin{bmatrix} x_2 \\ y_2 \\ z_2 \end{bmatrix} = \left[C^{\mathcal{B}/\mathcal{N}}\right]^T [d_2]_{\mathcal{B}} = \left[C^{\mathcal{B}/\mathcal{N}}\right]^T \begin{bmatrix} -\frac{m_1}{m_1+m_2} L \\ 0 \\ 0 \end{bmatrix} = \frac{m_1 L}{m_1+m_2} \begin{bmatrix} -cos\,\theta\, cos\,\psi \\ -cos\,\theta\, sin\,\psi \\ sin\,\theta \end{bmatrix} \quad (2.13)$$

The inertial velocity of the crafts may be obtained by using the transport theorem [40, 41]

$$\left\{\frac{d(\boldsymbol{R}_C+\boldsymbol{d}_i)}{dt}\right\}_{\mathcal{E}} = \left\{\frac{d(\boldsymbol{R}_C+\boldsymbol{d}_i)}{dt}\right\}_{\mathcal{N}} + \boldsymbol{\Omega}^{\mathcal{N}/\mathcal{E}} \times \{\boldsymbol{R}_C + \boldsymbol{d}_i\}_{\mathcal{N}} \quad (2.14)$$

Defining the inertial velocity as $\boldsymbol{v}_i$, it is

$$\boldsymbol{v}_i = \left\{\frac{d(\boldsymbol{R}_C+\boldsymbol{d}_i)}{dt}\right\}_{\mathcal{E}} = \dot{x}_i\hat{n}_1 + \dot{y}_i\hat{n}_2 + \dot{z}_i\hat{n}_3 + \begin{vmatrix} \hat{n}_1 & \hat{n}_2 & \hat{n}_3 \\ 0 & 0 & \Omega \\ x_i + R_C & y_i & z_i \end{vmatrix} = (\dot{x}_i - \Omega y_i)\hat{n}_1 + \left(\dot{y}_i + \Omega(x_i + R_C)\right)\hat{n}_2 + \dot{z}_i\hat{n}_3 \quad (2.15)$$

The kinetic energy of the system is given by

$$T = \frac{1}{2} m_1 \boldsymbol{v}_1 . \boldsymbol{v}_1 + \frac{1}{2} m_2 \boldsymbol{v}_2 . \boldsymbol{v}_2 \quad (2.16)$$

Substituting Eqs. (2.12), (2.13), and (2.15) into Eq. (2.16) the required formula for kinetic energy will be obtained as

$$T = \frac{1}{2}\frac{m_1 m_2}{m_1+m_2}\left(\dot{L}^2 + L^2\left(\dot{\theta}^2 + \left(\dot{\psi} + \Omega\right)^2 cos^2\,\theta\right)\right) + \frac{1}{2}(m_1 + m_2)\Omega^2 R_C^2 \quad (2.17)$$

where the separation distance between the two craft is given by

$$L = \sqrt{(x_1 - x_2)^2 + (y_1 - y_2)^2 + (z_1 - z_2)^2} \quad (2.18)$$

The gravitational potential of the Earth on the two-craft formation is written as

$$V_g = -GM_1\left(\frac{m_1}{|\boldsymbol{R}_C+\boldsymbol{d}_1|} + \frac{m_2}{|\boldsymbol{R}_C+\boldsymbol{d}_2|}\right) \quad (2.19)$$

The terms $\frac{1}{|\boldsymbol{R}_C+\boldsymbol{d}_i|}$ may be approximated by the Taylor series Expansions up to the second order terms. The results are given by

$$\frac{1}{|\boldsymbol{R}_C+\boldsymbol{d}_1|}=\frac{1}{R_c}\left(1-\frac{m_2}{m_1+m_2}\left(\frac{L}{R_c}\right)\left(\widehat{\boldsymbol{R}}_c.\widehat{\boldsymbol{d}}_1\right)+\frac{1}{2}\left(\frac{m_2}{m_1+m_2}\frac{L}{R_c}\right)^2\left(3\left(\widehat{\boldsymbol{R}}_c.\widehat{\boldsymbol{d}}_1\right)^2-1\right)\right) \quad (2.20)$$

$$\frac{1}{|\boldsymbol{R}_C+\boldsymbol{d}_2|}=\frac{1}{R_c}\left(1-\frac{m_1}{m_1+m_2}\left(\frac{L}{R_c}\right)\left(\widehat{\boldsymbol{R}}_c.\widehat{\boldsymbol{d}}_2\right)+\frac{1}{2}\left(\frac{m_1}{m_1+m_2}\frac{L}{R_c}\right)^2\left(3\left(\widehat{\boldsymbol{R}}_c.\widehat{\boldsymbol{d}}_2\right)^2-1\right)\right) \quad (2.21)$$

where $\widehat{\boldsymbol{R}}_c$ and $\widehat{\boldsymbol{d}}_i$ are the unit vectors of the $\boldsymbol{R}_C$ and $\boldsymbol{d}_i$, respectively. So,

$$\boldsymbol{d}_1=\frac{m_2}{m_1+m_2}L\widehat{\boldsymbol{d}}_1 \quad (2.22)$$

$$\boldsymbol{d}_2=\frac{m_1}{m_1+m_2}L\widehat{\boldsymbol{d}}_2 \quad (2.23)$$

where

$$\widehat{\boldsymbol{d}}_1=cos\,\theta\,cos\,\psi\,\hat{n}_1+cos\,\theta\,sin\,\psi\,\hat{n}_2-sin\,\theta\,\hat{n}_3 \quad (2.24)$$

$$\widehat{\boldsymbol{d}}_2=-cos\,\theta\,cos\,\psi\,\hat{n}_1-cos\,\theta\,sin\,\psi\,\hat{n}_2+sin\,\theta\,\hat{n}_3 \quad (2.25)$$

Now, V_g may be rewritten as

$$V_g=-\frac{\mu_1}{R_c}\left((m_1+m_2)+\frac{1}{2}\frac{m_1m_2}{m_1+m_2}\left(\frac{L}{R_c}\right)^2\left(3\left(\widehat{\boldsymbol{R}}_c.\widehat{\boldsymbol{d}}_1\right)^2-1\right)\right) \quad (2.26)$$

The Coulomb potential of the system is

$$V_c=k_c\frac{q_1q_2}{L^2}exp\left(\frac{-L}{\lambda_d}\right) \quad (2.27)$$

where k_c is the Coulomb constant and q_i is the electrostatic charge of each satellite. The term λ_d is called debye length which controls the lower bound on the electrostatic field strength of plasma shielding between the craft and varies between $80-1400$ meters at GEO.

The nonlinear equations of motion are derived using the Lagrange's equations. The Lagrangian function is defined as $\mathcal{L}=T-V$. The most famous form of the Lagrangian equation is

$$\frac{d}{dt}\frac{\partial\mathcal{L}}{\partial\dot{q}^j}-\frac{\partial\mathcal{L}}{\partial q^j}=\mathcal{Q}_j \quad (2.28)$$

where $q^j=(L,\psi,\theta)$ with $j=(1\ldots3)$ and $\mathcal{Q}_j$'s are generalized forces.

The nonlinear equations of motion for orbit-radial direction of a two-craft coulomb formation at earth circular orbits may be derived as

$$\ddot{L} - L\left(\dot{\theta}^2 + \left(\dot{\psi} + \Omega\right)^2 cos^2\,\theta - \Omega^2(1 - 3\,cos^2\,\theta\,cos^2\,\psi)\right) = \frac{Q_L}{m} \quad (2.29)$$

$$\ddot{\psi} - 2\dot{\theta}\,tan\,\theta\left(\dot{\psi} + \Omega\right) + 2\frac{\dot{L}}{L}\left(\dot{\psi} + \Omega\right) + 3\Omega^2\,cos\,\psi\,sin\,\psi = \frac{Q_\psi}{mL^2\,cos^2\,\theta} \quad (2.30)$$

$$\ddot{\theta} + 2\frac{\dot{L}}{L}\dot{\theta} + cos\,\theta\,sin\,\theta\left(\left(\dot{\psi} + \Omega\right)^2 + 3\Omega^2\,cos^2\,\psi\right) = \frac{Q_\theta}{mL^2} \quad (2.31)$$

which are in agreement with the equations given in [7]. The terms Q_L, Q_ψ, and Q_θ are the generalized forces, and the constant, m, is defined as $m = \frac{m_1 m_2}{m_1 + m_2}$. The Coulomb force, $\mathrm{F_{cf}}$, acting between the two crafts is given by

$$F_{cf} = -Q_L = -k_c\frac{q_1 q_2}{L^2}exp\left(\frac{-L}{\lambda_d}\right)\left(1 + \frac{L}{\lambda_d}\right) \quad (2.32)$$

The other generalized forces are defined by $Q_\psi = F_\psi L$ and $Q_\theta = F_\theta L$ where F_ψ and F_θ are the electric propulsion (EP) thrusting forces that introduce net formation torques in the ψ and θ directions. Note that to avoid any potential plume exhaust impingement issues both the EP thruster forces are directed in orthogonal directions to the formation line of sight vector [7]. The inputs are $u_L = \frac{k_c q_1 q_2}{m}$, $u_\psi = \frac{F_\psi}{m}$, $u_\theta = \frac{F_\theta}{m}$. The Eqs. (2.29)-(2.31) are rewritten as

$$\ddot{L} - L\left(\dot{\theta}^2 + \left(\dot{\psi} + \Omega\right)^2 cos^2\,\theta - \Omega^2(1 - 3\,cos^2\,\theta\,cos^2\,\psi)\right) = \frac{Q_L}{m} = \frac{-F_{cf}}{m} = bu_L \quad (2.33)$$

$$\ddot{\psi} - 2\dot{\theta}\,tan\,\theta\left(\dot{\psi} + \Omega\right) + 2\frac{\dot{L}}{L}\left(\dot{\psi} + \Omega\right) + 3\Omega^2\,cos\,\psi\,sin\,\psi = \frac{F_\psi}{mL\,cos^2\,\theta} = \frac{u_\psi}{L\,cos^2\,\theta} \quad (2.34)$$

$$\ddot{\theta} + 2\frac{\dot{L}}{L}\dot{\theta} + cos\,\theta\,sin\,\theta\left(\left(\dot{\psi} + \Omega\right)^2 + 3\Omega^2\sigma\,cos^2\,\psi\right) = \frac{F_\theta}{mL} = \frac{u_\theta}{L} \quad (2.35)$$

where

$$b = \frac{1}{\mathrm{L}^2}\exp\left(\frac{-\mathrm{L}}{\lambda_\mathrm{d}}\right)\left(1 + \frac{\mathrm{L}}{\lambda_\mathrm{d}}\right)$$

Consider the following state and input vectors

$$\boldsymbol{x} = (x_1, x_2, x_3, x_4, x_5, x_6)^T = \left(L, \psi, \theta, \dot{L}, \dot{\psi}, \dot{\theta}\right)^T \quad (2.36)$$

$$\boldsymbol{u} = \left(u_L, u_\psi, u_\theta\right)^T \tag{2.37}$$

The equations of motion will be written in the first order differential form as $\dot{\mathbf{x}} = \mathbf{F}(\mathbf{x}, \mathbf{u})$ which may be converted to an input affine form given by $\dot{\mathbf{x}} = \mathbf{f}(\mathbf{x}) + \mathbf{B}(\mathbf{x})\mathbf{u}$. The equations of motion should cast into a state dependent form while making sure that zero condition is an equilibrium point. The reason is discussed in Sections 5.1.2 and 6.1. Then, the equations are transformed to the SDC factorized form defined as $\dot{\mathbf{x}} = \mathbf{A}(\mathbf{x})\mathbf{x} + \mathbf{B}(\mathbf{x})\mathbf{u}$. The equations of motion may be written in first-order differential form as

$$\begin{bmatrix}\dot{x}_1\\ \dot{x}_2\\ \dot{x}_3\\ \dot{x}_4\\ \dot{x}_5\\ \dot{x}_6\end{bmatrix} = \begin{bmatrix} x_4 \\ x_5 \\ x_6 \\ x_1\left({x_6}^2 + (x_5+\Omega)^2\cos^2 x_3 - \Omega^2\left(1 - 3\cos^2 x_2 \cos^2 x_3\right)\right) \\ -2\frac{x_4}{x_1}(x_5+\Omega) + 2x_6 \tan x_3\,(x_5+\Omega) - 3\Omega^2 \cos x_2 \sin x_2 \\ -2\frac{x_4}{x_1}x_6 - \cos x_3 \sin x_3\left((x_5+\Omega)^2 + 3\Omega^2\cos^2 x_2\right)\end{bmatrix} + \begin{bmatrix}0 & 0 & 0\\ 0 & 0 & 0\\ 0 & 0 & 0\\ b & 0 & 0\\ 0 & \frac{1}{x_1\cos^2 x_3} & 0\\ 0 & 0 & \frac{1}{x_1}\end{bmatrix}\begin{bmatrix}u_L\\ u_\psi\\ u_\theta\end{bmatrix} \tag{2.38}$$

By considering an equilibrium as

$$\dot{\boldsymbol{x}} = \boldsymbol{F}(\boldsymbol{x}, \boldsymbol{u}) \;\rightarrow\; \boldsymbol{F}(\boldsymbol{x}_e, \boldsymbol{u}_e) = \mathbf{0} \tag{2.39}$$

$$\boldsymbol{x}_e = \left(L_{ref}, 0,0,0,0,0\right)^T \quad , \quad \boldsymbol{u}_e = \left(u_{L_e}, 0,0,0,0,0\right)^T \tag{2.40}$$

and defining new variables, $\tilde{\mathbf{x}} = \mathbf{x} - \mathbf{x}_e$, and $\tilde{\mathbf{u}} = \mathbf{u} - \mathbf{u}_e$

$$\dot{\tilde{\boldsymbol{x}}} = \tilde{\boldsymbol{F}}(\tilde{\boldsymbol{x}} + \boldsymbol{x}_e, \tilde{\boldsymbol{u}} + \boldsymbol{u}_e) \tag{2.41}$$

One may get new representation of the first order differential equations given by

$$\begin{bmatrix}\dot{\tilde{x}}_1\\ \dot{\tilde{x}}_2\\ \dot{\tilde{x}}_3\\ \dot{\tilde{x}}_4\\ \dot{\tilde{x}}_5\\ \dot{\tilde{x}}_6\end{bmatrix}=\begin{bmatrix}\tilde{x}_4\\ \tilde{x}_5\\ \tilde{x}_6\\ \left(\tilde{x}_1+L_{ref}\right)\left(\tilde{x}_6{}^2+(\tilde{x}_5+\Omega)^2\cos^2\tilde{x}_3-\Omega^2(1-3\cos^2\tilde{x}_2\cos^2\tilde{x}_3)\right)\\ -2\frac{\tilde{x}_4}{(\tilde{x}_1+L_{ref})}(\tilde{x}_5+\Omega)+2\tilde{x}_6\tan\tilde{x}_3\,(\tilde{x}_5+\Omega)-3\Omega^2\cos\tilde{x}_2\sin\tilde{x}_2\\ -2\frac{\tilde{x}_4}{(\tilde{x}_1+L_{ref})}\tilde{x}_6-\cos\tilde{x}_3\sin\tilde{x}_3\,((\tilde{x}_5+\Omega)^2+3\Omega^2\cos^2\tilde{x}_2)\end{bmatrix}+$$
$$\begin{bmatrix}0 & 0 & 0\\ 0 & 0 & 0\\ 0 & 0 & 0\\ b & 0 & 0\\ 0 & \frac{1}{(\tilde{x}_1+L_{ref})\cos^2\tilde{x}_3} & 0\\ 0 & 0 & \frac{1}{(\tilde{x}_1+L_{ref})}\end{bmatrix}\begin{bmatrix}\tilde{u}_L\\ \tilde{u}_\psi\\ \tilde{u}_\theta\end{bmatrix}+\begin{bmatrix}0\\ 0\\ 0\\ bu_{L_e}\\ 0\\ 0\end{bmatrix} \tag{2.42}$$

The fourth element of the Eq. (2.42) is

$$\dot{\tilde{x}}_4=\tilde{f}_4(\tilde{\boldsymbol{x}})+b\tilde{u}_L+bu_{L_e} \tag{2.43}$$

The term $\tilde{f}_4$ may be rearranged as

$$\tilde{f}_4=\left(\tilde{x}_1+L_{ref}\right)\left(\tilde{x}_6{}^2+(\tilde{x}_5+\Omega)^2\cos^2\tilde{x}_3-\Omega^2(1-3\cos^2\tilde{x}_2\cos^2\tilde{x}_3)\right)=$$
$$\tilde{x}_1\left(\tilde{x}_6{}^2+(\tilde{x}_5+\Omega)^2\cos^2\tilde{x}_3-\Omega^2(1-3\cos^2\tilde{x}_2\cos^2\tilde{x}_3)\right)+L_{ref}\left(\tilde{x}_6{}^2+\left(2\Omega\tilde{x}_5+\tilde{x}_5{}^2\right)\cos^2\tilde{x}_3\right)+L_{ref}\Omega^2(-3\sin^2\tilde{x}_2-4\sin^2\tilde{x}_3+3\sin^2\tilde{x}_2\sin^2\tilde{x}_3)+$$
$$3L_{ref}\Omega^2 \tag{2.44}$$

The constant term in the Eq. (2.43), u_{l_e}, is given by

$$u_{l_e}=\frac{k_c(q_1q_2)_e}{m} \tag{2.45}$$

where q_1q_2 for charges for a radially aligned two spacecraft formation is [7]

$$(q_1q_2)_e=-3\Omega^2\frac{L_{ref}^3}{k_c}m\left(\frac{\lambda_d}{L_{ref}+\lambda_d}\right)exp\left(\frac{L_{ref}}{\lambda_d}\right) \tag{2.46}$$

which can be obtained from the Eqs. (2.29)-(2.31) by putting all the parameters $\dot{L},\ddot{L},\psi,\dot{\psi},\ddot{\psi},\varphi,\dot{\varphi},and\ \ddot{\varphi}$ equal to zero and defining $L=L_{ref}$. Then, the equilibrium input becomes

$$bu_{l_e}=3L_{ref}\Omega^2 \tag{2.47}$$

Substituting Eqs. (2.44) & (2.47) into Eq. (2.43), the constant terms cancel each other. There are infinite numbers of choices for SDC factorization. One such choice

of the $\widetilde{\mathbf{A}}$ and $\widetilde{\mathbf{B}}$ matrices that the pair of them is controllable and the controllability matrix if full rank is given below.

$$\widetilde{\boldsymbol{A}}(\tilde{\boldsymbol{x}}) = \begin{bmatrix} 0 & 0 & 0 & 1 & 0 & 0 \\ 0 & 0 & 0 & 0 & 1 & 0 \\ 0 & 0 & 0 & 0 & 0 & 1 \\ \tilde{A}_{41} & \tilde{A}_{42} & \tilde{A}_{43} & 0 & \tilde{A}_{45} & \tilde{A}_{46} \\ 0 & \tilde{A}_{52} & 0 & \tilde{A}_{54} & \tilde{A}_{55} & \tilde{A}_{56} \\ 0 & 0 & \tilde{A}_{63} & \tilde{A}_{64} & 0 & 0 \end{bmatrix} \tag{2.48}$$

where

$$\tilde{A}_{41} = \left(\tilde{x}_6{}^2 + (\tilde{x}_5 + \Omega)^2 \cos^2 \tilde{x}_3 - \Omega^2(1 - 3\cos^2 \tilde{x}_2 \cos^2 \tilde{x}_3)\right)$$

$$\tilde{A}_{42} = -3L_{ref}\Omega^2 \frac{\sin^2 \tilde{x}_2}{\tilde{x}_2},\ \tilde{A}_{43} = L_{ref}\Omega^2(-4 + 3\sin^2 \tilde{x}_2)\frac{\sin^2 \tilde{x}_3}{\tilde{x}_3}$$

$$\tilde{A}_{45} = L_{ref}(\tilde{x}_5 + 2\Omega)\cos^2 \tilde{x}_3,\ \tilde{A}_{46} = L_{ref}\tilde{x}_6$$

$$\tilde{A}_{52} = -3\Omega^2 \cos \tilde{x}_2 \frac{\sin \tilde{x}_2}{\tilde{x}_2},\ \tilde{A}_{54} = \frac{-2\Omega}{\tilde{x}_1 + L_{ref}},\ ,\ \tilde{A}_{55} = \frac{-2\tilde{x}_4}{\tilde{x}_1 + L_{ref}},\ \tilde{A}_{56} = 2(\tilde{x}_5 + \Omega)\tan \tilde{x}_3$$

$$\tilde{A}_{63} = -((\tilde{x}_5 + \Omega)^2 + 3\Omega^2 \cos^2 \tilde{x}_2)\cos \tilde{x}_3 \frac{\sin \tilde{x}_3}{\tilde{x}_3},\ \tilde{A}_{64} = \frac{-2\tilde{x}_6}{\tilde{x}_1 + L_{ref}}$$

and

$$\widetilde{\boldsymbol{B}}(\tilde{\boldsymbol{x}}) = \begin{bmatrix} 0 & 0 & 0 \\ 0 & 0 & 0 \\ 0 & 0 & 0 \\ b & 0 & 0 \\ 0 & \frac{1}{(\tilde{x}_1 + L_{ref})\cos^2 \tilde{x}_3} & 0 \\ 0 & 0 & \frac{1}{(\tilde{x}_1 + L_{ref})} \end{bmatrix} \tag{2.49}$$

2.2 Along-Track Configuration

Following the same approach presented in Sec. 2.1, the nonlinear equations of motion for along-track configuration of a two-craft coulomb formation may be written as

$$\ddot{L} - L\left(\dot{\varphi}^2 + \left(\dot{\psi} + \Omega\right)^2 \cos^2 \varphi - \Omega^2(1 - 3\cos^2 \varphi \sin^2 \psi)\right) = \frac{Q_L}{m} = \frac{-F_{cf}}{m} = bu_L \tag{2.50}$$

$$\ddot{\psi} - 2\dot{\varphi}\tan \varphi \left(\dot{\psi} + \Omega\right) + 2\frac{\dot{L}}{L}\left(\dot{\psi} + \Omega\right) - 3\Omega^2 \cos \psi \sin \psi = \frac{Q_\psi}{mL^2 \cos^2 \varphi} = \frac{F_\psi}{mL \cos^2 \varphi} = \frac{u_\psi}{L \cos^2 \varphi} \tag{2.51}$$

$$\ddot{\varphi} + 2\frac{\dot{L}}{L}\dot{\varphi} + cos\,\varphi\,sin\,\varphi\left(\left(\dot{\psi}+\Omega\right)^2 + 3\Omega^2\,sin^2\,\psi\right) = \frac{Q_\varphi}{mL^2} = \frac{F_\varphi}{mL} = \frac{u_\varphi}{L} \quad (2.52)$$

where $Q_\varphi = F_\varphi L$, and F_φ is the electric propulsion (EP) thrusting force that introduce net formation torques in the φ direction. Consider the following state and input vectors

$$\boldsymbol{x} = (x_1, x_2, x_3, x_4, x_5, x_6)^T = \left(L, \psi, \varphi, \dot{L}, \dot{\psi}, \dot{\varphi}\right)^T$$

$$\boldsymbol{u} = \left(u_L, u_\psi, u_\varphi\right)^T$$

For along-track configuration considering a reference separation distance between the spacecraft and the equations as represented in (2.39)-(2.41), the state space form of the equations of motion becomes

$$\begin{bmatrix}\dot{\tilde{x}}_1\\ \dot{\tilde{x}}_2\\ \dot{\tilde{x}}_3\\ \dot{\tilde{x}}_4\\ \dot{\tilde{x}}_5\\ \dot{\tilde{x}}_6\end{bmatrix} = \begin{bmatrix} \tilde{x}_4 \\ \tilde{x}_5 \\ \tilde{x}_6 \\ \left(\tilde{x}_1 + L_{ref}\right)\left(\tilde{x}_6{}^2 + (\tilde{x}_5+\Omega)^2\,cos^2\,\tilde{x}_3 - \Omega^2(1-3\,cos^2\,\tilde{x}_3\,sin^2\,\tilde{x}_2)\right) \\ 2\tilde{x}_6\,tan\,\tilde{x}_3\,(\tilde{x}_5+\Omega) - 2\frac{\tilde{x}_4}{(\tilde{x}_1+L_{ref})}(\tilde{x}_5+\Omega) + 3\Omega^2\,cos\,\tilde{x}_2\,sin\,\tilde{x}_2 \\ -2\frac{\tilde{x}_4}{(\tilde{x}_1+L_{ref})}\tilde{x}_6 - cos\,\tilde{x}_3\,sin\,\tilde{x}_3\,((\tilde{x}_5+\Omega)^2 + 3\Omega^2\,sin^2\,\tilde{x}_2) \end{bmatrix} +$$

$$\begin{bmatrix} 0 & 0 & 0 \\ 0 & 0 & 0 \\ 0 & 0 & 0 \\ b & 0 & 0 \\ 0 & \frac{1}{(\tilde{x}_1+L_{ref})\,cos^2\,\tilde{x}_3} & 0 \\ 0 & 0 & \frac{1}{(\tilde{x}_1+L_{ref})} \end{bmatrix}\begin{bmatrix}\tilde{u}_L\\ \tilde{u}_\psi\\ \tilde{u}_\varphi\end{bmatrix} + \begin{bmatrix} 0 \\ bu_{L_e} \\ 0 \\ 0 \\ 0 \\ 0 \end{bmatrix} \quad (2.53)$$

The constant term in the Eq.(2.53), u_{l_e}, for along-track formation is

$$u_{l_e} = 0 \quad (2.54)$$

The multiplication term $q_1 q_2$ for charges for an along-track two spacecraft formation becomes [7]

$$(q_1 q_2)_{along-track} = 0 \quad (2.55)$$

In this formulation, $\tilde{\mathbf{f}}(\mathbf{0}) = \mathbf{0}$, and SDC factorization for along-track formation is given as

$$\widetilde{\boldsymbol{A}}(\tilde{\boldsymbol{x}}) = \begin{bmatrix} 0 & 0 & 0 & 1 & 0 & 0 \\ 0 & 0 & 0 & 0 & 1 & 0 \\ 0 & 0 & 0 & 0 & 0 & 1 \\ \tilde{A}_{41} & \tilde{A}_{42} & \tilde{A}_{43} & 0 & \tilde{A}_{45} & \tilde{A}_{46} \\ 0 & \tilde{A}_{52} & 0 & \tilde{A}_{54} & \tilde{A}_{55} & \tilde{A}_{56} \\ 0 & 0 & \tilde{A}_{63} & \tilde{A}_{64} & 0 & 0 \end{bmatrix} \tag{2.56}$$

where

$$\tilde{A}_{41} = \tilde{x}_6{}^2 + (\tilde{x}_5 + \Omega)^2 \cos^2 \tilde{x}_3 - \Omega^2(1 - 3\cos^2 \tilde{x}_3 \sin^2 \tilde{x}_2)$$

$$\tilde{A}_{42} = 3L_{ref}\Omega^2 \cos^2 \tilde{x}_3 \frac{\sin^2 \tilde{x}_2}{\tilde{x}_2},\ \tilde{A}_{43} = -L_{ref}\Omega^2 \frac{\sin^2 \tilde{x}_3}{\tilde{x}_3}$$

$$\tilde{A}_{45} = L_{ref}(\tilde{x}_5 + 2\Omega) \cos^2 \tilde{x}_3\ ,\tilde{A}_{46} = L_{ref}\tilde{x}_6$$

$$\tilde{A}_{52} = 3\Omega^2 \cos \tilde{x}_2 \frac{\sin \tilde{x}_2}{\tilde{x}_2},\ \tilde{A}_{54} = \frac{-2\Omega}{\tilde{x}_1 + L_{ref}},\ \tilde{A}_{55} = \frac{-2\tilde{x}_4}{\tilde{x}_1 + L_{ref}},\ \tilde{A}_{56} = 2(\tilde{x}_5 + \Omega) \tan \tilde{x}_3$$

$$\tilde{A}_{63} = -((\tilde{x}_5 + \Omega)^2 + 3\Omega^2 \sin^2 \tilde{x}_2) \cos \tilde{x}_3 \frac{\sin \tilde{x}_3}{\tilde{x}_3},\ \tilde{A}_{64} = \frac{-2\tilde{x}_6}{\tilde{x}_1 + L_{ref}}$$

The matrix $\widetilde{\mathbf{B}}(\tilde{\mathbf{x}})$ is as the same as Eq. (2.49).

2.3 Orbit-Normal Configuration

The nonlinear equations of motion for orbit-normal configuration of a two-craft coulomb formation are derived as

$$\ddot{L} - L\left(\dot{\theta}^2 \cos^2 \varphi + \dot{\varphi}^2 - \Omega^2 \cos^2 \varphi \cos^2 \theta + \Omega\dot{\theta} \sin 2\varphi \cos \theta - 2\Omega\dot{\varphi} \sin \theta\right) - 3\Omega^2 L \cos^2 \varphi \sin^2 \theta = \frac{Q_L}{m} = \frac{-F_{cf}}{m} = bu_L \tag{2.57}$$

$$\ddot{\theta} + 2\frac{\dot{L}}{L}\dot{\theta} - 2\dot{\varphi}\dot{\theta} \tan \varphi + 2\Omega\frac{\dot{L}}{L}\tan \varphi \cos \theta + 2\Omega\dot{\varphi} \cos \theta - 4\Omega^2 \cos \theta \sin \theta = \frac{Q_\theta}{mL^2 \cos^2 \varphi} = \frac{F_\theta}{mL \cos^2 \varphi} = \frac{u_\theta}{L \cos^2 \varphi} \tag{2.58}$$

$$\ddot{\varphi} + 2\frac{\dot{L}}{L}(\dot{\varphi} - \Omega \sin \theta) + \cos \varphi \sin \varphi \left(\dot{\theta}^2 - \Omega^2 \cos^2 \theta + 3\Omega^2 \sin^2 \theta\right) - 2\Omega\dot{\theta} \cos^2 \varphi \cos \theta = \frac{Q_\varphi}{mL^2} = \frac{F_\varphi}{mL} = \frac{u_\varphi}{L} \tag{2.59}$$

Define new states and inputs as

$$\boldsymbol{x} = (x_1, x_2, x_3, x_4, x_5, x_6)^T = \left(L, \theta, \varphi, \dot{L}, \dot{\theta}, \dot{\varphi}\right)^T \tag{2.60}$$

$$\boldsymbol{u} = \left(u_L, u_\theta, u_\varphi\right)^T \tag{2.61}$$

For the orbit-normal configuration considering again a reference separation distance between the spacecraft, the first order differential equations are given by

$$\begin{bmatrix}\dot{\tilde{x}}_1\\ \dot{\tilde{x}}_2\\ \dot{\tilde{x}}_3\\ \dot{\tilde{x}}_4\\ \dot{\tilde{x}}_5\\ \dot{\tilde{x}}_6\end{bmatrix} =$$

$$\begin{bmatrix} \tilde{x}_4 \\ \tilde{x}_5 \\ \tilde{x}_6 \\ (\tilde{x}_1 + L_{ref})\begin{pmatrix}\tilde{x}_5{}^2\, cos^2\,\tilde{x}_3 + \tilde{x}_6{}^2 - \Omega^2\, cos^2\,\tilde{x}_3\, cos^2\,\tilde{x}_2 + \Omega\tilde{x}_5\, sin\, 2\tilde{x}_3\, cos\,\tilde{x}_2 - \\ 2\Omega\tilde{x}_6\, sin\,\tilde{x}_2 + 3\Omega^2\, cos^2\,\tilde{x}_3\, sin^2\,\tilde{x}_2\end{pmatrix} \\ \begin{pmatrix}-2\frac{\tilde{x}_4}{(\tilde{x}_1+L_{ref})}\tilde{x}_5 + 2\tilde{x}_6\tilde{x}_5 tan\tilde{x}_3 - 2\Omega\frac{\tilde{x}_4}{(\tilde{x}_1+L_{ref})}tan\tilde{x}_3\, cos\,\tilde{x}_2 - \\ 2\Omega\tilde{x}_6\, cos\,\tilde{x}_2 + 4\Omega^2\, cos\,\tilde{x}_2\, sin\,\tilde{x}_2\end{pmatrix} \\ \begin{pmatrix}-2\frac{\tilde{x}_4}{(\tilde{x}_1+L_{ref})}(\tilde{x}_6 - \Omega\, sin\,\tilde{x}_2) - cos\,\tilde{x}_3\, sin\,\tilde{x}_3\,(\tilde{x}_5{}^2 - \Omega^2\, cos^2\,\tilde{x}_2 + 3\Omega^2\, sin^2\,\tilde{x}_2) + \\ 2\Omega\tilde{x}_5\, cos^2\,\tilde{x}_3\, cos\,\tilde{x}_2\end{pmatrix} \end{bmatrix} +$$

$$\begin{bmatrix}0 & 0 & 0\\ 0 & 0 & 0\\ 0 & 0 & 0\\ b & 0 & 0\\ 0 & \frac{1}{(\tilde{x}_1+L_{ref})\,cos^2\,\tilde{x}_3} & 0\\ 0 & 0 & \frac{1}{(\tilde{x}_1+L_{ref})}\end{bmatrix}\begin{bmatrix}\tilde{u}_L\\ \tilde{u}_\theta\\ \tilde{u}_\varphi\end{bmatrix} + \begin{bmatrix}0\\ bu_{L_e}\\ 0\\ 0\\ 0\\ 0\end{bmatrix} \tag{2.62}$$

Now in the new form of equations the fourth entry in vector valued function $\tilde{\boldsymbol{f}}$ simplifies as

$$\tilde{f}_4 = (\tilde{x}_1)\big(\tilde{x}_5{}^2\, cos^2\,\tilde{x}_3 + \tilde{x}_6{}^2 - \Omega^2\, cos^2\,\tilde{x}_3\, cos^2\,\tilde{x}_2 + \Omega\tilde{x}_5\, sin\, 2\tilde{x}_3\, cos\,\tilde{x}_2 - 2\Omega\tilde{x}_6\, sin\,\tilde{x}_2 + 3\Omega^2\, cos^2\,\tilde{x}_3\, sin^2\,\tilde{x}_2\big) + \big(L_{ref}\big)\big(\tilde{x}_5{}^2\, cos^2\,\tilde{x}_3 + \tilde{x}_6{}^2 + \Omega\tilde{x}_5\, sin\, 2\tilde{x}_3\, cos\,\tilde{x}_2 - 2\Omega\tilde{x}_6\, sin\,\tilde{x}_2 + 3\Omega^2\, cos^2\,\tilde{x}_3\, sin^2\,\tilde{x}_2\big) - L_{ref}\Omega^2(sin^2\,\tilde{x}_3\, sin^2\,\tilde{x}_2 - sin^2\,\tilde{x}_2 - sin^2\,\tilde{x}_3) - L_{ref}\Omega^2 \tag{2.63}$$

The constant term in the Eq. (2.43),u_{l_e} , for orbit-normal configuration obtained as

$$u_{l_e} = \frac{k_c(q_1q_2)_e}{m} \tag{2.64}$$

where q_1q_2 for charges for an orbit normal two spacecraft formation is [7]

$$(q_1 q_2)_e = \Omega^2 \frac{L_{ref}^3}{k_c} m \left(\frac{\lambda_d}{L_{ref}+\lambda_d}\right) exp\left(\frac{L_{ref}}{\lambda_d}\right) \tag{2.65}$$

Then, the equilibrium input obtained as

$$bu_{l_e} = -L_{ref}\Omega^2 \tag{2.66}$$

Substituting Eqs. (2.63) & (2.66) into Eq. (2.62), the constant terms cancel each other. Therefore, the equations are manipulated to the proper structure and the necessary condition on $\tilde{\boldsymbol{f}}$ is satisfied. The following SDC factorization is used here.

$$\widetilde{\boldsymbol{A}}(\tilde{\boldsymbol{x}}) = \begin{bmatrix} 0 & 0 & 0 & 1 & 0 & 0 \\ 0 & 0 & 0 & 0 & 1 & 0 \\ 0 & 0 & 0 & 0 & 0 & 1 \\ \tilde{A}_{41} & \tilde{A}_{42} & \tilde{A}_{43} & 0 & \tilde{A}_{45} & \tilde{A}_{26} \\ 0 & \tilde{A}_{52} & 0 & \tilde{A}_{54} & \tilde{A}_{55} & \tilde{A}_{56} \\ 0 & 0 & \tilde{A}_{63} & \tilde{A}_{64} & \tilde{A}_{65} & 0 \end{bmatrix} \tag{2.67}$$

where

$$\tilde{A}_{41} = \left(\tilde{x}_5{}^2\, cos^2\, \tilde{x}_3 + \tilde{x}_6{}^2 - \Omega^2\, cos^2\, \tilde{x}_3\, cos^2\, \tilde{x}_2 + \Omega \tilde{x}_5\, sin\, 2\tilde{x}_3\, cos\, \tilde{x}_2 - 2\Omega \tilde{x}_6\, sin\, \tilde{x}_2 + 3\Omega^2\, cos^2\, \tilde{x}_3\, sin^2\, \tilde{x}_2\right)$$

$$\tilde{A}_{42} = \left(L_{ref}\Omega^2\right)(3\, cos^2\, \tilde{x}_3\, sin^2\, \tilde{x}_2 - sin^2\, \tilde{x}_3\, sin^2\, \tilde{x}_2 + sin^2\, \tilde{x}_2)/\tilde{x}_2$$

$$\tilde{A}_{43} = L_{ref}\Omega^2 \frac{sin^2\, \tilde{x}_3}{\tilde{x}_3},\ \tilde{A}_{45} = L_{ref}(\tilde{x}_5)\, cos^2\, \tilde{x}_3 + L_{ref}\Omega\, sin\, 2\tilde{x}_3\, cos\, \tilde{x}_2$$

$$\tilde{A}_{46} = L_{ref}(\tilde{x}_6 - 2\Omega\, sin\, \tilde{x}_2),\ \tilde{A}_{52} = 4\Omega^2\, cos\, \tilde{x}_2 \frac{sin\, \tilde{x}_2}{\tilde{x}_2}$$

$$\tilde{A}_{54} = \frac{-2\tilde{x}_5}{\tilde{x}_1 + L_{ref}} - 2\Omega \frac{1}{\tilde{x}_1 + L_{ref}} tan\tilde{x}_3\, cos\, \tilde{x}_2$$

$$\tilde{A}_{55} = 2\tilde{x}_6\, tan\, \tilde{x}_3,\ \tilde{A}_{56} = -2\Omega\, cos\, \tilde{x}_2,\ \tilde{A}_{64} = \frac{-2(\tilde{x}_6 - \Omega\, sin\, \tilde{x}_2)}{\tilde{x}_1 + L_{ref}}$$

$$\tilde{A}_{63} = -((\tilde{x}_5)^2 - \Omega^2\, cos^2\, \tilde{x}_2 + 3\Omega^2\, sin^2\, \tilde{x}_2)\, cos\, \tilde{x}_3 \frac{sin\, \tilde{x}_3}{\tilde{x}_3},$$

and the matrix $\widetilde{\mathbf{B}}(\tilde{\mathbf{x}})$ is the same as given in Eq. (2.49).

CHAPTER 3

TWO-CRAFT EQUATIONS OF MOTION AND SDC FACTORIZATIONS AT LIBRATION POINTS

3.1 Earth-Moon Collinear Libration Points

3.1.1 Orbit-Radial Configuration

The problem of describing the relative motion of a two-craft Coulomb formation at Earth-moon collinear libration point is considered in this section. The masses of two craft are infinitesimal with respect to the masses of two primaries, Earth and moon. Since the orbital motion of the two primaries is not affected by the two-craft, it is reasonable to assume a circular orbital motion for the primaries about their center of mass (barycenter) showed by the point $\mathcal{S}$ in the Figure 3. The constant angular velocity of the orbital motion of the two primaries is given by $\Omega = \sqrt{G(M_1 + M_2)/D^3}$, where G is the universal gravitational constant, M_1 and M_2 are the masses of the Earth and moon, respectively and D is the constant relative distance between them. An inertial frame with its center at the barycenter is defined here as $\mathcal{S}: \{\hat{e}_1, \hat{e}_2, \hat{e}_3\}$ with (X, Y, Z) coordinates, which its axes are aligned with the Earth centered inertial frame, $\mathcal{E}: \{\hat{e}_1, \hat{e}_2, \hat{e}_3\}$ defined in the Section 2.1 and just its center is different. The other coordinate systems are $\mathcal{N}: \{\hat{n}_1, \hat{n}_2, \hat{n}_3\}$ and $\mathcal{B}: \{\hat{b}_1, \hat{b}_2, \hat{b}_3\}$ frames which are also defined in the Sec. 2.1. Note that in this section, the centers of Hill's frame $\mathcal{N}$ and Body frame $\mathcal{B}$ are located at the L_2 libration point.

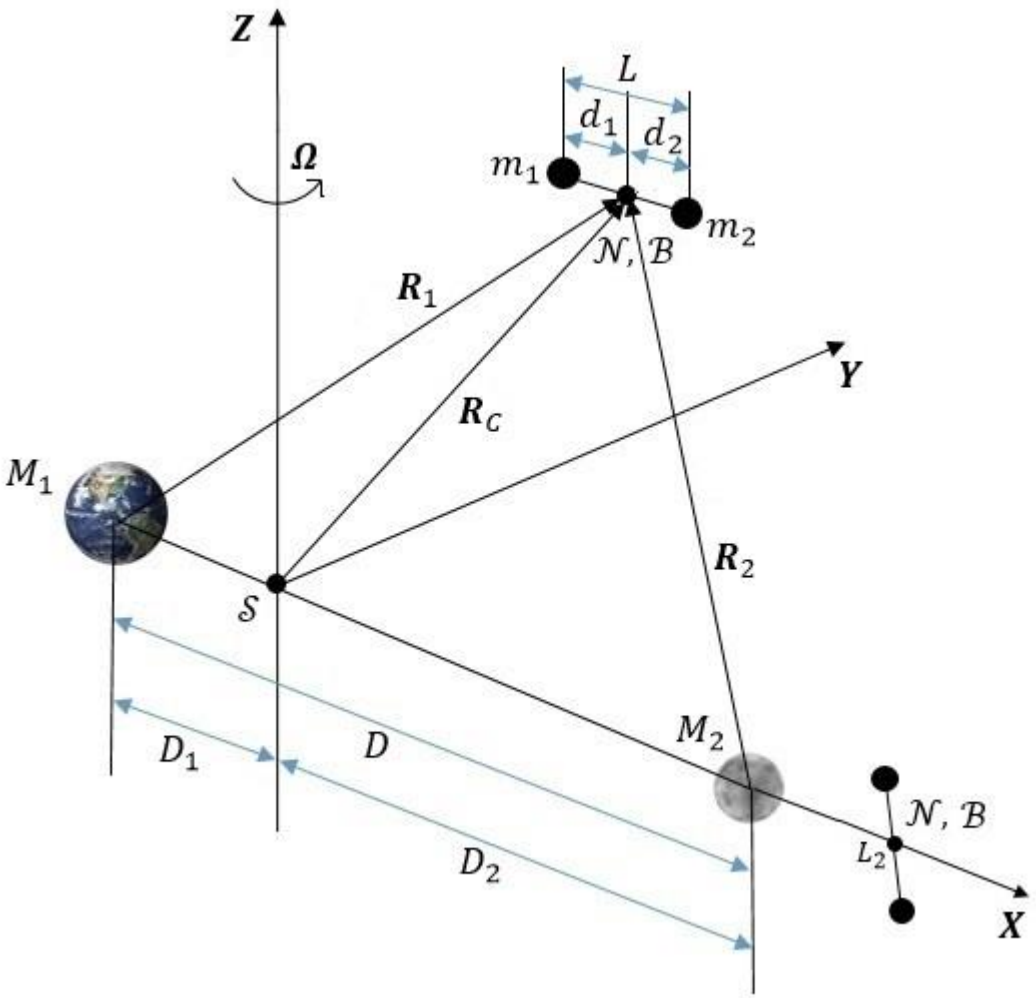

Figure 3. Formation configuration at Earth-moon collinear libration point.

The angular velocity is defined as

$$\boldsymbol{\Omega} = \boldsymbol{\Omega}^{\mathcal{N}/\mathcal{S}} = \boldsymbol{\Omega}^{\mathcal{N}/\mathcal{E}} = \Omega\, \hat{\boldsymbol{n}}_3 = \Omega\, \hat{\boldsymbol{e}}_3 \tag{3.1}$$

For the Earth-moon system, the parameters showed in Figure 3 are given by [40]

$$\mu_1 = GM_1 = 398{,}601\,\frac{km^3}{s^2}$$

$$\mu_2 = GM_2 = 4887\,\frac{km^3}{s^2}$$

$$M_1 = 81.3045 M_2$$

$$D = 384{,}748\ km$$

$$D_1 = 0.01215\, D = 4674\ km$$

$$D_1 = 98785\, D = 380{,}073\ km$$

$$\Omega = 2.661699\ \times 10^{-6}\, \frac{rad}{s}$$

The two-craft Coulomb formation is assumed to behave like a rigid body. The relative attitude between the $\mathcal{N}$ and $\mathcal{B}$ frames is represented using the 3-2-1 sequence of Euler angle rotations. As illustrated in Figure 2, the Euler angles are defined as $\psi, \theta, and\ \varphi$, which are yaw, pitch, and roll angles from Hill orbit frame to the formation body-fixed frame. The details about rotation matrices are given in the Sec. 2.1.

The satellites are assumed to be point masses, so the assumption $\varphi = 0$ is applied to the rotation matrix and the new direction cosine matrix used in this thesis will be obtained as

$$C^{\mathcal{B}/\mathcal{N}} = \begin{bmatrix} cos\,\theta\, cos\,\psi & cos\,\theta\, sin\,\psi & -sin\,\theta \\ -sin\,\psi & cos\,\psi & 0 \\ sin\,\theta\, cos\,\psi & sin\,\theta\, sin\,\psi & cos\,\theta \end{bmatrix} \tag{3.2}$$

The positions of two primaries in the Synodic frame are given by $(-D_1, 0{,}0)$ and $(D_2, 0{,}0)$, respectively. The planar position of the collinear libration point L_2 in the Synodic frame $\mathcal{S}$ is given by $(X_0, 0{,}0)$. So, the planar position vector of the libration point L_2 from the two primaries in the Synodic frame becomes

$$\boldsymbol{R}_1 = (X_0 + D_1)\hat{\boldsymbol{e}}_1 + 0\hat{\boldsymbol{e}}_2 + 0\hat{\boldsymbol{e}}_3 \tag{3.3}$$

$$\boldsymbol{R}_2 = (X_0 - D_2)\hat{\boldsymbol{e}}_1 + 0\hat{\boldsymbol{e}}_2 + 0\hat{\boldsymbol{e}}_3 \tag{3.4}$$

Based on the information represented in Figure 3, the relative distance of the two-craft formation is shown by L and the masses m_1 and m_2 are located at the distances d_1 and d_2 respectively with respect to the formation center of mass. Since the origin of the Hill frame and formation center of mass are coincident to each other, the center of mass condition may be represented as

$$m_1\boldsymbol{d}_1 + m_2\boldsymbol{d}_2 = \boldsymbol{0} \tag{3.5}$$

For the orbit-radial configuration, the relative distance vector of the two-craft is aligned with the orbit-radial direction. By analyzing the geometry of the formation, one may obtain

$$\boldsymbol{L} = L\,\widehat{\boldsymbol{b}}_1 \tag{3.6}$$

$$\boldsymbol{L} = \boldsymbol{d}_1 - \boldsymbol{d}_2 \tag{3.7}$$

Substituting Eqs. (3.6)-(3.7) into Eq. (3.5)gives

$$m_1\boldsymbol{d}_1 + m_2\boldsymbol{d}_2 = \boldsymbol{0} \rightarrow m_1(\boldsymbol{L} + \boldsymbol{d}_2) + m_2\boldsymbol{d}_2 = \boldsymbol{0} \rightarrow \boldsymbol{d}_2 = -\frac{m_1}{m_1+m_2} L\,\widehat{\boldsymbol{b}}_1 \tag{3.8}$$

and

$$\boldsymbol{d}_1 = \frac{m_2}{m_1+m_2} L\,\widehat{\boldsymbol{b}}_1 \tag{3.9}$$

Vector $\boldsymbol{d}_1$ in Hill orbit frame in a matrix notation may be written as

$$[d_1]_{\mathcal{N}} = \begin{bmatrix} x_1 \\ y_1 \\ z_1 \end{bmatrix} = \left[C^{\mathcal{B}/\mathcal{N}}\right]^T [d_1]_{\mathcal{B}} = \left[C^{\mathcal{B}/\mathcal{N}}\right]^T \begin{bmatrix} \frac{m_2}{m_1+m_2} L \\ 0 \\ 0 \end{bmatrix} = \frac{m_2 L}{m_1+m_2} \begin{bmatrix} cos\,\theta\, cos\,\psi \\ cos\,\theta\, sin\,\psi \\ -sin\,\theta \end{bmatrix} \tag{3.10}$$

Similarly, the position vector of the mass m_2 in the $\mathcal{N}$ frame can be written as

$$[d_2]_{\mathcal{N}} = \begin{bmatrix} x_2 \\ y_2 \\ z_2 \end{bmatrix} = \left[C^{\mathcal{B}/\mathcal{N}}\right]^T [d_2]_{\mathcal{B}} = \left[C^{\mathcal{B}/\mathcal{N}}\right]^T \begin{bmatrix} -\frac{m_1}{m_1+m_2} L \\ 0 \\ 0 \end{bmatrix} = \frac{m_1 L}{m_1+m_2} \begin{bmatrix} -cos\,\theta\, cos\,\psi \\ -cos\,\theta\, sin\,\psi \\ sin\,\theta \end{bmatrix} \tag{3.11}$$

The inertial velocity of the two-craft may be obtained by using the transport theorem [40, 41]

$$\left\{\frac{d(\boldsymbol{R}_C+\boldsymbol{d}_i)}{dt}\right\}_{\mathcal{S}} = \left\{\frac{d(\boldsymbol{R}_C+\boldsymbol{d}_i)}{dt}\right\}_{\mathcal{N}} + \boldsymbol{\Omega}^{\mathcal{N}/\mathcal{S}} \times \{\boldsymbol{R}_C + \boldsymbol{d}_i\}_{\mathcal{N}} \tag{3.12}$$

Defining the inertial velocity as $\boldsymbol{v}_i$, it is

$$\boldsymbol{v}_i = \left\{\frac{d(\boldsymbol{R}_C+\boldsymbol{d}_i)}{dt}\right\}_{\mathcal{S}} = \dot{x}_i\hat{n}_1 + \dot{y}_i\hat{n}_2 + \dot{z}_i\hat{n}_3 + \begin{vmatrix} \hat{n}_1 & \hat{n}_2 & \hat{n}_3 \\ 0 & 0 & \Omega \\ x_i + R_C & y_i & z_i \end{vmatrix} = (\dot{x}_i - \Omega y_i)\hat{n}_1 + \left(\dot{y}_i + \Omega(x_i + R_C)\right)\hat{n}_2 + \dot{z}_i\hat{n}_3 \tag{3.13}$$

The kinetic energy of the system is given by

$$T = \frac{1}{2} m_1 \boldsymbol{v}_1.\boldsymbol{v}_1 + \frac{1}{2} m_2 \boldsymbol{v}_2.\boldsymbol{v}_2 \tag{3.14}$$

Substituting Eqs.(3.10), (3.11), and (3.13) into Eq. (3.14)the required formula for kinetic energy will be obtained as

$$T = \frac{1}{2}\frac{m_1 m_2}{m_1+m_2}\left(\dot{L}^2 + L^2\left(\dot{\theta}^2 + \left(\dot{\psi}+\Omega\right)^2 cos^2\theta\right)\right) + \frac{1}{2}(m_1+m_2)\Omega^2 R_C^2 \quad (3.15)$$

where the separation distance between the two craft is given by

$$L = \sqrt{(x_1-x_2)^2 + (y_1-y_2)^2 + (z_1-z_2)^2} \quad (3.16)$$

The gravitational potential of the Earth-moon on the two-craft formation is written as

$$V_g = -GM_1\left(\frac{m_1}{|\boldsymbol{R}_1+\boldsymbol{d}_1|} + \frac{m_2}{|\boldsymbol{R}_1+\boldsymbol{d}_2|}\right) - GM_2\left(\frac{m_1}{|\boldsymbol{R}_2+\boldsymbol{d}_1|} + \frac{m_2}{|\boldsymbol{R}_2+\boldsymbol{d}_2|}\right) \quad (3.17)$$

The terms $\frac{1}{|\boldsymbol{R}_i+\boldsymbol{d}_i|}$ may be approximated by the Taylor series expansions up to the second order terms. The results are given by

$$\frac{1}{|\boldsymbol{R}_1+\boldsymbol{d}_1|} = \frac{1}{R_1}\left(1 - \frac{m_2}{m_1+m_2}\left(\frac{L}{R_1}\right)\left(\widehat{\boldsymbol{R}}_1.\widehat{\boldsymbol{d}}_1\right) + \frac{1}{2}\left(\frac{m_2}{m_1+m_2}\frac{L}{R_1}\right)^2\left(3\left(\widehat{\boldsymbol{R}}_1.\widehat{\boldsymbol{d}}_1\right)^2 - 1\right)\right) \quad (3.18)$$

$$\frac{1}{|\boldsymbol{R}_1+\boldsymbol{d}_2|} = \frac{1}{R_1}\left(1 - \frac{m_1}{m_1+m_2}\left(\frac{L}{R_1}\right)\left(\widehat{\boldsymbol{R}}_1.\widehat{\boldsymbol{d}}_2\right) + \frac{1}{2}\left(\frac{m_1}{m_1+m_2}\frac{L}{R_1}\right)^2\left(3\left(\widehat{\boldsymbol{R}}_1.\widehat{\boldsymbol{d}}_2\right)^2 - 1\right)\right) \quad (3.19)$$

$$\frac{1}{|\boldsymbol{R}_2+\boldsymbol{d}_1|} = \frac{1}{R_2}\left(1 - \frac{m_2}{m_1+m_2}\left(\frac{L}{R_2}\right)\left(\widehat{\boldsymbol{R}}_2.\widehat{\boldsymbol{d}}_1\right) + \frac{1}{2}\left(\frac{m_2}{m_1+m_2}\frac{L}{R_2}\right)^2\left(3\left(\widehat{\boldsymbol{R}}_2.\widehat{\boldsymbol{d}}_1\right)^2 - 1\right)\right) \quad (3.20)$$

$$\frac{1}{|\boldsymbol{R}_2+\boldsymbol{d}_2|} = \frac{1}{R_2}\left(1 - \frac{m_1}{m_1+m_2}\left(\frac{L}{R_2}\right)\left(\widehat{\boldsymbol{R}}_2.\widehat{\boldsymbol{d}}_2\right) + \frac{1}{2}\left(\frac{m_1}{m_1+m_2}\frac{L}{R_2}\right)^2\left(3\left(\widehat{\boldsymbol{R}}_2.\widehat{\boldsymbol{d}}_2\right)^2 - 1\right)\right) \quad (3.21)$$

where $\widehat{\boldsymbol{R}}_i$ and $\widehat{\boldsymbol{d}}_i$ are the unit vectors of the $\boldsymbol{R}_i$ and $\boldsymbol{d}_\mathrm{i}$, respectively. So,

$$\boldsymbol{d}_1 = \frac{m_2}{m_1+m_2}L\widehat{\boldsymbol{d}}_1 \quad (3.22)$$

$$\boldsymbol{d}_2 = \frac{m_1}{m_1+m_2}L\widehat{\boldsymbol{d}}_2 \quad (3.23)$$

where

$$\widehat{\boldsymbol{d}}_1 = cos\,\theta\,cos\,\psi\,\widehat{\boldsymbol{n}}_1 + cos\,\theta\,sin\,\psi\,\widehat{\boldsymbol{n}}_2 - sin\,\theta\,\widehat{\boldsymbol{n}}_3 \quad (3.24)$$

$$\widehat{\boldsymbol{d}}_2 = -cos\,\theta\,cos\,\psi\,\widehat{\boldsymbol{n}}_1 - cos\,\theta\,sin\,\psi\,\widehat{\boldsymbol{n}}_2 + sin\,\theta\,\widehat{\boldsymbol{n}}_3 \quad (3.25)$$

Now, V_g can be rewritten as

$$V_g = -\frac{\mu_1}{R_1}\left((m_1+m_2) + \frac{1}{2}\frac{m_1 m_2}{m_1+m_2}\left(\frac{L}{R_1}\right)^2\left(3\left(\widehat{\boldsymbol{R}}_1.\widehat{\boldsymbol{d}}_1\right)^2 - 1\right)\right) - \frac{\mu_2}{R_2}\left((m_1+m_2) + \frac{1}{2}\frac{m_1 m_2}{m_1+m_2}\left(\frac{L}{R_2}\right)^2\left(3\left(\widehat{\boldsymbol{R}}_2.\widehat{\boldsymbol{d}}_2\right)^2 - 1\right)\right) \quad (3.26)$$

The Coulomb potential of the system is

$$V_c = k_c \frac{q_1 q_2}{L^2} exp\left(\frac{-L}{\lambda_d}\right) \tag{3.27}$$

where k_c is the Coulomb constant and q_{i} is the electrostatic charge of each satellite. The term λ_d is called debye length which controls the lower bound on the electrostatic field strength of plasma shielding between the craft and varies between $80 - 1400$ meters at GEO.

The nonlinear equations of motion are derived using the Lagrange's equations. The Lagrangian function is defined as $\mathcal{L} = T - V$. The most famous form of the Lagrangian equation is

$$\frac{d}{dt}\frac{\partial \mathcal{L}}{\partial \dot{q}^j} - \frac{\partial \mathcal{L}}{\partial q^j} = \mathcal{Q}_j \tag{3.28}$$

where $q^j = (L, \psi, \theta)$ with $j = (1 \ldots 3)$ and $\mathcal{Q}_j$'s are generalized forces.

The nonlinear equations of motion for orbit-radial configuration for a two-craft Coulomb formation at Earth-moon collinear libration points are derived as

$$\ddot{L} - L\left(\dot{\theta}^2 + \left(\dot{\psi} + \Omega\right)^2 cos^2\,\theta - \Omega^2\sigma(1 - 3\,cos^2\,\theta\,cos^2\,\psi)\right) = \frac{\mathcal{Q}_L}{m} \tag{3.29}$$

$$\ddot{\psi} - 2\dot{\theta}\,tan\,\theta\left(\dot{\psi} + \Omega\right) + 2\frac{\dot{L}}{L}\left(\dot{\psi} + \Omega\right) + 3\Omega^2\sigma\,cos\,\psi\,sin\,\psi = \frac{\mathcal{Q}_\psi}{mL^2\,cos^2\,\theta} \tag{3.30}$$

$$\ddot{\theta} + 2\frac{\dot{L}}{L}\dot{\theta} + cos\,\theta\,sin\,\theta\left(\left(\dot{\psi} + \Omega\right)^2 + 3\Omega^2\sigma\,cos^2\,\psi\right) = \frac{\mathcal{Q}_\theta}{mL^2} \tag{3.31}$$

which are in agreement with those given in [8]. The constant, m, is defined as, $m = \frac{m_1 m_2}{m_1 + m_2}$, and the mass ratio ρ is defined as $\rho = \frac{M_2}{M_1 + M_2}$, and $1 - \rho = \frac{M_1}{M_1 + M_2}$. The parameter σ is defined as

$$\sigma = \frac{1-\rho}{\left|\left(\frac{X_0}{D}\right)+\rho\right|^3} + \frac{\rho}{\left|\left(\frac{X_0}{D}\right)-1+\rho\right|^3} \tag{3.32}$$

Note that if $\sigma = 1$, the Eqs. (3.29)-(3.31) would be exactly the same as the equations of motion for radial direction of a two-craft coulomb formation in circular Earth orbits represented in Eqs. (2.29)-(2.31). The terms $\mathcal{Q}_L, \mathcal{Q}_\psi, \mathcal{Q}_\theta$ are the generalized forces associated with L, ψ and θ, respectively. For a two spacecraft

Coulomb formation, with F_{cf} being the Coulomb force acting between the two crafts, $\mathcal{Q}_L = -F_{cf}$, we have

$$F_{cf} = -k_c \frac{q_1 q_2}{L^2} exp\left(\frac{-L}{\lambda_d}\right)\left(1 + \frac{L}{\lambda_d}\right) \tag{3.33}$$

And $\mathcal{Q}_\psi = F_\psi L$ and $\mathcal{Q}_\theta = F_\theta L$ where F_ψ and F_θ are the electric propulsion (EP) thrusting forces that introduce net formation torques in the ψ and θ directions. Note that to avoid any potential plume exhaust impingement issues both the EP thruster forces are directed in orthogonal directions to the formation line of sight vector. The equations of motion should cast in to a state dependent form while making sure that zero condition is an equilibrium point. Consider the following state and input vectors

$$\boldsymbol{x} = (x_1, x_2, x_3, x_4, x_5, x_6)^T = \left(L, \psi, \theta, \dot{L}, \dot{\psi}, \dot{\theta}\right)^T \tag{3.34}$$

$$\boldsymbol{u} = \left(u_L, u_\psi, u_\theta\right)^T \tag{3.35}$$

By considering an equilibrium as

$$\dot{\boldsymbol{x}} = \boldsymbol{F}(\boldsymbol{x}, \boldsymbol{u}) \;\rightarrow\; \boldsymbol{F}(\boldsymbol{x_e}, \boldsymbol{u_e}) = \boldsymbol{0} \tag{3.36}$$

$$\boldsymbol{x_e} = \left(L_{ref}, 0,0,0,0,0\right)^T \quad , \quad \boldsymbol{u_e} = \left(u_{L_e}, 0,0,0,0,0\right)^T \tag{3.37}$$

and defining new variables, $\tilde{\mathbf{x}} = \mathbf{x} - \mathbf{x}_e$, and $\tilde{\mathbf{u}} = \mathbf{u} - \mathbf{u}_e$, we have

$$\dot{\tilde{\boldsymbol{x}}} = \tilde{\boldsymbol{F}}(\tilde{\boldsymbol{x}} + \boldsymbol{x_e}, \tilde{\boldsymbol{u}} + \boldsymbol{u_e}) \tag{3.38}$$

The state space equations of motion in new definition for state and input variables may be written as

$$\begin{bmatrix}\dot{\tilde{x}}_1\\ \dot{\tilde{x}}_2\\ \dot{\tilde{x}}_3\\ \dot{\tilde{x}}_4\\ \dot{\tilde{x}}_5\\ \dot{\tilde{x}}_6\end{bmatrix}=\begin{bmatrix}\tilde{x}_4\\ \tilde{x}_5\\ \tilde{x}_6\\ (\tilde{x}_1+L_{ref})\left(\tilde{x}_6{}^2+(\tilde{x}_5+\Omega)^2\cos^2\tilde{x}_3-\Omega^2\sigma\,(1-3\cos^2\tilde{x}_3\cos^2\tilde{x}_2)\right)\\ 2\tilde{x}_6\tan\tilde{x}_3\,(\tilde{x}_5+\Omega)-2\frac{\tilde{x}_4}{(\tilde{x}_1+L_{ref})}(\tilde{x}_5+\Omega)-3\Omega^2\sigma\cos\tilde{x}_2\sin\tilde{x}_2\\ -2\frac{\tilde{x}_4}{(\tilde{x}_1+L_{ref})}\tilde{x}_6-\cos\tilde{x}_3\sin\tilde{x}_3\,((\tilde{x}_5+\Omega)^2+3\Omega^2\sigma\cos^2\tilde{x}_2)\end{bmatrix}+$$
$$\begin{bmatrix}0 & 0 & 0\\ 0 & 0 & 0\\ 0 & 0 & 0\\ b & 0 & 0\\ 0 & \frac{1}{(\tilde{x}_1+L_{ref})\cos^2\tilde{x}_3} & 0\\ 0 & 0 & \frac{1}{(\tilde{x}_1+L_{ref})}\end{bmatrix}\begin{bmatrix}\tilde{u}_L\\ \tilde{u}_\psi\\ \tilde{u}_\theta\end{bmatrix}+\begin{bmatrix}0\\ 0\\ 0\\ bu_{L_e}\\ 0\\ 0\end{bmatrix} \tag{3.39}$$

The fourth component in Eq. (3.39) can be shown as

$$\dot{\tilde{x}}_4=\tilde{f}_4(\tilde{\mathbf{x}})+b\tilde{u}_L+bu_{L_e} \tag{3.40}$$

The simplified form of $\tilde{f}_4(\tilde{\mathbf{x}})$ is

$$\tilde{f}_4(\tilde{x})=\tilde{x}_1\left(\tilde{x}_6{}^2+(\tilde{x}_5+\Omega)^2\cos^2\tilde{x}_3-\Omega^2\sigma\,(1-3\cos^2\tilde{x}_3\cos^2\tilde{x}_2)\right)+ L_{ref}\left(\tilde{x}_6{}^2+\left(2\Omega\tilde{x}_5+\tilde{x}_5{}^2\right)\cos^2\tilde{x}_3\right)+L_{ref}\Omega^2(-\sin^2\tilde{x}_3+3\sigma(-\sin^2\tilde{x}_2-\sin^2\tilde{x}_3+\sin^2\tilde{x}_3\sin^2\tilde{x}_2)+\ (2\sigma+1)L_{ref}\Omega^2 \tag{3.41}$$

The constant term in the Eq. (3.40), u_{L_e}, is

$$u_{L_e}=\frac{k_c(q_1q_2)_e}{m} \tag{3.42}$$

By putting all the parameters $\dot{L},\ddot{L},\psi,\dot{\psi},\ddot{\psi},\varphi,\dot{\varphi},and\ \ddot{\varphi}$ equal to zero and defining $L=L_{ref}$ in Eqs. (3.29)-(3.31), the q_1q_2 term for charges for a radially aligned two spacecraft formation is given by

$$\mathcal{Q}_{ref}=(q_1q_2)_e=-(2\sigma+1)\Omega^2\frac{L_{ref}^3}{k_c}m\left(\frac{\lambda_d}{L_{ref}+\lambda_d}\right)exp\left(\frac{L_{ref}}{\lambda_d}\right) \tag{3.43}$$

Then, the equilibrium input becomes

$$bu_{L_e}=(2\sigma+1)L_{ref}\Omega^2 \tag{3.44}$$

So, the system is conformed to the proper structure and conditions ($\tilde{\mathbf{f}}(\tilde{\mathbf{x}}) \in C^1(\Gamma)$ with $\tilde{\mathbf{f}}(\mathbf{0}) = \mathbf{0}$, without bias term) such that a suitable form for applying state dependent factorized control methods is obtained. There are many choices for SDC factorization, where the $\tilde{\mathbf{f}}(\tilde{\mathbf{x}})$ is converted to $\mathbf{A}(\tilde{\mathbf{x}})\tilde{\mathbf{x}}$. One such choice is given below.

$$\tilde{\boldsymbol{A}}(\tilde{\boldsymbol{x}}) = \begin{bmatrix} 0 & 0 & 0 & 1 & 0 & 0 \\ 0 & 0 & 0 & 0 & 1 & 0 \\ 0 & 0 & 0 & 0 & 0 & 1 \\ \tilde{A}_{41} & \tilde{A}_{42} & \tilde{A}_{43} & 0 & \tilde{A}_{45} & \tilde{A}_{46} \\ 0 & \tilde{A}_{52} & 0 & \tilde{A}_{54} & \tilde{A}_{55} & \tilde{A}_{56} \\ 0 & 0 & \tilde{A}_{63} & \tilde{A}_{64} & 0 & 0 \end{bmatrix} \tag{3.45}$$

where

$$\tilde{A}_{41} = \left(\tilde{x}_6{}^2 + (\tilde{x}_5 + \Omega)^2 \cos^2 \tilde{x}_3 - \Omega^2 \sigma \left(1 - 3\cos^2 \tilde{x}_3 \cos^2 \tilde{x}_2\right)\right)$$

$$\tilde{A}_{42} = -3L_{ref}\Omega^2\sigma \frac{\sin^2 \tilde{x}_2}{\tilde{x}_2},\ \tilde{A}_{43} = L_{ref}\Omega^2(-1 + 3\sigma(-1 + \sin^2 \tilde{x}_2)) \frac{\sin^2 \tilde{x}_3}{\tilde{x}_3}$$

$$\tilde{A}_{45} = L_{ref}(\tilde{x}_5 + 2\Omega)\cos^2 \tilde{x}_3,\ \tilde{A}_{46} = L_{ref}\tilde{x}_6,\ \tilde{A}_{54} = \frac{-2\Omega}{\tilde{x}_1 + L_{ref}}$$

$$\tilde{A}_{52} = -3\Omega^2\sigma \cos \tilde{x}_2 \frac{\sin \tilde{x}_2}{\tilde{x}_2},\ \tilde{A}_{55} = \frac{-2\tilde{x}_4}{\tilde{x}_1 + L_{ref}},\ \tilde{A}_{56} = 2(\tilde{x}_5 + \Omega)\tan \tilde{x}_3$$

$$\tilde{A}_{64} = \frac{-2\tilde{x}_6}{\tilde{x}_1 + L_{ref}},\ \tilde{A}_{63} = -((\tilde{x}_5 + \Omega)^2 + 3\Omega^2\sigma \cos^2 \tilde{x}_2)\cos \tilde{x}_3 \frac{\sin \tilde{x}_3}{\tilde{x}_3}$$

and

$$\tilde{\boldsymbol{B}}(\tilde{\boldsymbol{x}}) = \begin{bmatrix} 0 & 0 & 0 \\ 0 & 0 & 0 \\ 0 & 0 & 0 \\ b & 0 & 0 \\ 0 & \frac{1}{(\tilde{x}_1 + L_{ref})\cos^2 \tilde{x}_3} & 0 \\ 0 & 0 & \frac{1}{(\tilde{x}_1 + L_{ref})} \end{bmatrix} \tag{3.46}$$

3.1.2 Along-Track Configuration

Following the same approach presented in Sec. 3.1.1, the nonlinear equations of motion for along-track configuration for a two-craft coulomb formation at Earth-moon collinear libration points may be written as

$$\ddot{L} - L\left(\dot{\varphi}^2 + \left(\dot{\psi} + \Omega\right)^2 cos^2\,\varphi - \Omega^2\sigma\,(1 - 3\,cos^2\,\varphi\,sin^2\,\psi)\right) = \frac{Q_L}{m} \quad (3.47)$$

$$\ddot{\psi} - 2\dot{\varphi}\,tan\,\varphi\left(\dot{\psi} + \Omega\right) + 2\frac{\dot{L}}{L}\left(\dot{\psi} + \Omega\right) - 3\Omega^2\sigma\,cos\,\psi\,sin\,\psi = \frac{Q_\psi}{mL^2\,cos^2\,\varphi} \quad (3.48)$$

$$\ddot{\varphi} + 2\frac{\dot{L}}{L}\dot{\varphi} + cos\,\varphi\,sin\,\varphi\left(\left(\dot{\psi} + \Omega\right)^2 + 3\Omega^2\sigma\,sin^2\,\psi\right) = \frac{Q_\varphi}{mL^2} \quad (3.49)$$

where $Q_\varphi = F_\varphi L$, and F_φ is the electric propulsion (EP) thrusting force that introduce net formation torques in the φ direction. Note that if $\sigma = 1$, the Eqs. (3.47)-(3.49) would be exactly the same as the equations of motion for along-track configuration of a two-craft coulomb formation in Earth circular orbits. Defining the states and inputs as

$$\boldsymbol{x} = (x_1, x_2, x_3, x_4, x_5, x_6)^T = \left(L, \psi, \varphi, \dot{L}, \dot{\psi}, \dot{\varphi}\right)^T \quad (3.50)$$

$$\boldsymbol{u} = \left(u_L, u_\psi, u_\varphi\right)^T \quad (3.51)$$

By using the same procedure at the previous section, one obtains

$$\begin{bmatrix} \dot{\tilde{x}}_1 \\ \dot{\tilde{x}}_2 \\ \dot{\tilde{x}}_3 \\ \dot{\tilde{x}}_4 \\ \dot{\tilde{x}}_5 \\ \dot{\tilde{x}}_6 \end{bmatrix} = \begin{bmatrix} \tilde{x}_4 \\ \tilde{x}_5 \\ \tilde{x}_6 \\ \left(\tilde{x}_1 + L_{ref}\right)\left(\tilde{x}_6{}^2 + (\tilde{x}_5 + \Omega)^2\,cos^2\,\tilde{x}_3 - \Omega^2\sigma(1 - 3\,cos^2\,\tilde{x}_3\,sin^2\,\tilde{x}_2)\right) \\ 2\tilde{x}_6\,tan\,\tilde{x}_3\,(\tilde{x}_5 + \Omega) - 2\frac{\tilde{x}_4}{(\tilde{x}_1 + L_{ref})}(\tilde{x}_5 + \Omega) + 3\Omega^2\sigma\,cos\,\tilde{x}_2\,sin\,\tilde{x}_2 \\ -2\frac{\tilde{x}_4}{(\tilde{x}_1 + L_{ref})}\tilde{x}_6 - cos\,\tilde{x}_3\,sin\,\tilde{x}_3\,((\tilde{x}_5 + \Omega)^2 + 3\Omega^2\sigma\,sin^2\,\tilde{x}_2) \end{bmatrix} +$$

$$\begin{bmatrix} 0 & 0 & 0 \\ 0 & 0 & 0 \\ 0 & 0 & 0 \\ b & 0 & 0 \\ 0 & \frac{1}{(\tilde{x}_1 + L_{ref})\,cos^2\,\tilde{x}_3} & 0 \\ 0 & 0 & \frac{1}{(\tilde{x}_1 + L_{ref})} \end{bmatrix} \begin{bmatrix} \tilde{u}_L \\ \tilde{u}_\psi \\ \tilde{u}_\varphi \end{bmatrix} + \begin{bmatrix} 0 \\ 0 \\ 0 \\ bu_{L_e} \\ 0 \\ 0 \end{bmatrix} \quad (3.52)$$

The fourth component in Eq. (3.52) can be written as

$$\dot{\tilde{x}}_4 = \tilde{f}_4(\tilde{\boldsymbol{x}}) + b\tilde{u}_L + bu_{L_e} \quad (3.53)$$

The simplified form of $\tilde{f}_4(\tilde{\mathbf{x}})$ is given by

$$\tilde{f}_4(\tilde{\boldsymbol{x}}) = \tilde{x}_1\left(\tilde{x}_6{}^2 + (\tilde{x}_5 + \Omega)^2\, cos^2\, \tilde{x}_3 - \Omega^2\sigma(1 - 3\, cos^2\, \tilde{x}_3\, sin^2\, \tilde{x}_2)\right) + L_{ref}\left(\tilde{x}_6{}^2 + \left(2\Omega\tilde{x}_5 + \tilde{x}_5{}^2\right) cos^2\, \tilde{x}_3\right) + L_{ref}\Omega^2(-sin^2\, \tilde{x}_3 + 3\sigma(sin^2\, \tilde{x}_2 - sin^2\, \tilde{x}_3\, sin^2\, \tilde{x}_2) + (1 - \sigma)L_{ref}\Omega^2 \tag{3.54}$$

The term, u_{L_e} , is

$$u_{L_e} = \frac{k_c(q_1q_2)_e}{m} \tag{3.55}$$

where q_1q_2 for charges for an along track formation is obtained as

$$\mathcal{Q}_{ref} = (q_1q_2)_e = (\sigma - 1)\Omega^2 \frac{L_{ref}^3}{mk_c} exp\left(\frac{-L_{ref}}{\lambda_d}\right)\left(1 + \frac{L_{ref}}{\lambda_d}\right) \tag{3.56}$$

Then, the equilibrium input becomes

$$bu_{L_e} = (1 - \sigma)L_{ref}\Omega^2 \tag{3.57}$$

Again, among many choices for SDC factorization, the following is selected.

$$\tilde{\boldsymbol{A}}(\tilde{\boldsymbol{x}}) = \begin{bmatrix} 0 & 0 & 0 & 1 & 0 & 0 \\ 0 & 0 & 0 & 0 & 1 & 0 \\ 0 & 0 & 0 & 0 & 0 & 1 \\ \tilde{A}_{41} & \tilde{A}_{42} & \tilde{A}_{43} & 0 & \tilde{A}_{45} & \tilde{A}_{46} \\ 0 & \tilde{A}_{52} & 0 & \tilde{A}_{54} & \tilde{A}_{55} & \tilde{A}_{56} \\ 0 & 0 & \tilde{A}_{63} & \tilde{A}_{64} & 0 & 0 \end{bmatrix} \tag{3.58}$$

where

$$\tilde{A}_{41} = \left(\tilde{x}_6{}^2 + (\tilde{x}_5 + \Omega)^2\, cos^2\, \tilde{x}_3 - \Omega^2\sigma\, (1 - 3\, cos^2\, \tilde{x}_3\, sin^2\, \tilde{x}_2)\right)$$

$$\tilde{A}_{42} = 3L_{ref}\Omega^2\sigma\frac{sin^2\, \tilde{x}_2}{\tilde{x}_2},\ \tilde{A}_{43} = L_{ref}\Omega^2(-1 - 3\sigma\, sin^2\, \tilde{x}_2)\frac{sin^2\, \tilde{x}_3}{\tilde{x}_3}$$

$$\tilde{A}_{45} = L_{ref}(\tilde{x}_5 + 2\Omega)\, cos^2\, \tilde{x}_3,\tilde{A}_{46} = L_{ref}\tilde{x}_6,\ \tilde{A}_{52} = 3\Omega^2\sigma\, cos\, \tilde{x}_2\frac{sin\, \tilde{x}_2}{\tilde{x}_2}$$

$$\tilde{A}_{54} = \frac{-2\Omega}{\tilde{x}_1 + L_{ref}},\ \tilde{A}_{55} = \frac{-2\tilde{x}_4}{\tilde{x}_1 + L_{ref}},\ \tilde{A}_{56} = 2(\tilde{x}_5 + \Omega)\, tan\, \tilde{x}_3$$

$$\tilde{A}_{63} = -((\tilde{x}_5 + \Omega)^2 + 3\Omega^2\sigma\, sin^2\, \tilde{x}_2)\, cos\, \tilde{x}_3\frac{sin\, \tilde{x}_3}{\tilde{x}_3},\ \tilde{A}_{64} = \frac{-2\tilde{x}_6}{\tilde{x}_1 + L_{ref}}$$

The matrix $\tilde{\mathbf{B}}(\tilde{\mathbf{x}})$ is given by Eq. (3.46).

3.1.3 Orbit-Normal Configuration

The nonlinear equations of motion for orbit-normal configuration of a two-craft coulomb formation at Earth-moon collinear libration points are obtained as

$$\ddot{L} - L\left(\dot{\theta}^2 cos^2\varphi + \dot{\varphi}^2 + \Omega^2 - \Omega^2 cos^2\varphi cos^2\theta + \Omega\dot{\theta}\, sin\, 2\varphi\, cos\,\theta - 2\Omega\dot{\varphi}\, sin\,\theta\right) + \Omega^2 L\,\sigma(1 - 3\, cos^2\varphi\, sin^2\theta) = \frac{Q_L}{m} \tag{3.59}$$

$$\ddot{\theta} + 2\frac{\dot{L}}{L}\dot{\theta} - 2\dot{\varphi}\dot{\theta}\, tan\,\varphi + 2\Omega\frac{\dot{L}}{L} tan\,\varphi\, cos\,\theta + 2\Omega\dot{\varphi}\, cos\,\theta - \Omega^2\, cos\,\theta\, sin\,\theta - 3\Omega^2\sigma\, cos\,\theta\, sin\,\theta = \frac{Q_\theta}{mL^2\, cos^2\varphi} \tag{3.60}$$

$$\ddot{\varphi} + 2\frac{\dot{L}}{L}(\dot{\varphi} - \Omega\, sin\,\theta) + cos\,\varphi\, sin\,\varphi\left(\dot{\theta}^2 - \Omega^2 cos^2\theta + 3\Omega^2\sigma\, sin^2\theta\right) - 2\Omega\dot{\theta}\, cos^2\varphi\, cos\,\theta = \frac{Q_\varphi}{mL^2} \tag{3.61}$$

Note that if $\sigma = 1$, the Eqs. (3.59)-(3.61) would be exactly the same as the equations of motion for orbit-normal configuration of a two-craft coulomb formation in Earth circular orbit. Define new states and inputs as

$$\boldsymbol{x} = (x_1, x_2, x_3, x_4, x_5, x_6)^T = \left(L, \theta, \varphi, \dot{L}, \dot{\theta}, \dot{\varphi}\right)^T \tag{3.62}$$

$$\boldsymbol{u} = \left(u_L, u_\theta, u_\varphi\right)^T \tag{3.63}$$

The following equations are obtained

$$\begin{bmatrix}\dot{\tilde{x}}_1\\ \dot{\tilde{x}}_2\\ \dot{\tilde{x}}_3\\ \dot{\tilde{x}}_4\\ \dot{\tilde{x}}_5\\ \dot{\tilde{x}}_6\end{bmatrix} = \begin{bmatrix} \tilde{x}_4 \\ \tilde{x}_5 \\ \tilde{x}_6 \\ (\tilde{x}_1 + L_{ref})\begin{pmatrix} \tilde{x}_5{}^2 \cos^2\tilde{x}_3 + \tilde{x}_6{}^2 + \Omega^2(1-\cos^2\tilde{x}_3\cos^2\tilde{x}_2) + \\ \Omega\tilde{x}_5 \sin 2\tilde{x}_3 \cos\tilde{x}_2 - 2\Omega\tilde{x}_6 \sin\tilde{x}_2 - \\ \Omega^2\sigma(1-3\cos^2\tilde{x}_3\sin^2\tilde{x}_2 \end{pmatrix} \\ \begin{pmatrix} -2\frac{\tilde{x}_4}{(\tilde{x}_1+L_{ref})}\tilde{x}_5 + 2\tilde{x}_6\tilde{x}_5 tan\tilde{x}_3 - 2\Omega\frac{\tilde{x}_4}{(\tilde{x}_1+L_{ref})}tan\tilde{x}_3\cos\tilde{x}_2 - \\ 2\Omega\tilde{x}_6\cos\tilde{x}_2 + \Omega^2\cos\tilde{x}_2\sin\tilde{x}_2\,(1+3\sigma) \end{pmatrix} \\ \begin{pmatrix} -2\frac{\tilde{x}_4}{(\tilde{x}_1+L_{ref})}(\tilde{x}_6 - \Omega\sin\tilde{x}_2) - \\ \cos\tilde{x}_3\sin\tilde{x}_3\left(\tilde{x}_5{}^2 - \Omega^2\cos^2\tilde{x}_2 + 3\Omega^2\sigma\sin^2\tilde{x}_2\right) + \\ 2\Omega\tilde{x}_5\cos^2\tilde{x}_3\cos\tilde{x}_2 \end{pmatrix} \end{bmatrix} + \begin{bmatrix} 0 & 0 & 0 \\ 0 & 0 & 0 \\ 0 & 0 & 0 \\ b & 0 & 0 \\ 0 & \frac{1}{(\tilde{x}_1+L_{ref})\cos^2\tilde{x}_3} & 0 \\ 0 & 0 & \frac{1}{(\tilde{x}_1+L_{ref})} \end{bmatrix}\begin{bmatrix}\tilde{u}_L\\ \tilde{u}_\theta\\ \tilde{u}_\varphi\end{bmatrix} + \begin{bmatrix} 0\\0\\0\\bu_{L_e}\\0\\0\end{bmatrix} \tag{3.64}$$

Here $q_1 q_2$ for charges for an orbit normal configuration becomes

$$Q_{ref} = (q_1 q_2)_{orbit-normal} = \sigma\,\Omega^2\frac{L_{ref}^3}{mk_c}exp\left(\frac{-L_{ref}}{\lambda_d}\right)\left(1+\frac{L_{ref}}{\lambda_d}\right) \tag{3.65}$$

By following the similar procedures that is used in Sec. 3.1.1, we have

$$\widetilde{\boldsymbol{A}}(\tilde{\boldsymbol{x}}) = \begin{bmatrix} 0 & 0 & 0 & 1 & 0 & 0 \\ 0 & 0 & 0 & 0 & 1 & 0 \\ 0 & 0 & 0 & 0 & 0 & 1 \\ \tilde{A}_{41} & \tilde{A}_{42} & \tilde{A}_{43} & 0 & \tilde{A}_{45} & \tilde{A}_{46} \\ 0 & \tilde{A}_{52} & 0 & \tilde{A}_{54} & \tilde{A}_{55} & \tilde{A}_{56} \\ 0 & \tilde{A}_{62} & 0 & \tilde{A}_{64} & \tilde{A}_{65} & 0 \end{bmatrix} \tag{3.66}$$

where

$$\tilde{A}_{41} = \begin{pmatrix} \tilde{x}_5{}^2\cos^2\tilde{x}_3 + \tilde{x}_6{}^2 + \Omega^2(1-\cos^2\tilde{x}_3\cos^2\tilde{x}_2) + \Omega\tilde{x}_5\sin 2\tilde{x}_3\cos\tilde{x}_2 - 2\Omega\tilde{x}_6\sin\tilde{x}_2 - \\ \Omega^2\sigma(1-3\cos^2\tilde{x}_3\sin^2\tilde{x}_2) \end{pmatrix}$$

$$\tilde{A}_{42} = \left(L_{ref}\Omega^2\right)(3\sigma\cos^2\tilde{x}_3\sin^2\tilde{x}_2 - \sin^2\tilde{x}_3\sin^2\tilde{x}_2 + \sin^2\tilde{x}_2)/\tilde{x}_2$$

$$\tilde{A}_{43} = L_{ref}\Omega^2\frac{\sin^2\tilde{x}_3}{\tilde{x}_3},\ \tilde{A}_{45} = L_{ref}(\tilde{x}_5)\cos^2\tilde{x}_3 + L_{ref}\Omega\sin 2\tilde{x}_3\cos\tilde{x}_2$$

$$\tilde{A}_{46} = L_{ref}(\tilde{x}_6 - 2\Omega \sin \tilde{x}_2),\ \tilde{A}_{52} = \Omega^2 \cos \tilde{x}_2\,(1+3\sigma)\frac{\sin \tilde{x}_2}{\tilde{x}_2}$$

$$\tilde{A}_{54} = \frac{-2\tilde{x}_5}{\tilde{x}_1 + L_{ref}} - 2\Omega \frac{1}{\tilde{x}_1 + L_{ref}} tan\tilde{x}_3 \cos \tilde{x}_2,\ \tilde{A}_{55} = 2\tilde{x}_6 \tan \tilde{x}_3,\ \tilde{A}_{56} = -2\Omega \cos \tilde{x}_2,$$

$$\tilde{A}_{63} = -((\tilde{x}_5)^2 - \Omega^2 \cos^2 \tilde{x}_2 + 3\Omega^2 \sigma \sin^2 \tilde{x}_2) \cos \tilde{x}_3 \frac{\sin \tilde{x}_3}{\tilde{x}_3}$$

$$\tilde{A}_{64} = \frac{-2(\tilde{x}_6 - \Omega \sin \tilde{x}_2)}{\tilde{x}_1 + L_{ref}},\ \tilde{A}_{65} = 2\Omega \cos \tilde{x}_2 \cos^2 \tilde{x}_3$$

In addition, the matrix $\widetilde{\mathbf{B}}(\tilde{\mathbf{x}})$ is the same as given in Eq. (3.46).

3.2 Orbit-Radial Configuration at Earth-Moon Triangular Libration Points

The nonlinear equations of motion of an orbit-radially aligned two-craft Coulomb formation at Earth-moon triangular libration point is derived and discussed in this section. The procedure is similar to that presented in Sec. 3.1.1. The formation center of mass is located at triangular libration point L_4 as shown in Figure 4. The planar position of the point L_4 in the Synodic frame $\mathcal{S}$ is given by $(X_0, Y_0, 0)$. The planar position vector of the libration point L_4 from the two primaries in the Synodic frame becomes

$$\boldsymbol{R}_1 = (X_0 + D_1)\hat{\boldsymbol{e}}_1 + Y_0\hat{\boldsymbol{e}}_2 + 0\hat{\boldsymbol{e}}_3 \tag{3.67}$$

$$\boldsymbol{R}_2 = (X_0 - D_2)\hat{\boldsymbol{e}}_1 + Y_0\hat{\boldsymbol{e}}_2 + 0\hat{\boldsymbol{e}}_3 \tag{3.68}$$

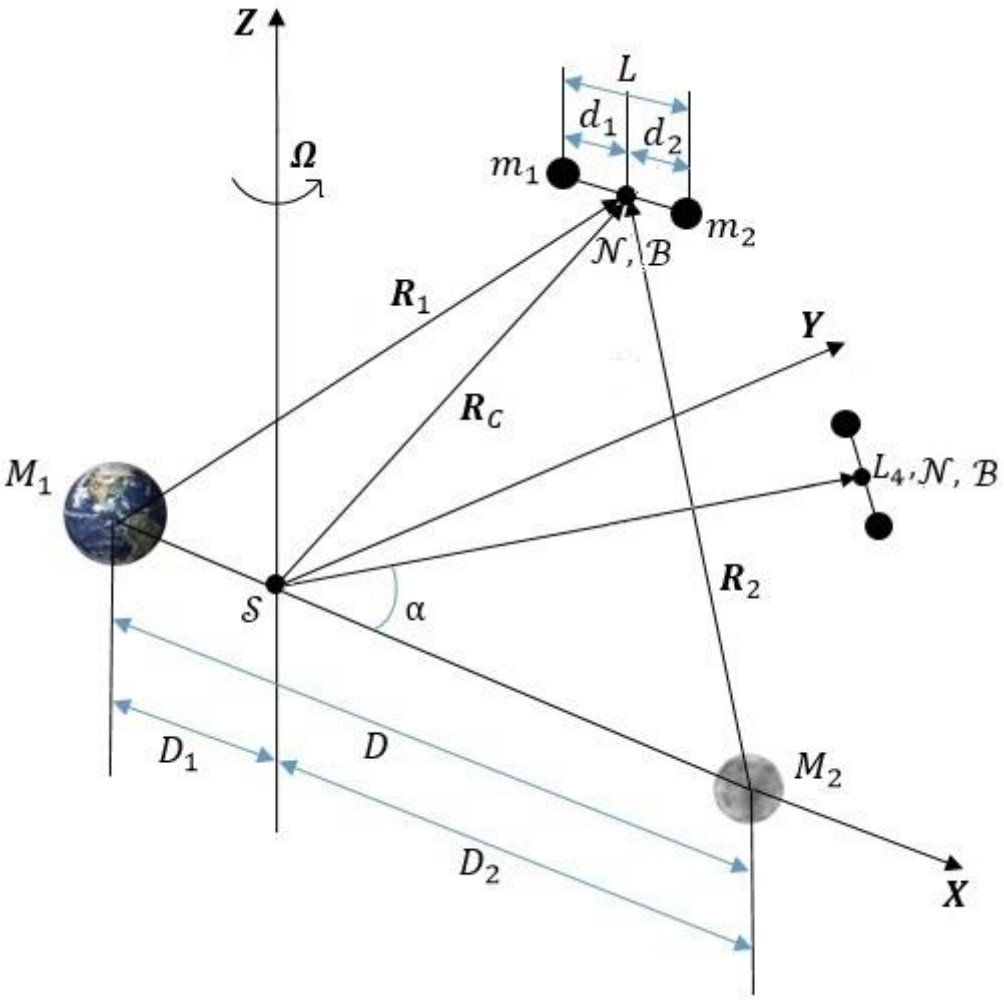

Figure 4. Formation configuration at Earth-moon triangular libration point.

The kinetic energy and Coulomb potential energy equations are the same as those represented in Sec. 3.1.1. However, the gravitational potential energy is different from that represented in Eq. (3.17) because the vector $\boldsymbol{R}_i$ is in Synodic frame and $\boldsymbol{d}_i$ is given in Hill's frame. Since the Synodic frame and Hill's frame are not aligned to each other in this section, it is necessary to convert the $\boldsymbol{R}_i$ vector from Synodic to Hill coordinate system using the transformation matrix

$$C^{\mathcal{N}/\mathcal{S}} = \begin{bmatrix} cos\,\alpha & sin\,\alpha & 0 \\ -sin\,\alpha & cos\,\alpha & 0 \\ 0 & 0 & 1 \end{bmatrix} \tag{3.69}$$

So, the planar position vector of the libration point L_4 from the two primaries in the Hill's frame becomes

$$\boldsymbol{R}_1 = \big((X_0 + D_1)\cos\alpha + Y_0 \sin\alpha\big)\hat{\boldsymbol{n}}_1 + (-(X_0 + D_1)\sin\alpha + Y_0\cos\alpha)\hat{\boldsymbol{n}}_2 + 0\hat{\boldsymbol{n}}_3 \quad (3.70)$$

$$\boldsymbol{R}_2 = \big((X_0 - D_2)\cos\alpha + Y_0 \sin\alpha\big)\hat{\boldsymbol{n}}_1 + (-(X_0 - D_2)\sin\alpha + Y_0\cos\alpha)\hat{\boldsymbol{n}}_2 + 0\hat{\boldsymbol{n}}_3 \quad (3.71)$$

where the magnitudes of the vectors are

$$R_1 = |\boldsymbol{R}_1| = D \quad (3.72)$$

$$R_2 = |\boldsymbol{R}_2| = D \quad (3.73)$$

For the triangular libration point L_4, we have [40]

$$X_0 = (\rho - 0.5)D \quad (3.74)$$

$$Y_0 = \frac{\sqrt{3}}{2}D \quad (3.75)$$

The nonlinear equations of motion for a two-craft coulomb formation at Earth-moon triangular libration points in orbit-radial configuration become

$$\ddot{L} - L\left(\dot{\theta}^2 + \left(\dot{\psi} + \Omega\right)^2 \cos^2\theta - \Omega^2\right) - \frac{3}{4}L\Omega^2\cos^2\theta\left((1-\rho)(A_\alpha\cos\psi + B_\alpha\sin\psi)^2 + \rho(C_\alpha\cos\psi + D_\alpha\sin\psi)^2\right) = \frac{Q_L}{m} \quad (3.76)$$

$$\ddot{\psi} - 2\dot{\theta}\tan\theta\left(\dot{\psi} + \Omega\right) + 2\frac{\dot{L}}{L}\left(\dot{\psi} + \Omega\right) - \frac{3}{4}\Omega^2\left((1-\rho)\left(A_\alpha B_\alpha\cos 2\psi + \frac{B_\alpha^2 - A_\alpha^2}{2}\sin 2\psi\right) + \rho\left(C_\alpha D_\alpha\cos 2\psi + \frac{D_\alpha^2 - C_\alpha^2}{2}\sin 2\psi\right)\right) = \frac{Q_\psi}{mL^2\cos^2\theta} \quad (3.77)$$

$$\ddot{\theta} + 2\frac{\dot{L}}{L}\dot{\theta} + \cos\theta\sin\theta\left(\left(\dot{\psi} + \Omega\right)^2 + \frac{3}{4}\Omega^2\big((1-\rho)(A_\alpha\cos\psi + B_\alpha\sin\psi)^2 + \rho(C_\alpha\cos\psi + D_\alpha\sin\psi)^2\big)\right) = \frac{Q_\theta}{mL^2} \quad (3.78)$$

where

$A_\alpha = cos\alpha + \sqrt{3}sin\alpha$ $\qquad$ $C_\alpha = -cos\alpha + \sqrt{3}sin\alpha$

$B_\alpha = -sin\alpha + \sqrt{3}cos\alpha$ $\qquad$ $D_\alpha = sin\alpha + \sqrt{3}cos\alpha$

Now by using the new state and control variables defined in the Eqs. (3.34)-(3.38) , one may get

$$\begin{bmatrix}\dot{\tilde{x}}_1\\ \dot{\tilde{x}}_2\\ \dot{\tilde{x}}_3\\ \dot{\tilde{x}}_4\\ \dot{\tilde{x}}_5\\ \dot{\tilde{x}}_6\end{bmatrix} =$$

$$\begin{bmatrix} \tilde{x}_4 \\ \tilde{x}_5 \\ \tilde{x}_6 \\ \left(\tilde{x}_1 + L_{ref}\right)\begin{pmatrix} (\tilde{x}_6^2 + (\tilde{x}_5 + \Omega)^2 \cos^2 \tilde{x}_3 - \Omega^2) + \\ \frac{3}{4}\Omega^2 \cos^2 \tilde{x}_3 \begin{pmatrix} (1-\rho)(A_\alpha \cos \tilde{x}_2 + B_\alpha \sin \tilde{x}_2)^2 + \\ \rho(C_\alpha \cos \tilde{x}_2 + D_\alpha \sin \tilde{x}_2)^2 \end{pmatrix} \end{pmatrix} \\ \begin{pmatrix} 2\tilde{x}_6 \tan \tilde{x}_3 \,(\tilde{x}_5 + \Omega) - 2\frac{\tilde{x}_4}{(\tilde{x}_1 + L_{ref})}(\tilde{x}_5 + \Omega) + \\ \frac{3}{4}\Omega^2 \begin{pmatrix} (1-\rho)\left(A_\alpha B_\alpha \cos 2\tilde{x}_2 + \frac{B_\alpha^2 - A_\alpha^2}{2} \sin 2\tilde{x}_2\right) + \\ \rho\left(C_\alpha D_\alpha \cos 2\tilde{x}_2 + \frac{D_\alpha^2 - C_\alpha^2}{2} \sin 2\tilde{x}_2\right) \end{pmatrix} \end{pmatrix} \\ -2\frac{\tilde{x}_4}{(\tilde{x}_1 + L_{ref})}\tilde{x}_6 - \cos \tilde{x}_3 \sin \tilde{x}_3 \begin{pmatrix} (\tilde{x}_5 + \Omega)^2 + \\ \frac{3}{4}\Omega^2 \begin{pmatrix} (1-\rho)(A_\alpha \cos \tilde{x}_2 + B_\alpha \sin \tilde{x}_2)^2 + \\ \rho(C_\alpha \cos \tilde{x}_2 + D_\alpha \sin \tilde{x}_2)^2 \end{pmatrix} \end{pmatrix} \end{bmatrix} +$$

$$\begin{bmatrix} 0 & 0 & 0 \\ 0 & 0 & 0 \\ 0 & 0 & 0 \\ b & 0 & 0 \\ 0 & \frac{1}{(\tilde{x}_1 + L_{ref})\cos^2 \tilde{x}_3} & 0 \\ 0 & 0 & \frac{1}{(\tilde{x}_1 + L_{ref})} \end{bmatrix} \begin{bmatrix} \tilde{u}_L \\ \tilde{u}_\theta \\ \tilde{u}_\varphi \end{bmatrix} + \begin{bmatrix} 0 \\ 0 \\ 0 \\ bu_{L_e} \\ 0 \\ 0 \end{bmatrix} \tag{3.79}$$

The fourth component in Eq. (3.79) can be shown as

$$\dot{\tilde{x}}_4 = \tilde{f}_4(\tilde{\mathbf{x}}) + b\tilde{u}_L + bu_{L_e} \tag{3.80}$$

The simplified form of $\tilde{f}_4(\tilde{\mathbf{x}})$ is given by

$$\tilde{f}_4(\tilde{\mathbf{x}}) = \tilde{x}_1(\tilde{x}_6^2 + (\tilde{x}_5 + \Omega)^2 \cos^2 \tilde{x}_3 - \Omega^2) + \frac{3}{4}\tilde{x}_1\Omega^2 \cos^2 \tilde{x}_3 \left((1-\rho)(A_\alpha \cos \tilde{x}_2 + B_\alpha \sin \tilde{x}_2)^2 + \rho(C_\alpha \cos \tilde{x}_2 + D_\alpha \sin \tilde{x}_2)^2\right) + L_{ref}(\tilde{x}_6^2 + (\tilde{x}_5^2 + 2\tilde{x}_5\Omega)\cos^2 \tilde{x}_3) + \frac{3}{4}L_{ref}\Omega^2 \cos^2 \tilde{x}_3 \left((1-\rho)(A_\alpha B_\alpha \sin 2\tilde{x}_2 + B_\alpha^2 \sin^2 \tilde{x}_2) + \rho(C_\alpha D_\alpha \sin 2\tilde{x}_2 + D_\alpha^2 \sin^2 \tilde{x}_2)\right) + L_{ref}\Omega^2 \sin^2 \tilde{x}_3 \left(-1 - \frac{3}{4}(1 - \sin^2 \tilde{x}_2)(A_\alpha^2 - \rho A_\alpha^2 + \rho C_\alpha^2)\right) + \frac{3}{4}L_{ref}\Omega^2 \sin^2 \tilde{x}_2 (-A_\alpha^2 + \rho A_\alpha^2 - \rho C_\alpha^2) + \frac{3}{4}L_{ref}\Omega^2 \left(1 + 2\sin^2 \alpha + \sqrt{3}\sin 2\alpha\,(1 - 2\rho)\right) \tag{3.81}$$

The constant term in the Eq. (3.80), u_{L_e} , is

$$u_{L_e} = \frac{k_c (q_1 q_2)_e}{m} \tag{3.82}$$

where $q_1 q_2$ for charges for a radially aligned two spacecraft formation is obtained as

$$Q_{ref} = (q_1 q_2)_e = -\frac{3}{4}\Big(1 + 2\,sin^2\,\alpha + \sqrt{3}\,sin\,2\alpha\,(1 - 2\rho)\Big)\,\Omega^2\,\frac{L_{ref}^3}{k_c}\,m\left(\frac{\lambda_d}{L_{ref}+\lambda_d}\right)exp\left(\frac{L_{ref}}{\lambda_d}\right) \tag{3.83}$$

Then, the equilibrium input becomes

$$bu_{L_e} = \frac{3}{4}L_{ref}\Omega^2\left(1 + 2\,sin^2\,\alpha + \sqrt{3}\,sin\,2\alpha\,(1 - 2\rho)\right) \tag{3.84}$$

Substituting Eqs. (3.81) & (3.84) into Eq.(3.80), the constant terms cancel each other.

The fifth component of Eq. (3.79) may be simplified as

$$\tilde{f}_5(\tilde{\boldsymbol{x}}) = 2\tilde{x}_6\,tan\,\tilde{x}_3\,(\tilde{x}_5 + \Omega) - 2\,\frac{\tilde{x}_4}{(\tilde{x}_1+L_{ref})}\,(\tilde{x}_5 + \Omega) + \frac{3}{4}\Omega^2\left((1 - \rho)\left(-2A_\alpha B_\alpha\,sin^2\,\tilde{x}_2 + \frac{B_\alpha^2 - A_\alpha^2}{2}\,sin\,2\tilde{x}_2\right) + \rho\left(-2C_\alpha D_\alpha\,sin^2\,\tilde{x}_2 + \frac{D_\alpha^2 - C_\alpha^2}{2}\,sin\,2\tilde{x}_2\right)\right) + \frac{3}{4}\Omega^2\left(sin\,2\alpha + \sqrt{3}\,cos\,2\alpha\,(1 - 2\rho)\right) \tag{3.85}$$

The last term in Eq. (3.85) is a constant term and its value is

$$\frac{3}{4}\Omega^2\left(sin\,2\alpha + \sqrt{3}\,cos\,2\alpha\,(1 - 2\rho)\right) = -0.108421 \times 10^{-14} \tag{3.86}$$

and its effect is negligible on the differential equations and will be dropped from the equation. There are many choices for SDC factorization where the term $\tilde{\mathbf{f}}(\tilde{\mathbf{x}})$ is converted to $\mathbf{A(x)x}$. One such choice, which is used in the numerical simulations, is given as

$$\tilde{\boldsymbol{A}}(\tilde{\boldsymbol{x}}) = \begin{bmatrix} 0 & 0 & 0 & 1 & 0 & 0 \\ 0 & 0 & 0 & 0 & 1 & 0 \\ 0 & 0 & 0 & 0 & 0 & 1 \\ \tilde{A}_{41} & \tilde{A}_{42} & \tilde{A}_{43} & 0 & \tilde{A}_{45} & \tilde{A}_{46} \\ 0 & \tilde{A}_{52} & 0 & \tilde{A}_{54} & 0 & \tilde{A}_{56} \\ 0 & 0 & \tilde{A}_{63} & \tilde{A}_{64} & 0 & 0 \end{bmatrix} \tag{3.87}$$

where

$\tilde{A}_{41} = (\tilde{x}_6^2 + (\tilde{x}_5 + \Omega)^2 \cos^2 \tilde{x}_3 - \Omega^2) + \frac{3}{4}\Omega^2 \cos^2 \tilde{x}_3 \big((1-\rho)(A_\alpha \cos \tilde{x}_2 + B_\alpha \sin \tilde{x}_2)^2 + \rho(C_\alpha \cos \tilde{x}_2 + D_\alpha \sin \tilde{x}_2)^2\big)$,

$\tilde{A}_{42} = \frac{3}{4} L_{ref} \Omega^2 \cos^2 \tilde{x}_3 \big((1-\rho)(2A_\alpha B_\alpha \cos \tilde{x}_2 + B_\alpha^2 \sin \tilde{x}_2) + \rho(2C_\alpha D_\alpha \cos \tilde{x}_2 + D_\alpha^2 \sin \tilde{x}_2)\big) \frac{\sin \tilde{x}_2}{\tilde{x}_2} + \frac{3}{4} L_{ref} \Omega^2 \sin \tilde{x}_2 \, (-A_\alpha^2 + \rho A_\alpha^2 - \rho C_\alpha^2) \frac{\sin \tilde{x}_2}{\tilde{x}_2}$,

$\tilde{A}_{43} = L_{ref} \Omega^2 \left(-1 - \frac{3}{4}(1 - \sin^2 \tilde{x}_2)(A_\alpha^2 - \rho A_\alpha^2 + \rho C_\alpha^2)\right) \frac{\sin^2 \tilde{x}_3}{\tilde{x}_3}$,

$\tilde{A}_{45} = L_{ref}(\tilde{x}_5 + 2\Omega) \cos^2 \tilde{x}_3$, $\tilde{A}_{46} = L_{ref} \tilde{x}_6$

$\tilde{A}_{52} = \frac{3}{4}\Omega^2 \big((1-\rho)(-2A_\alpha B_\alpha \sin \tilde{x}_2 + (B_\alpha^2 - A_\alpha^2) \cos \tilde{x}_2) + \rho(-2C_\alpha D_\alpha \sin \tilde{x}_2 + (D_\alpha^2 - C_\alpha^2) \cos \tilde{x}_2)\big) \frac{\sin \tilde{x}_2}{\tilde{x}_2}$,

$\tilde{A}_{54} = \frac{-2(\tilde{x}_5 + \Omega)}{\tilde{x}_1 + L_{ref}}$, $\tilde{A}_{56} = 2(\tilde{x}_5 + \Omega) \tan \tilde{x}_3$, $\tilde{A}_{64} = \frac{-2\tilde{x}_6}{\tilde{x}_1 + L_{ref}}$

$\tilde{A}_{63} = -\cos \tilde{x}_3 \left((\tilde{x}_5 + \Omega)^2 + \frac{3}{4}\Omega^2 \big((1-\rho)(A_\alpha \cos \tilde{x}_2 + B_\alpha \sin \tilde{x}_2)^2 + \rho(C_\alpha \cos \tilde{x}_2 + D_\alpha \sin \tilde{x}_2)^2\big)\right) \frac{\sin \tilde{x}_3}{\tilde{x}_3}$,

In addition, the matrix $\widetilde{\mathbf{B}}(\tilde{\mathbf{x}})$ is the same as given in Eq. (3.46).

CHATER 4

THREE-CRAFT EQUATIONS OF MOTION AND SDC FACTORIZATIONS AT DEEP SPACE

4.1 Planar Three Bodies Dynamic

The notation presented here is similar to that used in [12]. Consider a formation of three charged craft operating in deep space as shown in Figure 5.

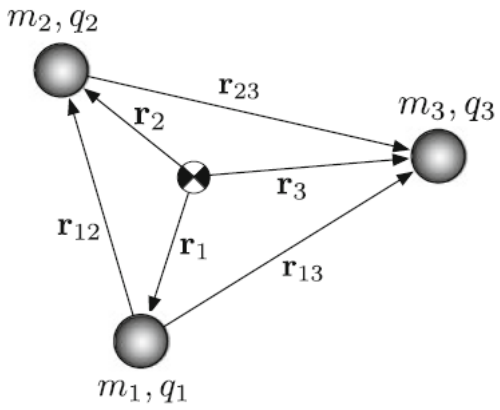

Figure 5. Three-craft Coulomb formation [12].

Also, consider a collinear configuration of craft, as shown in Figure 6.

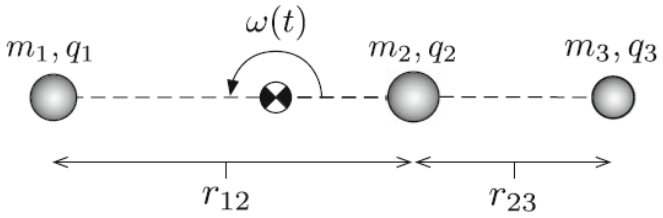

Figure 6. Collinear invariant shape Coulomb formation [12].

The frame $\mathcal{B}$: $\{\hat{b}_1, \hat{b}_2, \hat{b}_3\}$ is aligned such that the craft 1 is confined to the $\hat{b}_1$ axis for all time, while the craft 2 and 3 are free to move about in the $\hat{b}_1 - \hat{b}_2$ plane. The origin of the $\mathcal{B}$ frame is aligned with the center of mass of the formation, and the frame rotates about this point as craft 1 moves around the center of mass. This configuration is shown in Figure 7. Here, only planar dynamics are derived. The angular velocity of the $\mathcal{B}$ frame relative to the inertial frame is, $\omega^{\mathcal{B}/\mathcal{N}} = \dot{\theta}\hat{b}_3$.

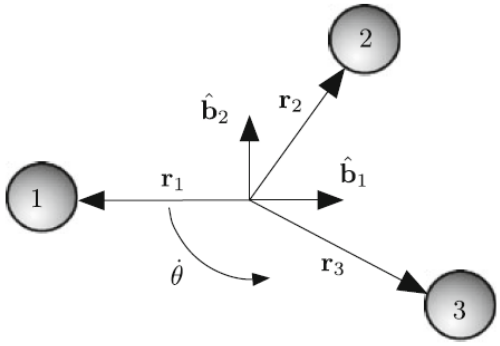

Figure 7. The rotating B frame

In the absence of plasma shielding effects, the Coulomb forces experienced on craft 'i' is expressed as

$$\boldsymbol{F}_i = \sum_{j=1, j\neq i}^{3} k_c \frac{q_i q_j}{r_{ij}^2} \hat{e}_{ji} \tag{4.1}$$

Where $k_c = 8.99\times10^9 Nm/\mathrm{C}^2$ is the Coulomb constant, q_i is the charge on craft i, and $\hat{e}_{ji}$ is the unit vector from craft j to craft i.

The nonlinear equations of motion for craft 1, 2 and 3 in a planar 3-body dynamic configuration may be written as [12]

$$\ddot{x}_1 = \frac{k_c q_1}{m_1}\left(q_2 \frac{x_1 - x_2}{r_{12}^3} + q_3 \frac{x_1 - x_3}{r_{13}^3}\right) + x_1\dot{\theta}^2 \tag{4.2}$$

$$\ddot{\theta} = -\frac{k_c q_1}{m_1 x_1}\left(q_2 \frac{y_2}{r_{12}^3} + q_3 \frac{y_3}{r_{13}^3}\right) - \frac{2\dot{\theta}\dot{x}_1}{x_1} \tag{4.3}$$

$$\ddot{x}_2 = \frac{k_c q_2}{m_2}\left(q_1 \frac{x_2 - x_1}{r_{12}^3} + q_3 \frac{x_2 - x_3}{r_{13}^3}\right) \tag{4.4}$$

$$\ddot{y}_2 = \frac{k_c q_2}{m_2}\left(q_1 \frac{y_2}{r_{12}^3} + q_3 \frac{y_2 - y_3}{r_{23}^3}\right) + y_2\dot{\theta}^2 - x_2\ddot{\theta} - 2\dot{x}_2\dot{\theta} \tag{4.5}$$

$$\ddot{x}_3 = \frac{k_c q_3}{m_3}\left(q_1 \frac{x_3 - x_1}{r_{13}^3} + q_2 \frac{x_3 - x_2}{r_{23}^3}\right) + x_3\dot{\theta}^2 + y_3\ddot{\theta} + 2\dot{y}_3\dot{\theta} \tag{4.6}$$

$$\ddot{y}_3 = \frac{k_c q_3}{m_3}\left(q_1 \frac{y_3}{r_{13}^3} + q_2 \frac{y_3 - y_2}{r_{23}^3}\right) + y_3\dot{\theta}^2 - x_3\ddot{\theta} - 2\dot{x}_3\dot{\theta} \tag{4.7}$$

Note that these equations imply an 11-dimensional state space, described by the state variables

$$\boldsymbol{x} = \left(x_1, \dot{x}_1, x_2, \dot{x}_2, y_2, \dot{y}_2, x_3, \dot{x}_3, y_3, \dot{y}_3, \dot{\theta}\right)^T \tag{4.8}$$

The inputs are defined as

$$\boldsymbol{u} = (u_1, u_2, u_3)^T = (k_c q_1 q_2, k_c q_2 q_3, k_c q_1 q_3)^T \tag{4.9}$$

By using the states and inputs defined above, the equations of motion may be written in state space form as

$$\dot{\boldsymbol{x}} = \begin{bmatrix} 0 & 1 & 0 & 0 & 0 & 0 & 0 & 0 & 0 & 0 & 0 \\ \dot{\theta}^2 & 0 & 0 & 0 & 0 & 0 & 0 & 0 & 0 & 0 & 0 \\ 0 & 0 & 0 & 1 & 0 & 0 & 0 & 0 & 0 & 0 & 0 \\ 0 & 0 & \dot{\theta}^2 & -\frac{2\dot{\theta}\dot{x}_1}{x_1} & 0 & 0 & 0 & 0 & 0 & 0 & 2\dot{y}_2 \\ 0 & 0 & 0 & 0 & 0 & 1 & 0 & 0 & 0 & 0 & 0 \\ 0 & 0 & \frac{2\dot{\theta}\dot{x}_1}{x_1} & 0 & \dot{\theta}^2 & 0 & 0 & 0 & 0 & 0 & -2\dot{x}_2 \\ 0 & 0 & 0 & 0 & 0 & 0 & 0 & 1 & 0 & 0 & 0 \\ 0 & 0 & 0 & 0 & 0 & 0 & \dot{\theta}^2 & 0 & -\frac{2\dot{\theta}\dot{x}_1}{x_1} & 2\dot{\theta} & 0 \\ 0 & 0 & 0 & 0 & 0 & 0 & 0 & 0 & 0 & 1 & 0 \\ 0 & 0 & 0 & 0 & 0 & 0 & \frac{2\dot{\theta}\dot{x}_1}{x_1} & -2\dot{\theta} & \dot{\theta}^2 & 0 & 0 \\ 0 & 0 & 0 & 0 & 0 & 0 & 0 & 0 & 0 & 0 & -\frac{2\dot{x}_1}{x_1} \end{bmatrix} \begin{bmatrix} x_1 \\ \dot{x}_1 \\ x_2 \\ \dot{x}_2 \\ y_2 \\ \dot{y}_2 \\ x_3 \\ \dot{x}_3 \\ y_3 \\ \dot{y}_3 \\ \dot{\theta} \end{bmatrix} +$$

$$\begin{bmatrix} 0 & 0 & 0 \\ \frac{1}{m_1}\left(\frac{x_1-x_2}{r_{12}^3}\right) & 0 & \frac{1}{m_1}\left(\frac{x_1-x_3}{r_{13}^3}\right) \\ 0 & 0 & 0 \\ \frac{1}{m_2}\left(\frac{x_2-x_1}{r_{12}^3}\right) - \frac{1}{m_1 x_1}\left(\frac{y_2^2}{r_{12}^3}\right) & \frac{1}{m_2}\left(\frac{x_2-x_3}{r_{23}^3}\right) & -\frac{1}{m_1 x_1}\left(\frac{y_2 y_3}{r_{13}^3}\right) \\ 0 & 0 & 0 \\ \frac{1}{m_2}\left(\frac{y_2}{r_{12}^3}\right) + \frac{x_2}{m_1 x_1}\left(\frac{y_2}{r_{12}^3}\right) & \frac{1}{m_2}\left(\frac{y_2-y_3}{r_{23}^3}\right) & \frac{x_2}{m_1 x_1}\left(\frac{y_3}{r_{13}^3}\right) \\ 0 & 0 & 0 \\ -\frac{1}{m_1 x_1}\left(\frac{y_2 y_3}{r_{12}^3}\right) & \frac{1}{m_3}\left(\frac{x_3-x_2}{r_{23}^3}\right) & \frac{1}{m_3}\left(\frac{x_3-x_1}{r_{13}^3}\right) - \frac{1}{m_1 x_1}\left(\frac{y_3^2}{r_{13}^3}\right) \\ 0 & 0 & 0 \\ \frac{1}{m_1 x_1}\left(\frac{x_3 y_2}{r_{12}^3}\right) & \frac{1}{m_3}\left(\frac{y_3-y_2}{r_{23}^3}\right) & \frac{1}{m_3}\left(\frac{y_3}{r_{13}^3}\right) + \frac{1}{m_1 x_1}\left(\frac{x_3 y_3}{r_{13}^3}\right) \\ -\frac{1}{m_1 x_1}\left(\frac{y_2}{r_{12}^3}\right) & 0 & -\frac{1}{m_1 x_1}\left(\frac{y_3}{r_{13}^3}\right) \end{bmatrix} \begin{bmatrix} u_1 \\ u_2 \\ u_3 \end{bmatrix} \tag{4.10}$$

4.2 SDC Factorization Form

The above formulation is applicable if, $\mathbf{f}(0) = \mathbf{0}$. Thus, a state dependent factorization is necessary while making sure that, $\mathbf{f}(0) = \mathbf{0}$. However, an investigation of Eq. (4.10) indicates that there are singularities when $\mathbf{x} = 0$. This problem can be solved by considering

$$\dot{\boldsymbol{x}} = \boldsymbol{F}(\boldsymbol{x}, \boldsymbol{u}) \;\rightarrow\; \boldsymbol{F}(\boldsymbol{x}_e, \boldsymbol{u}_e) = \mathbf{0} \tag{4.11}$$

$$\boldsymbol{x}_e = \left(x_{1_e}, 0, x_{2_e}, 0,0,0, x_{3_e}, 0,0,0, \dot{\theta}_e\right)^T \quad , \quad \boldsymbol{u}_e = \left(u_{1_e}, u_{2_e}, u_{3_e}\right)^T \tag{4.12}$$

and defining new variables, $\tilde{\mathbf{x}} = \mathbf{x} - \mathbf{x}_e$, and $\tilde{\mathbf{u}} = \mathbf{u} - \mathbf{u}_e$, we have

$$\dot{\tilde{\boldsymbol{x}}} = \tilde{\boldsymbol{F}}(\tilde{\boldsymbol{x}} + \boldsymbol{x}_e, \tilde{\boldsymbol{u}} + \boldsymbol{u}_e) \tag{4.13}$$

Considering a reference separation distance between three spacecraft, Eq. (4.10) may be written as

$$\dot{\tilde{\boldsymbol{x}}} = \tilde{\boldsymbol{A}}(\tilde{\boldsymbol{x}})\tilde{\boldsymbol{x}} + \tilde{\boldsymbol{B}}(\tilde{\boldsymbol{x}})\tilde{\boldsymbol{u}} \tag{4.14}$$

There are infinite numbers of choices for SDC factorization. One such choice is given below.

$$\tilde{\boldsymbol{A}}(\tilde{\boldsymbol{x}}) = \begin{bmatrix} 0 & 1 & 0 & 0 & 0 & 0 & 0 & 0 & 0 & 0 & 0 \\ \tilde{A}_{21} & 0 & \tilde{A}_{23} & 0 & 0 & 0 & \tilde{A}_{27} & 0 & 0 & 0 & \tilde{A}_{211} \\ 0 & 0 & 0 & 1 & 0 & 0 & 0 & 0 & 0 & 0 & 0 \\ \tilde{A}_{41} & 0 & \tilde{A}_{43} & 0 & \tilde{A}_{45} & \tilde{A}_{46} & \tilde{A}_{47} & 0 & \tilde{A}_{49} & 0 & \tilde{A}_{411} \\ 0 & 0 & 0 & 0 & 0 & 1 & 0 & 0 & 0 & 0 & 0 \\ 0 & \tilde{A}_{62} & 0 & \tilde{A}_{64} & \tilde{A}_{65} & 0 & 0 & 0 & \tilde{A}_{69} & 0 & 0 \\ 0 & 0 & 0 & 0 & 0 & 0 & 0 & 1 & 0 & 0 & 0 \\ \tilde{A}_{81} & 0 & \tilde{A}_{83} & 0 & \tilde{A}_{85} & 0 & \tilde{A}_{87} & 0 & \tilde{A}_{89} & \tilde{A}_{810} & \tilde{A}_{811} \\ 0 & 0 & 0 & 0 & 0 & 0 & 0 & 0 & 0 & 1 & 0 \\ 0 & \tilde{A}_{102} & 0 & 0 & \tilde{A}_{105} & 0 & 0 & \tilde{A}_{108} & \tilde{A}_{109} & 0 & 0 \\ 0 & \tilde{A}_{112} & 0 & 0 & \tilde{A}_{115} & 0 & 0 & 0 & \tilde{A}_{119} & 0 & 0 \end{bmatrix} \tag{4.15}$$

Where

$$\tilde{A}_{21} = \dot{\tilde{\theta}}^2 + 2\dot{\tilde{\theta}}\dot{\theta}_e + \dot{\theta}_e{}^2 + \frac{1}{m_1}\frac{u_{1_e}}{\tilde{r}_{12}} + \frac{1}{m_1}\frac{u_{3_e}}{\tilde{r}_{13}}, \tilde{A}_{23} = -\frac{1}{m_1}\frac{u_{1_e}}{\tilde{r}_{12}}, \tilde{A}_{27} = -\frac{1}{m_1}\frac{u_{3_e}}{\tilde{r}_{13}}$$

$$\tilde{A}_{211} = \dot{\tilde{\theta}}x_{1_e} + 2\dot{\theta}_e x_{1_e}, \tilde{A}_{41} = -\frac{1}{m_2}\frac{u_{1_e}}{\tilde{r}_{12}}, \tilde{A}_{43} = \dot{\tilde{\theta}}^2 + 2\dot{\tilde{\theta}}\dot{\theta}_e + \dot{\theta}_e{}^2 + \frac{1}{m_2}\frac{u_{1_e}}{\tilde{r}_{12}} + \frac{1}{m_2}\frac{u_{2_e}}{\tilde{r}_{23}},$$

$$\tilde{A}_{45} = -\frac{2\left(\dot{\tilde{\theta}}+\dot{\theta}_e\right)\dot{\tilde{x}}_1}{\left(\tilde{x}_1+x_{1_e}\right)} - \frac{1}{m_1\left(\tilde{x}_1+x_{1_e}\right)}\frac{u_{1_e}}{\tilde{r}_{12}}\tilde{y}_2, \tilde{A}_{46} = 2\left(\dot{\tilde{\theta}} + \dot{\theta}_e\right), \tilde{A}_{47} = -\frac{1}{m_2}\frac{u_{2_e}}{\tilde{r}_{23}}$$

$$\tilde{A}_{49} = -\frac{1}{m_1\left(\tilde{x}_1+x_{1_e}\right)}\frac{u_{3_e}}{\tilde{r}_{13}}\tilde{y}_2, \tilde{A}_{411} = \dot{\tilde{\theta}}x_{2_e} + 2\dot{\theta}_e x_{2_e}, \tilde{A}_{62} = \frac{2\left(\dot{\tilde{\theta}}+\dot{\theta}_e\right)}{\left(\tilde{x}_1+x_{1_e}\right)}\left(\tilde{x}_2 + x_{2_e}\right),$$

$$\tilde{A}_{64} = -2\left(\dot{\tilde{\theta}} + \dot{\theta}_e\right), \tilde{A}_{65} = \dot{\tilde{\theta}}^2 + 2\dot{\tilde{\theta}}\dot{\theta}_e + \dot{\theta}_e{}^2 + \frac{1}{m_2}\frac{u_{1_e}}{\tilde{r}_{12}} + \frac{1}{m_2}\frac{u_{2_e}}{\tilde{r}_{23}} + \frac{\left(\tilde{x}_2+x_{2_e}\right)}{m_1\left(\tilde{x}_1+x_{1_e}\right)}\frac{u_{1_e}}{\tilde{r}_{12}},$$

$$\tilde{A}_{69} = -\frac{1}{m_2}\frac{u_{2_e}}{\tilde{r}_{23}} + \frac{\left(\tilde{x}_2+x_{2_e}\right)}{m_1\left(\tilde{x}_1+x_{1_e}\right)}\frac{u_{3_e}}{\tilde{r}_{13}}, \tilde{A}_{81} = -\frac{1}{m_3}\frac{u_{3_e}}{\tilde{r}_{13}}, \tilde{A}_{83} = -\frac{1}{m_3}\frac{u_{2_e}}{\tilde{r}_{23}},$$

$$\tilde{A}_{85} = -\frac{1}{m_1\left(\tilde{x}_1+x_{1_e}\right)}\frac{u_{1_e}}{\tilde{r}_{12}}\tilde{y}_3, \tilde{A}_{87} = \dot{\tilde{\theta}}^2 + 2\dot{\tilde{\theta}}\dot{\theta}_e + \dot{\theta}_e{}^2 + \frac{1}{m_3}\frac{u_{2_e}}{\tilde{r}_{23}} + \frac{1}{m_3}\frac{u_{3_e}}{\tilde{r}_{13}},$$

$$\tilde{A}_{89} = -\frac{2\left(\dot{\tilde{\theta}}+\dot{\theta}_e\right)\dot{\tilde{x}}_1}{\left(\tilde{x}_1+x_{1_e}\right)} - \frac{1}{m_1\left(\tilde{x}_1+x_{1_e}\right)}\frac{u_{3_e}}{\tilde{r}_{13}}\tilde{y}_3, \tilde{A}_{810} = 2\left(\dot{\tilde{\theta}} + \dot{\theta}_e\right), \tilde{A}_{811} = \dot{\tilde{\theta}}x_{3_e} + 2\dot{\theta}_e x_{3_e},$$

$$\tilde{A}_{102} = \frac{2\left(\dot{\tilde{\theta}}+\dot{\theta}_e\right)\left(\tilde{x}_3+x_{3_e}\right)}{\left(\tilde{x}_1+x_{1_e}\right)}, \tilde{A}_{105} = \frac{\left(\tilde{x}_3+x_{3_e}\right)}{m_1\left(\tilde{x}_1+x_{1_e}\right)}\frac{u_{1_e}}{\tilde{r}_{12}} - \frac{1}{m_3}\frac{u_{2_e}}{\tilde{r}_{23}}, \tilde{A}_{108} = -2\left(\dot{\tilde{\theta}} + \dot{\theta}_e\right),$$

$$\tilde{A}_{109} = \dot{\tilde{\theta}}^2 + 2\dot{\tilde{\theta}}\dot{\theta}_e + {\dot{\theta}_e}^2 + \frac{1}{m_3}\frac{u_{2_e}}{\tilde{r}_{23}} + \frac{1}{m_3}\frac{u_{3_e}}{\tilde{r}_{13}} + \frac{(\tilde{x}_3 + x_{3_e})}{m_1(\tilde{x}_1 + x_{1_e})}\frac{u_{3_e}}{\tilde{r}_{13}},$$

$$\tilde{A}_{112} = -\frac{2\left(\dot{\tilde{\theta}} + \dot{\theta}_e\right)}{(\tilde{x}_1 + x_{1_e})}, \tilde{A}_{115} = -\frac{1}{m_1(\tilde{x}_1 + x_{1_e})}\frac{u_{1_e}}{\tilde{r}_{12}}, \tilde{A}_{119} = -\frac{1}{m_1(\tilde{x}_1 + x_{1_e})}\frac{u_{3_e}}{\tilde{r}_{13}},$$

And

$$\tilde{\boldsymbol{B}}(\tilde{x}) = \begin{bmatrix} 0 & 0 & 0 \\ \tilde{B}_{21} & 0 & \tilde{B}_{23} \\ 0 & 0 & 0 \\ \tilde{B}_{41} & \tilde{B}_{42} & \tilde{B}_{43} \\ 0 & 0 & 0 \\ \tilde{B}_{61} & \tilde{B}_{62} & \tilde{B}_{63} \\ 0 & 0 & 0 \\ \tilde{B}_{81} & \tilde{B}_{82} & \tilde{B}_{83} \\ 0 & 0 & 0 \\ \tilde{B}_{101} & \tilde{B}_{102} & \tilde{B}_{103} \\ \tilde{B}_{111} & 0 & \tilde{B}_{113} \end{bmatrix} \tag{4.16}$$

Where

$$\tilde{B}_{21} = \frac{1}{m_1}\left(\frac{\tilde{x}_1 + x_{1_e} - \tilde{x}_2 - x_{2_e}}{r_{12}^3}\right), \tilde{B}_{23} = \frac{1}{m_1}\left(\frac{\tilde{x}_1 + x_{1_e} - \tilde{x}_3 - x_{3_e}}{r_{13}^3}\right),$$

$$\tilde{B}_{41} = \frac{1}{m_2}\left(\frac{\tilde{x}_2 + x_{2_e} - \tilde{x}_1 - x_{1_e}}{r_{12}^3}\right) - \frac{1}{m_1(\tilde{x}_1 + x_{1_e})}\left(\frac{{\tilde{y}_2}^2}{r_{12}^3}\right), \tilde{B}_{42} = \frac{1}{m_2}\left(\frac{\tilde{x}_2 + x_{2_e} - \tilde{x}_3 - x_{3_e}}{r_{23}^3}\right),$$

$$\tilde{B}_{43} = -\frac{1}{m_1(\tilde{x}_1 + x_{1_e})}\left(\frac{\tilde{y}_2\tilde{y}_3}{r_{13}^3}\right), \tilde{B}_{61} = \frac{1}{m_2}\left(\frac{\tilde{y}_2}{r_{12}^3}\right) + \frac{(\tilde{x}_2 + x_{2_e})}{m_1(\tilde{x}_1 + x_{1_e})}\left(\frac{\tilde{y}_2}{r_{12}^3}\right),$$

$$\tilde{B}_{62} = \frac{1}{m_2}\left(\frac{\tilde{y}_2 - \tilde{y}_3}{r_{23}^3}\right), \tilde{B}_{63} = \frac{(\tilde{x}_2 + x_{2_e})}{m_1(\tilde{x}_1 + x_{1_e})}\left(\frac{\tilde{y}_3}{r_{13}^3}\right), \tilde{B}_{81} = -\frac{1}{m_1(\tilde{x}_1 + x_{1_e})}\left(\frac{\tilde{y}_2\tilde{y}_3}{r_{12}^3}\right),$$

$$\tilde{B}_{82} = \frac{1}{m_3}\left(\frac{\tilde{x}_3 + x_{3_e} - \tilde{x}_2 - x_{2_e}}{r_{23}^3}\right), \tilde{B}_{83} = \frac{1}{m_3}\left(\frac{\tilde{x}_3 + x_{3_e} - \tilde{x}_1 - x_{1_e}}{r_{13}^3}\right) - \frac{1}{m_1(\tilde{x}_1 + x_{1_e})}\left(\frac{{\tilde{y}_3}^2}{r_{13}^3}\right),$$

$$\tilde{B}_{101} = \frac{(\tilde{x}_3 + x_{3_e})}{m_1(\tilde{x}_1 + x_{1_e})}\left(\frac{\tilde{y}_2}{r_{12}^3}\right), \tilde{B}_{102} = \frac{1}{m_3}\left(\frac{\tilde{y}_3 - \tilde{y}_2}{r_{23}^3}\right), \tilde{B}_{103} = \frac{1}{m_3}\left(\frac{\tilde{y}_3}{r_{13}^3}\right) + \frac{(\tilde{x}_3 + x_{3_e})}{m_1(\tilde{x}_1 + x_{1_e})}\left(\frac{\tilde{y}_3}{r_{13}^3}\right),$$

$$\tilde{B}_{111} = -\frac{1}{m_1(\tilde{x}_1 + x_{1_e})}\left(\frac{\tilde{y}_2}{r_{12}^3}\right), \tilde{B}_{113} = -\frac{1}{m_1(\tilde{x}_1 + x_{1_e})}\left(\frac{\tilde{y}_3}{r_{13}^3}\right),$$

The system has a few important constraints. As the Coulomb forces are internal to the system, the forces between each two craft are equal and opposite. The center of mass is inertial and does not have acceleration because these electrostatic forces are the only forces acting on the system.

$$M\ddot{\boldsymbol{R}}_c = \boldsymbol{F}_{ext} = 0 \tag{4.17}$$

Then, the resulting four constraints equations are

$$0 = m_1\boldsymbol{r}_1 + m_2\boldsymbol{r}_2 + m_3\boldsymbol{r}_3 \tag{4.18}$$

$$0 = m_1\dot{\boldsymbol{r}}_1 + m_2\dot{\boldsymbol{r}}_2 + m_3\dot{\boldsymbol{r}}_3 \tag{4.19}$$

By knowing the positions and velocities of craft 1 and 2, the position and velocity of craft 3 can be computed. Since, there are no external forces and torques, the formation angular momentum is constant.

$$\dot{\boldsymbol{H}} = 0 \tag{4.20}$$

Now, the state space model is reduced and there is a 6-dimensional state space model. The reduced model can be described by the state variables

$$\boldsymbol{x}^* = (x_1, \dot{x}_1, x_2, \dot{x}_2, y_2, \dot{y}_2)^T \tag{4.21}$$

The final equations of motion are

$$\ddot{x}_1 = \frac{k_c q_1}{m_1}\left(q_2\frac{x_1 - x_2}{r_{12}^3} + q_3\frac{2x_1 + x_2}{r_{13}^3}\right) + x_1\dot{\theta}^2 \tag{4.22}$$

$$\ddot{x}_2 = \frac{k_c q_2}{m_2}\left(q_1\frac{x_2 - x_1}{r_{12}^3} + q_3\frac{2x_2 + x_1}{r_{23}^3}\right) + x_2\dot{\theta}^2 + y_2\ddot{\theta} + 2\dot{y}_2\dot{\theta} \tag{4.23}$$

$$\ddot{y}_2 = \frac{k_c q_2}{m_2}\left(q_1\frac{y_2}{r_{12}^3} + q_3\frac{2y_2}{r_{23}^3}\right) + y_2\dot{\theta}^2 - x_2\ddot{\theta} - 2\dot{x}_2\dot{\theta} \tag{4.24}$$

where

$$r_{13} = \sqrt{(2x_1 + x_2)^2 + y_2^2} \tag{4.25}$$

$$r_{23} = \sqrt{(x_1 + 2x_2)^2 + 4y_2^2} \tag{4.26}$$

The formation angular velocity equation is described as

$$\dot{\theta} = \frac{m_3 H_0 + (y_2\dot{x}_2 - x_2\dot{y}_2)(m_2^2 + m_2 m_3) - m_1 m_2(x_1\dot{y}_2 - \dot{x}_1 y_2)}{2m_1 m_2 x_1 x_2 + x_1^2(m_1^2 + m_1 m_3) + (m_2^2 + m_2 m_3)(x_2^2 + y_2^2)} \tag{4.27}$$

and H_0 is formation angular momentum.

CHAPTER 5

STATE DEPENDENT FACTORIZED OPTIMAL CONTROL METHODS

5.1 Review of Optimal Solutions to Unconstrained Nonlinear Optimal Control Problems

In this section, the nonautonomous problems that are nonlinear in the state and linear-affine in the control are considered. The initial state condition is specified, and the final state condition can be either specified or unknown. Both the state variables and controls are unconstrained, and the time span is fixed.

5.1.1 Statement of Unconstrained Nonlinear Optimal Control Problem

Consider a set of n first-order differential equations

$$\dot{\mathbf{x}} = \mathbf{f}\left(\mathbf{x},t\right) + \mathbf{B}\left(\mathbf{x},t\right)\mathbf{u} \tag{5.1}$$

with $\mathbf{f}:\mathbb{R}^{n+1} \to \mathbb{R}^n$ and $\mathbf{B}:\mathbb{R}^{n+1} \to \mathbb{R}^{n\times m}$. The goal is to find m control functions $\mathbf{u}(t)$ within the initial and final times, t_0, t_f, such that the performance index

$$J = \varphi\left(\mathbf{x}(t_f),t_f\right) + \int_{t_0}^{t_f} L\left(\mathbf{x}(t),\mathbf{u}(t),t\right)\mathrm{d}t \tag{5.2}$$

is minimized; $L:\mathbb{R}^{n+m+1} \to \mathbb{R}$, and $\varphi:\mathbb{R}^{n+1} \to \mathbb{R}$. The initial condition is assumed given, namely

$$\mathbf{x}(t_0) = \mathbf{x}_0 \tag{5.3}$$

While three different forms are examined for the final state condition. These describe the soft constrained problem (SCP), the hard constrained problem (HCP), and the mixed constrained problem (MCP), with the final state not specified, fully specified, and partly specified, respectively.

Defined the Hamiltonian $H(\mathbf{x},\boldsymbol{\lambda},\mathbf{u},t) = L(\mathbf{x},\mathbf{u},t) + \boldsymbol{\lambda}^T\left[\mathbf{f}(\mathbf{x},t) + \mathbf{B}(\mathbf{x},t)\mathbf{u}\right]$, the solution of the problem may be found using the Euler-Lagrange equations,

$$\dot{\mathbf{x}} = +\frac{\partial H}{\partial \boldsymbol{\lambda}}, \qquad \dot{\boldsymbol{\lambda}} = -\frac{\partial H}{\partial \mathbf{x}}, \qquad \frac{\partial H}{\partial \mathbf{u}} = \mathbf{0} \tag{5.4}$$

in which λ is the vector of costates. These Euler-Lagrange equations are the necessary conditions, and their alternative solutions are represented in Eqs. (5.10)-(5.14) for the ASRE approach 1 and Eqs. (5.18)-(5.19) for the ASRE approach 2.

5.1.2 Approximating Sequence of Riccati Equations Method

Suppose that $\mathbf{f}(\mathbf{x},t)$ in Eq. (5.1) is a continuously differentiable vector-valued function of $\mathbf{x}$ and t in an open set $\boldsymbol{\Gamma} \in \mathbb{R}^{n+1}$, $\mathbf{f}(\cdot) \in \mathcal{C}^1(\boldsymbol{\Gamma})$, and $\mathbf{B}(\mathbf{x},t) \in \mathcal{C}^0(\boldsymbol{\Gamma})$ is a continuous vector-valued function. In addition, $\mathbf{f}(\mathbf{0},t) = \mathbf{0}, \forall t \in \mathbb{R}$. Under these conditions [16], the State Dependent Coefficient (SDC) factorization of Eq. (5.1) may be written as

$$\dot{\mathbf{x}} = \mathbf{A}(\mathbf{x},t)\mathbf{x} + \mathbf{B}(\mathbf{x},t)\mathbf{u} \tag{5.5}$$

which is a stabilizable parameterization of the nonlinear system represented in Eq. (5.1) in a region $\boldsymbol{\Gamma}$ if the pair $\{\mathbf{A}(\mathbf{x},t), \mathbf{B}(\mathbf{x},t)\}$ is point-wise stabilizable in the linear sense for all $\mathbf{x} \in \boldsymbol{\Gamma}$. Redefinition of the objective function in the quadratic-like form is

$$J = \frac{1}{2}\mathbf{x}^T(t_f)S(\mathbf{x}(t_f),t_f)\mathbf{x}(t_f) + \frac{1}{2}\int_{t_0}^{t_f}\left(\mathbf{x}^T Q(\mathbf{x},t)\mathbf{x} + \mathbf{u}^T R(\mathbf{x},t)\mathbf{u}\right)dt \tag{5.6}$$

where $S(\mathbf{x}(t_f),t_f)$ and $Q(\mathbf{x},t)$ are positive semi-definite, and $R(\mathbf{x},t)$ is positive definite time-varying matrices.

5.1.2.1 Approach1

The ASRE approach presented in [23, 24] considers the following sequences of Time Varying Linear Quadratic Regulator (TVLQR) approximations

$$\dot{\mathbf{x}}^{[1]} = \mathbf{A}(\mathbf{x}_0)\,\mathbf{x}^{[1]}(t) + \mathbf{B}(\mathbf{x}_0)\,\mathbf{u}^{[1]}(t) \tag{5.7}$$

$$\dot{\mathbf{x}}^{[k+1]} = \mathbf{A}(\mathbf{x}^{[k]}(t),t)\,\mathbf{x}^{[k+1]} + \mathbf{B}(\mathbf{x}^{[k]}(t),t)\,\mathbf{u}^{[k+1]} \tag{5.8}$$

where the superscript denotes the iteration. The initial state is $\mathbf{x}^{[k+1]}(t_0) = \mathbf{x}_0$, and the corresponding linear-quadratic cost functional is

$$J^{[k+1]} = \frac{1}{2}\left(\mathbf{x}^{[k+1]}(t_f)\right)^T \mathbf{S}(\mathbf{x}^{[k]}(t_f),t_f)\left(\mathbf{x}^{[k+1]}(t_f)\right) +$$

$$\frac{1}{2}\int_{t_0}^{t_f}\left(\mathbf{x}^{[k+1]T}\mathbf{Q}(\mathbf{x}^{[k]}(t),t)\mathbf{x}^{[k+1]} + \mathbf{u}^{[k+1]T}\mathbf{R}(\mathbf{x}^{[k]}(t),t)\mathbf{u}^{[k+1]}\right)dt \tag{5.9}$$

Since each approximation is time-varying and linear-quadratic, the optimal control sequence is in the form [23]

$$\mathbf{u}^{[k+1]}(t) = -\mathbf{R}^{-1}(\mathbf{x}^{[k]}(t))\mathbf{B}^T(\mathbf{x}^{[k]}(t))\mathbf{P}^{[k+1]}(t)\mathbf{x}^{[k+1]}(t) \tag{5.10}$$

where the real, symmetric and positive-definite matrix $\mathbf{P}^{[k+1]}(t)$ is the solution of

$$\dot{\mathbf{P}}^{[k+1]}(t) = -\mathbf{Q}(\mathbf{x}^{[k]}(t)) - \mathbf{P}^{[k+1]}(t)\mathbf{A}(\mathbf{x}^{[k]}(t)) - \mathbf{A}^T(\mathbf{x}^{[k]}(t))\mathbf{P}^{[k+1]}(t) + \mathbf{P}^{[k+1]}(t)\mathbf{E}(\mathbf{x}^{[k]}(t))\mathbf{P}^{[k+1]}(t) \tag{5.11}$$

with

$$\mathbf{P}^{[k+1]}(t_f) = \mathbf{S}(\mathbf{x}^{[k]}(t_f)) \tag{5.12}$$

$$\mathbf{E}(\mathbf{x}^{[k]}(t)) = \mathbf{B}(\mathbf{x}^{[k]}(t))\mathbf{R}^{-1}(\mathbf{x}^{[k]}(t))\mathbf{B}^T(\mathbf{x}^{[k]}(t)) \tag{5.13}$$

Notice that the differential Riccati equation (5.11) has to be solved backward in time and the optimal state trajectory is obtained by integrating the following differential equation forward in time

$$\dot{\mathbf{x}}^{[k+1]}(t) = \left[\mathbf{A}(\mathbf{x}^{[k]}(t)) - \mathbf{E}(\mathbf{x}^{[k]}(t))\mathbf{P}^{[k+1]}(t)\right]\mathbf{x}^{[k+1]}(t) \tag{5.14}$$

5.1.2.2 Approach2

The sequence of TVLQR is solved by exploiting the structure of their Euler--Lagrange equations, so avoiding dealing with the matrix differential Riccati equation. This approach is described in [27, 28]. Rather than integrating Eq. (5.11), the approach in [27, 28] integrates the Hamiltonian matrix equation to obtain state transition sub-matrices that enable easy handling of partially specified terminal states.

Consider the system dynamic and quadratic objective function in Eqs. (5.5)-(5.6). The necessary conditions for this problem are obtained by applying Eq. (5.4), namely

$$\dot{\mathbf{x}} = \mathbf{A}(\mathbf{x},t)\,\mathbf{x} + \mathbf{B}(\mathbf{x},t)\,\mathbf{u}, \tag{5.15}$$

$$\dot{\boldsymbol{\lambda}} = -\mathbf{Q}(\mathbf{x},t)\,\mathbf{x} - \mathbf{A}^T(\mathbf{x},t)\,\boldsymbol{\lambda} \tag{5.16}$$

$$\mathbf{0} = \mathbf{R}(\mathbf{x},t)\,\mathbf{u} + \mathbf{B}^T(\mathbf{x},t)\,\boldsymbol{\lambda} \tag{5.17}$$

From Eq. (5.17), one may get

$$\mathbf{u} = -\mathbf{R}^{-1}(\mathbf{x},t)\mathbf{B}^T(\mathbf{x},t)\,\boldsymbol{\lambda} \tag{5.18}$$

which by substituting into Eqs. (5.15)-(5.16) it is possible to get

$$\begin{pmatrix} \dot{\mathbf{x}} \\ \dot{\boldsymbol{\lambda}} \end{pmatrix} = \begin{bmatrix} \mathbf{A}(\mathbf{x},t) & -\mathbf{B}(\mathbf{x},t)R^{-1}(\mathbf{x},t)\mathbf{B}^T(\mathbf{x},t) \\ -\mathbf{Q}(\mathbf{x},t) & -\mathbf{A}^T(\mathbf{x},t) \end{bmatrix} \begin{pmatrix} \mathbf{x} \\ \boldsymbol{\lambda} \end{pmatrix} \tag{5.19}$$

The solution of Eq. (5.19), which is a system of linear differential equations, is given by

$$\mathbf{x}(t) = \phi_{xx}(t_0,t)\,\mathbf{x}_0 + \phi_{x\lambda}(t_0,t)\,\lambda_0 \tag{5.20}$$

$$\boldsymbol{\lambda}(t) = \phi_{\lambda x}(t_0,t)\mathbf{x}_0 + \phi_{\lambda\lambda}(t_0,t)\lambda_0 \tag{5.21}$$

where $\mathbf{x}_0$ and λ_0 are the initial state and costate, respectively. The components of the state transition matrix ϕ_{xx}, $\phi_{x\lambda}$, $\phi_{\lambda x}$, and $\phi_{\lambda\lambda}$ are obtained by integrating the following dynamics

$$\begin{bmatrix} \dot{\phi}_{xx} & \dot{\phi}_{x\lambda} \\ \dot{\phi}_{\lambda x} & \dot{\phi}_{\lambda\lambda} \end{bmatrix} = \begin{bmatrix} \mathbf{A}(\mathbf{x},t) & -\mathbf{B}(\mathbf{x},t)\mathbf{R}^{-1}(\mathbf{x},t)\mathbf{B}^T(\mathbf{x},t) \\ -\mathbf{Q}(\mathbf{x},t) & -\mathbf{A}^T(\mathbf{x},t) \end{bmatrix} \begin{bmatrix} \phi_{xx} & \phi_{x\lambda} \\ \phi_{\lambda x} & \phi_{\lambda\lambda} \end{bmatrix} \tag{5.22}$$

with the required initial conditions defined as

$$\phi_{xx}(t_0,t_0) = \phi_{\lambda\lambda}(t_0,t_0) = \mathbf{I}_{n\times n}, \quad \phi_{x\lambda}(t_0,t_0) = \phi_{\lambda x}(t_0,t_0) = 0_{n\times n} \tag{5.23}$$

The issue here is computing λ_0 as only $\mathbf{x}_0$ is given. This is given by (refer to [42] for detailed derivation)

$$\lambda_0(\mathbf{x}_0,\mathbf{x}_f,t_0,t_f) = \phi_{x\lambda}{}^{-1}(t_0,t_f)\left[\mathbf{x}_f - \phi_{xx}(t_0,t_f)\,\mathbf{x}_0\right] \text{ for HCP}$$

$$\lambda_0(\mathbf{x}_0,t_0,t_f) = \left[\phi_{\lambda\lambda}(t_0,t_f) - \mathbf{S}(t_f)\phi_{x\lambda}(t_0,t_f)\right]^{-1}\left[\mathbf{S}(t_f)\phi_{xx}(t_0,t_f) - \phi_{\lambda x}(t_0,t_f)\right]\mathbf{x}_0 \text{ for SCP}$$

$$\lambda_0(\mathbf{x}_0,y_f,t_0,t_f) = (\xi_0(\mathbf{x}_0,y_f,t_0,t_f),\ \eta_0(\mathbf{x}_0,y_f,t_0,t_f)), \text{ for MCP}$$

(5.24)

where ξ and η are the component of λ related to the elements of the final state that are partially specified (their expressions are reported in [42]).

5.2 State Dependent Coefficient Direct Method

The problems treated in this section are the same as in Sec. 5.1 except that both the states and controls are constrained. The proposed SDC Direct method employs SDC factorization and Chebyshev polynomials. Constrained nonlinear optimal control problem formulation is recalled and reformulated to SDC form. The state variables are approximated and expanded to the Chebyshev polynomials. Then, the state derivatives are derived from the state variables. To this end, the control variables are obtained as a function of state variables and their derivatives. The CNOC problem is converted to quadratic programming problem, and a constrained optimization problem is solved.

5.2.1 *Statement of Constrained Nonlinear Optimal Control Problem*

The statement of the constrained problem is similar to that of the unconstrained case in Sect. 5.1.1, except that this time Eqs. (5.25)-(5.26) have to be considered.

$$\mathbf{x}_{\min} \le \mathbf{x}(t) \le \mathbf{x}_{\max} \tag{5.25}$$

$$\mathbf{u}_{\min} \le \mathbf{u}(t) \le \mathbf{u}_{\max} \tag{5.26}$$

The necessary conditions for $\dot{\mathbf{x}}$ and $\dot{\boldsymbol{\lambda}}$ represented in Eq. (5.4) are kept here, while the third condition, $\partial H / \partial \mathbf{u} = \mathbf{0}$, is replaced by the minimum principle

$$\mathbf{u} = \arg\min_{\mathbf{u}} H(\mathbf{x}, \boldsymbol{\lambda}, \mathbf{u}, t) \tag{5.27}$$

This new form of the necessary condition (minimum principle) on the Hamiltonian prevent the use of alternative solutions described in Eqs. (5.10)-(5.14) and Eqs. (5.18)-(5.19). Hence, the SDC Direct method to solve the constrained problems in needed.

5.2.2 *Converting Constrained Nonlinear Optimal Control Problems to Quadratic Programming Problems Using Chebyshev Polynomials*

From now, and without any loss of generality, we assume $t_0 = 0$. In order to use Chebyshev polynomials, the transformation time $\tau = 2t / t_f - 1$ is used; this is defined in $[-1,1]$. By using Chebyshev time transformation, TVLQR approximations in Eq. (5.8) are written as

$$\frac{\mathrm{d}\mathbf{x}^{[k+1]}}{\mathrm{d}\tau}(\tau) = \frac{t_f}{2}[\mathbf{A}(\mathbf{x}^{[k]}(\tau), \tau)\, \mathbf{x}^{[k+1]} + \mathbf{B}(\mathbf{x}^{[k]}(\tau), \tau)\, \mathbf{u}^{[k+1]}] \tag{5.28}$$

At the first iteration, the states, the state matrix, and the control matrix are written as $\mathbf{x}^{[k]} = \mathbf{x}_0$, $\mathbf{A}(\mathbf{x}^{[k]}(\tau), \tau) = \mathbf{A}(\mathbf{x}_0)$, and $\mathbf{B}(\mathbf{x}^{[k]}(\tau), \tau) = \mathbf{B}(\mathbf{x}_0)$, respectively. From the second iteration on, the state variables $\mathbf{x}^{[k+1]}$ are approximated by Chebyshev polynomials and the inputs $\mathbf{u}^{[k+1]}$ are obtained from the states and their derivatives. Note that $\mathbf{A}(\mathbf{x}^{[k]}(\tau), \tau)$ and $\mathbf{B}(\mathbf{x}^{[k]}(\tau), \tau)$ matrices for each iteration are evaluated by the states of the previous iteration. So, the state and input matrices are functions

of states and inputs of the previous iteration and they do not need to be approximated by Chebyshev polynomials in the current thesis. The other equations are written as

$$J^{[k+1]} = \frac{1}{2}\left(\mathbf{x}^{[k+1]}(1)\right)^T \mathbf{S}(\mathbf{x}^{[k]}(1),1)\left(\mathbf{x}^{[k+1]}(1)\right) +$$

$$\frac{t_f}{4}\int_{-1}^{1}\left(\mathbf{x}^{[k+1]T}\mathbf{Q}(\mathbf{x}^{[k]}(\tau),\tau)\,\mathbf{x}^{[k+1]} + \mathbf{u}^{[k+1]T}\mathbf{R}(\mathbf{x}^{[k]}(\tau),\mathbf{u}^{[k]}(\tau),\tau)\,\mathbf{u}^{[k+1]}\right)\mathrm{d}\tau \quad (5.29)$$

$$\mathbf{x}^{[k+1]}(-1) = \mathbf{x}_0 \quad (5.30)$$

$$\mathbf{x}_{\min} \le \mathbf{x}^{[k+1]}(\tau) \le \mathbf{x}_{\max} \quad (5.31)$$

$$\mathbf{u}_{\min} \le \mathbf{u}^{[k+1]}(\tau) \le \mathbf{u}_{\max} \quad (5.32)$$

For approximating the state variables, Chebyshev polynomials of first kind, $T_i(\tau)$, are used such that

$$x_j^{[k+1]}(\tau) = \sum_{i=0}^{N}{}' \, a_i^{(j)} T_i(\tau) \quad (5.33)$$

where the dash $\left(\sum'\right)$ denotes that the first term in the sum is to be halved, $j = 1,2,...,n$ is the number of states, N is the degree of the Chebyshev polynomial, and $a_i^{(j)}$ are unknown parameters. Eq. (5.33) may be rewritten in matrix form as

$$\begin{bmatrix} x_1^{k+1}(\tau) \\ x_2^{k+1}(\tau) \\ . \\ . \\ . \\ x_n^{k+1}(\tau) \end{bmatrix} = \begin{bmatrix} 0.5a_0^{(1)} & a_1^{(1)} & ... & a_N^{(1)} \\ 0.5a_0^{(2)} & a_1^{(2)} & ... & a_N^{(2)} \\ . & . & ... & . \\ . & . & ... & . \\ . & . & ... & . \\ 0.5a_0^{(n)} & a_1^{(n)} & ... & a_N^{(n)} \end{bmatrix} \begin{bmatrix} T_0(\tau) \\ T_1(\tau) \\ . \\ . \\ . \\ T_N(\tau) \end{bmatrix}$$

Using the Kronecker product yields a convenient notation

$$\mathbf{x}^{[k+1]}(\tau) = \left(\mathbf{I}_n \otimes \mathbf{T}^T(\tau)\right)\mathbf{a} \quad (5.34)$$

where $\mathbf{T}^T(\tau) = [T_0(\tau), T_1(\tau), ..., T_N(\tau)]$ is an $(1\times(N+1))$ row vector of Chebyshev polynomials, and $\mathbf{a}^T = [a_0^{(1)}/2, a_1^{(1)}, ..., a_N^{(1)}, a_0^{(2)}/2, ..., a_N^{(2)}, ..., a_0^{(n)}/2, ..., a_N^{(n)}]$ is an

$(1\times n(N+1))$ row vector of unknown parameters. Derivative of the state variables is governed by equation

$$\dot{x}_j^{[k+1]}(\tau)=\sum_{i=0}^{N}{}'a_i^{(j)}\dot{T}_i(\tau) \tag{5.35}$$

which may be written in matrix form as

$$\dot{\mathbf{x}}^{[k+1]}(\tau)=\left(\mathbf{I}_n\otimes\mathbf{T}^T(\tau)\mathbf{D}^T\right)\mathbf{a} \tag{5.36}$$

where $\dot{\mathbf{T}}=\mathbf{DT}$ is used here, and $\mathbf{D}$ matrix has a dimension of $(N+1)\times(N+1)$ which is defined as following. The derivative of Chebyshev polynomials is defined in [43] as

$$\frac{\mathrm{d}T_N(\tau)}{\mathrm{d}\tau}=2N\sum_{\substack{i=0\\ N-i\ odd}}^{N-1}{}'T_i(\tau) \tag{5.37}$$

From Eq. (5.37) it can be concluded that the derivative of the Chebyshev polynomials of the first kind may be written as

$$\frac{\mathrm{d}T_1(\tau)}{\mathrm{d}\tau}=T_0(\tau)$$

$$\frac{\mathrm{d}T_2(\tau)}{\mathrm{d}\tau}=4T_1(\tau)$$

$$\frac{\mathrm{d}T_3(\tau)}{\mathrm{d}\tau}=3T_0(\tau)+6T_2(\tau)$$

$$\frac{\mathrm{d}T_4(\tau)}{\mathrm{d}\tau}=8T_1(\tau)+8T_3(\tau)$$

$$\frac{\mathrm{d}T_5(\tau)}{\mathrm{d}\tau}=5T_0(\tau)+10T_2(\tau)+10T_4(\tau)$$

$$\frac{\mathrm{d}T_6(\tau)}{\mathrm{d}\tau}=12T_1(\tau)+12T_3(\tau)+12T_5(\tau)$$

$$\vdots$$

and from the definition of the Chebyshev polynomials of the first kind in [43], we have $\frac{\mathrm{d}T_0(\tau)}{\mathrm{d}\tau}=0$. Therefore, it may be proved that

$$\mathbf{D}=\begin{bmatrix}0&0&0&0&0&0&0&0&...&0\\1&0&0&0&0&0&0&0&...&0\\0&4&0&0&0&0&0&0&...&0\\3&0&6&0&0&0&0&0&...&0\\0&8&0&8&0&0&0&0&...&0\\5&0&10&0&10&0&0&0&...&0\\0&12&0&12&0&12&0&0&...&0\\7&0&14&0&14&0&14&0&...&0\\0&16&0&16&0&16&0&16&...&0\\.&.&.&.&.&.&.&.&.&.\end{bmatrix}$$

Also, for the technique represented in Sec. 5.2.3, it is required to get the second derivative of the state variables using the equation

$$\ddot{x}_j^{[k+1]}(\tau)=\sum_{i=0}^{N}{}'a_i^{(j)}\ddot{T}_i(\tau) \tag{5.38}$$

which in matrix form may be written as

$$\ddot{\mathbf{x}}^{[k+1]}(\tau)=\left(\mathbf{I}_n\otimes\mathbf{T}^T(\tau)\mathbf{D}^T\mathbf{D}^T\right)\mathbf{a} \tag{5.39}$$

where $\ddot{\mathbf{T}}=\mathbf{DDT}$ is used here. The second derivative of Chebyshev polynomials is defined in [43] as

$$\frac{\mathrm{d}^2T_N(\tau)}{\mathrm{d}\tau^2}=\sum_{\substack{i=0\\N-i\ even}}^{N-2}{}'(N-i)N(N+i)T_i(\tau) \tag{5.40}$$

From Eq. (5.40) it can be concluded that the second derivative of the Chebyshev polynomials of the first kind may be written as

$$\frac{\mathrm{d}^2 T_2(\tau)}{\mathrm{d}\tau^2} = 4T_0(\tau)$$

$$\frac{\mathrm{d}^2 T_3(\tau)}{\mathrm{d}\tau^2} = 24T_1(\tau)$$

$$\frac{\mathrm{d}^2 T_4(\tau)}{\mathrm{d}\tau^2} = 32T_0(\tau) + 48T_2(\tau)$$

$$\frac{\mathrm{d}^2 T_5(\tau)}{\mathrm{d}\tau^2} = 120T_1(\tau) + 80T_3(\tau)$$

$$\vdots$$

and from the definition of the Chebyshev polynomials of the first kind in [43], we have $\frac{\mathrm{d}^2 T_0(\tau)}{\mathrm{d}\tau^2} = 0$, and $\frac{\mathrm{d}^2 T_1(\tau)}{\mathrm{d}\tau^2} = 0$. So,

$$\mathbf{D}^2 = \begin{bmatrix} 0 & 0 & 0 & 0 & 0 & 0 & 0 & 0 & \dots & 0 \\ 0 & 0 & 0 & 0 & 0 & 0 & 0 & 0 & \dots & 0 \\ 4 & 0 & 0 & 0 & 0 & 0 & 0 & 0 & \dots & 0 \\ 0 & 24 & 0 & 0 & 0 & 0 & 0 & 0 & \dots & 0 \\ 32 & 0 & 48 & 0 & 0 & 0 & 0 & 0 & \dots & 0 \\ 0 & 120 & 0 & 80 & 0 & 0 & 0 & 0 & \dots & 0 \\ 108 & 0 & 192 & 0 & 120 & 0 & 0 & 0 & \dots & 0 \\ 0 & 336 & 0 & 280 & 0 & 168 & 0 & 0 & \dots & 0 \\ 256 & 0 & 480 & 0 & 384 & 0 & 224 & 0 & \dots & 0 \\ . & . & . & . & . & . & . & . & . & . \end{bmatrix}$$

Until now, the state variables are approximated and expanded to the Chebyshev polynomials. Moreover, the state derivatives are derived from the state variables. To this end, the control variables are obtained as a function of state variables and their derivatives. Here, it is assumed that the number of states, n, is equal to the number of inputs, m, and the $\mathbf{B}(\mathbf{x}^{[k]})$ matrix in Eq. (5.28) is square and invertible. Sec. 5.2.3 will handle the case in which the number of states, n, is greater than the number of inputs, m, and $\mathbf{B}(\mathbf{x}^{[k]})$ is not square and invertible. Now rearranging Eq. (5.28) gives us the required formula for inputs which is in the form

$$\mathbf{u}^{k+1}(\tau) = \mathbf{B}(\mathbf{x}^{[k]}(\tau))^{-1}\left[\frac{2}{t_f}\left(\mathbf{I}_n \otimes \mathbf{T}^T(\tau)\mathbf{D}^T\right)\mathbf{a} - \mathbf{A}(\mathbf{x}^{[k]}(\tau))\left(\mathbf{I}_n \otimes \mathbf{T}^T(\tau)\right)\mathbf{a}\right] \quad (5.41)$$

Without loss of generality, we consider that the matrices Q, R, and S are constant for convenience. Taking into account of all the approximations for states, state derivatives, and inputs and substituting them in Eq. (5.29) may give

$$\hat{J}^{[k+1]} = \frac{1}{2}\mathbf{a}^T\left(\mathbf{I}_n \otimes T(1)\right)\mathbf{S}\left(\mathbf{I}_n \otimes T^T(1)\right)\mathbf{a} + \frac{t_f}{4}\int_{-1}^{1}\left[\mathbf{a}^T\left(\mathbf{I}_n \otimes \mathbf{T}(\tau)\right)\mathbf{Q}\left(\mathbf{I}_n \otimes \mathbf{T}^T(\tau)\right)\mathbf{a}\right]\mathrm{d}\tau +$$
$$\frac{t_f}{4}\int_{-1}^{1}\left[\frac{2}{t_f}\mathbf{a}^T\left(\mathbf{I}_n \otimes \mathbf{DT}(\tau)\right) - \mathbf{a}^T\left(\mathbf{I}_n \otimes \mathbf{T}(\tau)\right)\mathbf{A}(\mathbf{x}^{[k]}(\tau))^T\right]\times$$
$$\mathbf{F}(\tau)\left[\frac{2}{t_f}\left(\mathbf{I}_n \otimes \mathbf{T}^T(\tau)\mathbf{D}^T\right)\mathbf{a} - \mathbf{A}(\mathbf{x}^{[k]}(\tau))\left(\mathbf{I}_n \otimes \mathbf{T}^T(\tau)\right)\mathbf{a}\right]\mathrm{d}\tau \quad (5.42)$$

where $\mathbf{F}(\tau) = (\mathbf{B}(\mathbf{x}^{[k]}(\tau))^{-1})^T\,\mathbf{R}\mathbf{B}(\mathbf{x}^{[k]}(\tau))^{-1}$, and $\hat{J}^{[k+1]}$ is an approximate value of $J^{[k+1]}$. Multiplication of the elements in Eq. (5.42) will give the formula for the approximated objective function in the form

$$\hat{J}^{[k+1]} = \frac{1}{2}\mathbf{a}^T\mathbf{h}_0\mathbf{a} + \frac{t_f}{4}\int_{-1}^{1}\left[\mathbf{a}^T\mathbf{h}_1\mathbf{a} + \frac{4}{{t_f}^2}\mathbf{a}^T\mathbf{h}_2\mathbf{a} + \mathbf{a}^T\mathbf{h}_3\mathbf{a} - \frac{2}{t_f}\mathbf{a}^T\mathbf{h}_4\mathbf{a} - \frac{2}{t_f}\mathbf{a}^T\mathbf{h}_5\mathbf{a}\right]\mathrm{d}\tau \quad (5.43)$$

where

$$\mathbf{h}_0 = \mathbf{S} \otimes T(1)T^T(1)$$

$$\mathbf{h}_1 = \mathbf{Q} \otimes \mathbf{T}(\tau)\mathbf{T}^T(\tau)$$

$$\mathbf{h}_2 = \mathbf{F}(\tau) \otimes \mathbf{DT}(\tau)\mathbf{T}^T(\tau)\mathbf{D}^T$$

$$\mathbf{h}_3 = (\mathbf{A}(\mathbf{x}^{[k]}(\tau)))^T\,\mathbf{F}(\tau)\mathbf{A}(\mathbf{x}^{[k]}(\tau)) \otimes \mathbf{T}(\tau)\mathbf{T}^T(\tau)$$

$$\mathbf{h}_4 = \mathbf{F}(\tau)\mathbf{A}(\mathbf{x}^{[k]}(\tau)) \otimes \mathbf{DT}(\tau)\mathbf{T}^T(\tau)$$

$$\mathbf{h}_5 = (\mathbf{A}(\mathbf{x}^{[k]}(\tau)))^T\,\mathbf{F}(\tau) \otimes \mathbf{T}(\tau)\mathbf{T}^T(\tau)\mathbf{D}^T$$

The current work computes the objective function numerically using the pointwise evaluations of the states, their derived derivatives, and the derived

controls. From Eq. (5.34) it can be concluded that the initial boundary condition in (5.30) may be written as

$$\mathbf{x}^{[k+1]}(-1) = \left(\mathbf{I}_n \otimes T^T(-1)\right)\mathbf{a} = \mathbf{x_0} \tag{5.44}$$

In addition, by substituting the state and control approximations defined in Eqs. (5.34) and (5.41) into Eqs. (5.31) and (5.32),one may obtain

$$\mathbf{x}_{\min} \le \left(\mathbf{I}_n \otimes \mathbf{T}^T(\tau)\right)\mathbf{a} \le \mathbf{x}_{\max} \tag{5.45}$$

$$\mathbf{u}_{\min} \le \mathbf{B}(\mathbf{x}^{[k]}(\tau))^{-1}\left[\frac{2}{t_f}\left(\mathbf{I}_n \otimes \mathbf{T}^T(\tau)\mathbf{D}^T\right)\mathbf{a} - \mathbf{A}(\mathbf{x}^{[k]}(\tau))\left(\mathbf{I}_n \otimes \mathbf{T}^T(\tau)\right)\mathbf{a}\right] \le \mathbf{u}_{\max} \tag{5.46}$$

Now we are dealing with a special type of mathematical optimization problem known as Quadratic Programming problem. The goal is minimization of a quadratic function, $\hat{J}^{[k+1]}$, of several variables, $\mathbf{a}$, subject to linear constraints on these variables. Inequality constraints result from the state and control constraints (bounds), and equality constraints result from the state boundary conditions. The unknowns are no longer $\mathbf{x}(t)$, $\mathbf{u}(t)$, but rather the coefficients $\mathbf{a}$. The minimization problem is summarized as follows

$$\begin{aligned} &\min_{\mathbf{a}} \ \hat{J}^{[k+1]} = \frac{1}{2}\mathbf{a}^T \mathcal{H}\, \mathbf{a} \\ &\text{s.t.} \quad \mathcal{A}\mathbf{a} - \mathbf{b} < 0 \\ &\qquad \mathcal{A}_{\text{eq}}\mathbf{a} - \mathbf{b}_{\text{eq}} = 0 \end{aligned} \tag{5.47}$$

where the quadratic function $\mathcal{H}$ will be described below for the different cases. The matrices and vectors for inequality constraints are defined as

$$\mathcal{A} = \begin{bmatrix} \mathbf{B}(\mathbf{x}^{[k]}(\tau))^{-1}\left[\frac{2}{t_f}\left(\mathbf{I}_n \otimes \mathbf{T}^T(\tau)\mathbf{D}^T\right) - \mathbf{A}(\mathbf{x}^{[k]}(\tau))\left(\mathbf{I}_n \otimes \mathbf{T}^T(\tau)\right)\right] \\ -\mathbf{B}(\mathbf{x}^{[k]}(\tau))^{-1}\left[\frac{2}{t_f}\left(\mathbf{I}_n \otimes \mathbf{T}^T(\tau)\mathbf{D}^T\right) - \mathbf{A}(\mathbf{x}^{[k]}(\tau))\left(\mathbf{I}_n \otimes \mathbf{T}^T(\tau)\right)\right] \\ \left(\mathbf{I}_n \otimes \mathbf{T}^T(\tau)\right) \\ -\left(\mathbf{I}_n \otimes \mathbf{T}^T(\tau)\right) \end{bmatrix} \tag{5.48}$$

$$\mathbf{b} = \begin{bmatrix} \mathbf{u}_{\max} \\ -\mathbf{u}_{\min} \\ \mathbf{x}_{\max} \\ -\mathbf{x}_{\min} \end{bmatrix} \tag{5.49}$$

and matrices and vectors for equality constraints are defined as

$$\mathcal{A}_{\text{eq}} = \left[\left(\mathbf{I}_n \otimes T^T(-1) \right) \right] \tag{5.50}$$

$$\mathbf{b}_{\text{eq}} = \left[\mathbf{x}_0 \right] \tag{5.51}$$

Consider that Eqs. (5.50) and (5.51) are valid for soft constrained problems in which the final state conditions are not specified. The matrices and vectors for equality constraints for hard constrained problems and mixed constrained problems are rewritten in Sec. 5.2.2.2 and Sec. 5.2.2.3, respectively. To summarize the proposed method, for the first iteration, the states, the state matrix, and the control matrix are written as $\mathbf{x}^{[k]} = \mathbf{x}_0$, $\mathbf{A}(\mathbf{x}^{[k]}(\tau), \tau) = \mathbf{A}(\mathbf{x}_0)$, and $\mathbf{B}(\mathbf{x}^{[k]}(\tau), \tau) = \mathbf{B}(\mathbf{x}_0)$, respectively. Furthemore, the TVLQR approximations represented in Eq. (5.28)

$$\frac{\mathrm{d}\mathbf{x}^{[k+1]}}{\mathrm{d}\tau}(\tau) = \frac{t_f}{2}[\mathbf{A}(\mathbf{x}^{[k]}(\tau), \tau)\, \mathbf{x}^{[k+1]} + \mathbf{B}(\mathbf{x}^{[k]}(\tau), \tau)\, \mathbf{u}^{[k+1]}]$$

followed by the herein equations in Sec. 5.2.2, help to understand that for the second, third, and the other iterations, the state variables $\mathbf{x}^{[k+1]}$ are approximated by Chebyshev polynomials and the inputs $\mathbf{u}^{[k+1]}$ will be obtained from the states and their derivatives. Note that $\mathbf{A}(\mathbf{x}^{[k]}(\tau), \tau)$ and $\mathbf{B}(\mathbf{x}^{[k]}(\tau), \tau)$ matrices for each iteration are evaluated by the states of the previous iteration. Next, the optimization problem in Eq. (5.47) with its equality and inequality constrained has to be solved to get the parameters in the $\mathbf{a}^T = [a_0^{(1)}/2, a_1^{(1)}, ..., a_N^{(1)},\ a_0^{(2)}/2, ..., a_N^{(2)}, ...,\ a_0^{(n)}/2, ..., a_N^{(n)}]$ matrix.

This optimization problem is a type of quadratic programming problem which is the problem of finding a vector $\mathbf{a}$ that minimizes a quadratic function $1/2\, \mathbf{a}^T \mathcal{H}\, \mathbf{a}$, subject to linear constraints. For implementations and numerical examples, the quadprog syntax of Matlab with the interior-point-convex algorithm is used to solve

the problems in the current thesis. To this end, the states, the state derivatives and the inputs are evaluated from Eqs. (5.34), (5.36), and (5.41), respectively.

5.2.2.1 Soft Constrained Problem

The quadratic function required for minimization problem (5.47) is given by

$$\mathcal{H} = \mathbf{h}_0 + \frac{t_f}{2}\int_{-1}^{1}\left[\mathbf{h}_1 + \frac{4}{{t_f}^2}\mathbf{h}_2 + \mathbf{h}_3 - \frac{2}{t_f}\mathbf{h}_4 - \frac{2}{t_f}\mathbf{h}_5\right]\mathrm{d}\tau \tag{5.52}$$

Since the final state is not specified, the equality constraint's matrices and vectors are as stated in Eqs. (5.50) and (5.51).

5.2.2.2 Hard Constrained Problem

The quadratic function required for minimization problem (5.47) is in the form of

$$\mathcal{H} = \frac{t_f}{2}\int_{-1}^{1}\left[\mathbf{h}_1 + \frac{4}{{t_f}^2}\mathbf{h}_2 + \mathbf{h}_3 - \frac{2}{t_f}\mathbf{h}_4 - \frac{2}{t_f}\mathbf{h}_5\right]\mathrm{d}\tau \tag{5.53}$$

where final state condition $\mathbf{x}_f$ is specified in this case. For HCP, the matrices and vectors for equality constraints of the optimization problem are expressed in the form of

$$\mathcal{A}_{\text{eq}} = \begin{bmatrix}\left(\mathbf{I}_n \otimes T^T(-1)\right)\\ \left(\mathbf{I}_n \otimes T^T(1)\right)\end{bmatrix} \tag{5.54}$$

$$\mathbf{b}_{\text{eq}} = \begin{bmatrix}\mathbf{x}_0\\ \mathbf{x}_f\end{bmatrix} \tag{5.55}$$

5.2.2.3 Mixed Constrained Problem

The quadratic function required for minimization problem (5.47) is given by

$$\mathcal{H} = \mathbf{h}_0 + \frac{t_f}{2}\int_{-1}^{1}\left[\mathbf{h}_1 + \frac{4}{{t_f}^2}\mathbf{h}_2 + \mathbf{h}_3 - \frac{2}{t_f}\mathbf{h}_4 - \frac{2}{t_f}\mathbf{h}_5\right]\mathrm{d}\tau \tag{5.56}$$

The final state is not fully specified in this case. Let the state to be decomposed as $x=(y,z)$, where $y=(x_1,\ldots,x_r)$ are the r known components at final time, whereas $z=(x_{r+1},\ldots,x_n)$ are the remaining $n-r$ free components at final time. So, the equality constraint conditions may be written as

$$\mathcal{A}_{\text{eq}}=\begin{bmatrix}\left(\mathbf{I}_n\otimes T^T(-1)\right)\\ \left(\mathbf{I}_{r\times n}\otimes T^T(1)\right)\end{bmatrix} \tag{5.57}$$

$$\mathbf{b}_{\text{eq}}=\begin{bmatrix}\mathbf{x}_0\\ \mathbf{y}_f\end{bmatrix} \tag{5.58}$$

Also, it is important to notice that matrix $\mathbf{S}$ in Eq. (5.43) for $\mathbf{h}_0$ term, should be updated as

$$\mathbf{S}=\begin{bmatrix}\mathbf{0}_{r\times r} & \mathbf{0}_{r\times(n-r)}\\ \mathbf{0}_{(n-r)\times r} & \mathbf{S}_{(n-r)\times(n-r)}\end{bmatrix}$$

where the terms $\mathbf{0}$'s in above matrix are zero matrices.

5.2.3 Number of Inputs Less than Number of States

Remember the approximated equation for $\mathbf{u}^{[k+1]}$ represented in (5.41), which shows that the inverse matrix of $\mathbf{B}(\mathbf{x}^{[k]})$ is required. For the case with $n=m$, the matrix $\mathbf{B}(\mathbf{x}^{[k]})$ is square and the necessary condition for that is to be invertible. However, for the case in which, $n>m$, the matrix $\mathbf{B}(\mathbf{x}^{[k]})$ is not square, so not invertible and the following technique briefly explained in [38] may be used. This technique is applicable to the systems that are written in the form of Eq.(5.59). Consider the dynamic system represented in Eq.(5.5), for the case $n>m$, to be written as

$$
\begin{aligned}
\dot{x}_1(t) &= A_{11}x_1(t)+A_{12}x_2(t)+\ldots+A_{1n}x_n(t)\\
&\vdots\\
\dot{x}_{q-1}(t) &= A_{(q-1)1}x_1(t)+A_{(q-1)2}x_2(t)+\ldots+A_{(q-1)n}x_n(t)\\
\dot{x}_q(t) &= A_{q1}x_1(t)+A_{q2}x_2(t)+\ldots+A_{qn}x_n(t)+B_{q1}u_1(t)+B_{q2}u_2(t)+\ldots+B_{qm}u_m(t)\\
&\vdots\\
\dot{x}_n(t) &= A_{n1}x_1(t)+A_{n2}x_2(t)+\ldots+A_{nn}x_n(t)+B_{n1}u_1(t)+B_{n2}u_2(t)+\ldots+B_{nm}u_m(t)
\end{aligned}
\tag{5.59}
$$

where the subscript q is defined as $q = n - m + 1$, and the **A** and **B** terms may be state dependent, and these terms are evaluated with the previous iteration's values at the current iteration. Converting the equations to Chebyshev time domain results in

$$
\begin{aligned}
\dot{x}_1(\tau) &= \frac{t_f}{2}\left(A_{11}x_1(\tau)+A_{12}x_2(\tau)+\ldots+A_{1n}x_n(\tau)\right)\\
&\vdots\\
\dot{x}_{q-1}(\tau) &= \frac{t_f}{2}\left(A_{(q-1)1}x_1(\tau)+A_{(q-1)2}x_2(\tau)+\ldots+A_{(q-1)n}x_n(\tau)\right)\\
\dot{x}_q(\tau) &= \frac{t_f}{2}\left(A_{q1}x_1(\tau)+A_{q2}x_2(\tau)+\ldots+A_{qn}x_n(\tau)+B_{q1}u_1(\tau)+B_{q2}u_2(\tau)+\ldots+B_{qm}u_m(\tau)\right)\\
&\vdots\\
\dot{x}_n(\tau) &= \frac{t_f}{2}\left(A_{n1}x_1(\tau)+A_{n2}x_2(\tau)+\ldots+A_{nn}x_n(\tau)+B_{n1}u_1(\tau)+B_{n2}u_2(\tau)+\ldots+B_{nm}u_m(\tau)\right)
\end{aligned}
\tag{5.60}
$$

Now, approximate the states $x_1(\tau), x_2(\tau), \ldots, x_{q-1}(\tau)$ by Chebyshev polynomials as represented in Eq. (5.35), and then obtain the first and second derivatives of them by using Eqs. (5.36) and (5.39). Rearrange the first $q-1$ terms in (5.59) as following to obtain the states $x_q(\tau), x_{q+1}(\tau), \ldots, x_n(\tau)$.

$$
\begin{aligned}
\frac{2}{t_f}\dot{x}_1(\tau)-A_{11}x_1(\tau)-\cdots-A_{1(q-1)}x_{q-1}(\tau) &= A_{1q}x_q(\tau)+\cdots+A_{1n}x_n(\tau)\\
&\vdots\\
\frac{2}{t_f}\dot{x}_{q-1}(\tau)-A_{(q-1)1}x_1(\tau)-\cdots-A_{(q-1)(q-1)}x_{q-1}(\tau) &= A_{qq}x_q(\tau)+\cdots+A_{qn}x_n(\tau)
\end{aligned}
\tag{5.61}
$$

By taking the derivative from both sides of Eq.(5.61), the terms $\dot{x}_q(\tau), \dot{x}_{q+1}(\tau), \ldots, \dot{x}_n(\tau)$ will be obtained. So,

$$\begin{aligned} \frac{2}{t_f}\ddot{x}_1(\tau) - A_{11}\dot{x}_1(\tau) - \cdots - A_{1(q-1)}\dot{x}_{q-1}(\tau) &= A_{1q}\dot{x}_q(\tau) + \cdots + A_{1n}\dot{x}_n(\tau) \\ &\vdots \\ \frac{2}{t_f}\ddot{x}_{q-1}(\tau) - A_{(q-1)1}\dot{x}_1(\tau) - \cdots - A_{(q-1)(q-1)}\dot{x}_{q-1}(\tau) &= A_{qq}\dot{x}_q(\tau) + \cdots + A_{qn}\dot{x}_n(\tau) \end{aligned} \tag{5.62}$$

To this end, from last m equations of (5.60) the required inputs will be found. These inputs $u_1, u_2, \ldots, u_m$ are obtained from

$$\begin{aligned} \frac{2}{t_f}\dot{x}_q(\tau) - A_{q1}x_1(\tau) - \cdots - A_{qn}x_n(\tau) &= B_{q1}u_1(\tau) + B_{q2}u_2(\tau) + \cdots + B_{qm}u_m(\tau) \\ &\vdots \\ \frac{2}{t_f}\dot{x}_n(\tau) - A_{n1}x_1(\tau) - \cdots - A_{nn}x_n(\tau) &= B_{n1}u_1(\tau) + B_{q2}u_2(\tau) + \cdots + B_{nm}u_m(\tau) \end{aligned} \tag{5.63}$$

Then, following the same approach represented in Sec. 5.2.2 gives the updated versions of the Eqs. (5.43), (5.46), and (5.48).

CHAPTER 6

APPLICATION OF STATE DEPENDENT RICCATI EQUATION METHOD TO SPACECRAFT COULOMB FORMATIONS

6.1 State Dependent Riccati Equation Method

Consider an autonomous, infinite-horizon, nonlinear regulator problem for minimizing the performance index

$$J = \frac{1}{2}\int_0^\infty \mathbf{x}^T Q(\mathbf{x})\mathbf{x} + \mathbf{u}^T R(\mathbf{x})\mathbf{u}dt \tag{6.1}$$

Subject to the nonlinear differential constraints

$$\dot{\mathbf{x}} = \mathbf{f}(\mathbf{x}) + \mathbf{B}(\mathbf{x})\mathbf{u} \tag{6.2}$$

With state vector $\mathbf{x} \in \mathbb{R}^n$ and input vector $\mathbf{u} \in \mathbb{R}^m$, such that $\mathbf{f}: \mathbb{R}^n \to \mathbb{R}^n$ and $\mathbf{B}: \mathbb{R}^n \to \mathbb{R}^{n\times m}$, with $\mathbf{B} \neq 0 \forall \mathbf{x}$, and $Q: \mathbb{R}^n \to \mathbb{R}^{n\times n}$ and $R: \mathbb{R}^n \to \mathbb{R}^{m\times m}$ for all $\mathbf{x}$ are positive semi-definite and positive-definite matrices, respectively, and $\mathbf{f}(0) = 0$, which does not have bias term [16, 44].

The SDRE approach for obtaining a suboptimal, locally asymptotically stabilizing solution of problem which stated in Eqs. (6.1)-(6.2) may be realized first by obtaining the state dependent coefficient (SDC) form of Eq. (6.2) as

$$\dot{\mathbf{x}} = \mathbf{A}(\mathbf{x})\mathbf{x} + \mathbf{B}(\mathbf{x})\mathbf{u} \tag{6.3}$$

The SDC representation in Eq. (6.3) is a stabilizable (respectively controllable) parameterization of the nonlinear system in Eq. (6.2) in a region Γ if the pair (A(x), B(x)) is point wise stabilizable (respectively controllable) in the linear sense for all $\mathbf{x} \in \Gamma$, and $\boldsymbol{f}(\mathbf{x})$ is a continuously differentiable vector-valued function of $\mathbf{x}$ on Γ, that is, $\mathbf{f}(.) \in C^1(\Gamma)$, and $\mathbf{B}(\mathbf{x})$ is a $C^0(\Gamma)$ matrix-valued function. Assuming that the

states are slowly varying and considering $\mathbf{A}$ and $\mathbf{B}$ matrices are constant, the Riccati equation may be solved as

$$P(\mathbf{x})\mathbf{A}(\mathbf{x}) + \mathbf{A}^T(\mathbf{x})P(\mathbf{x}) - P(\mathbf{x})\mathbf{B}(\mathbf{x})R^{(-1)}(\mathbf{x})\mathbf{B}^T(\mathbf{x})P(\mathbf{x}) + Q(\mathbf{x}) = 0 \tag{6.4}$$

Then, the feedback control is obtained just like the linear quadratic regulator case as

$$\mathbf{u}(\mathbf{x}) = -R^{(-1)}(\mathbf{x})\mathbf{B}^T(\mathbf{x})P(\mathbf{x})\mathbf{x} \tag{6.5}$$

6.2 Numerical Simulations

To demonstrate the effectiveness of the SDRE control method, nonlinear simulations are coded in the Matlab environment for each of the nonlinear formation equations. The objective in all the cases of two-craft configurations is to bring the satellites 25 m apart. Table 1 shows the simulation parameters for the two-craft implementations. For the two-craft numerical simulations, the weighting matrices are chosen as $\mathrm{Q} = \mathrm{diag}(10^6, 10^9, 10^9, 0,0,0)$ and $\mathrm{R} = \mathrm{diag}(10^{21}, 10^{20}, 10^{20})$.

Table 1. Simulation parameters for two-craft implementations.

Parameter	Value	Unit
m_1	150	kg
m_2	150	kg
L_{ref}	25	m
k_c	8.99×10^9	$\frac{Nm^2}{C^2}$
$\Omega_{Earth\ circular}$	7.2915×10^{-5}	$\frac{rad}{s}$
$\Omega_{Earth-moon}$	2.661699×10^{-6}	$\frac{rad}{s}$
σ	3.190432478	

For the planar three-craft formation equations presented in Chap. 4, the objective in all cases is to bring the satellites to a fixed shape and size. The parameters are given in Table 2. The weighting matrices for the quadratic performance index of three-craft formation are chosen as, $\mathrm{R} = \mathrm{diag}(10^{11}, 10^8, 10^9)$, and $Q = 10 \times I_6$.

The SDRE nonlinear feedback control of the formations is carried out, and the simulation results are given in the figures and tables.

Table 2. Simulation parameters for three-craft implementations.

Parameter	Value	Unit
m_1	100	kg
m_2	100	kg
m_3	100	kg
x_{1_e} (case 1)	44.616	m
x_{1_e} (case 2)	42.188	m
x_{2_e} (case 1)	19.125	m
x_{2_e} (case 2)	22.188	m
x_{3_e} (case 1)	-63.714	m
x_{3_e} (case 2)	-64.376	m
k_c	8.99e+9	$\frac{Nm^2}{C^2}$
H_0	350.972	$\frac{Kgm^2}{s}$
q_{1_e}	10	μC
q_{2_e}	10/7	μC
q_{3_e}	-200	μC

6.2.1 Orbit-Radial Two-craft Coulomb Formation at Earth Circular Orbits

The control objective is to bring the satellites $25\ m$ apart, and also bring the yaw and pitch angles to the zero. Figure 8 shows that the relative distance between the satellites settles down to desired distance, and attitudes are also stabilized and converged to zero. Therefore, the formation is brought back to the equilibrium radial configuration.

The initial deviation from the nominal state variables is chosen as $L = 15\ m$, $\psi = \frac{pi}{6}\ rad$, and $\theta = \frac{pi}{6}\ rad$. The simulation results show that all the state variables are regulated and going back to the equilibrium conditions. Therefore, the feedback control technique used here proves that even for the big initial errors for the states, the formation is regulated and stabilized around the equilibrium condition. Reference [5] shows the results of the linear equations of motion with small deviations from the nominal trajectory. A nonlinear Lyapunov-based feedback control is simulated in the literature and the results are given in [45]. In that paper, the only control action is the Coulomb force and there is no electrical force for changing the attitude of the formation. Furthermore, the nonlinear equations of motion used in the cited paper are not coupled and complex as those considered in the current thesis.

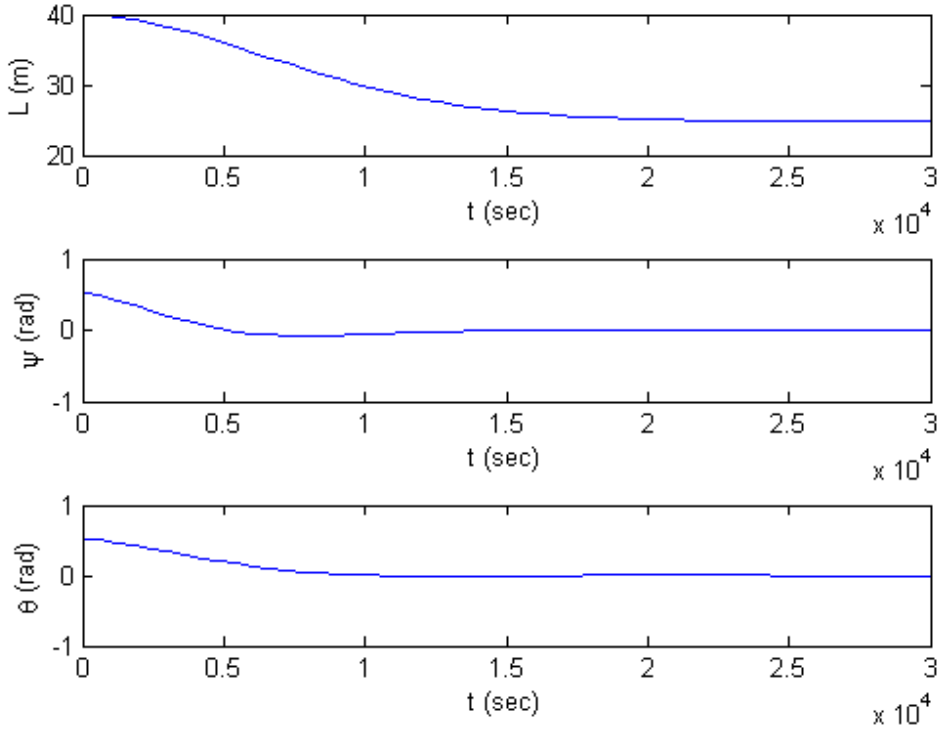

Figure 8. Separation distance, yaw angle, and pitch angle stabilizations using SDRE method for two-craft Earth circular orbit.

The control input histories shown in Figure 9 indicate that the requested control levels are reasonable and may be realized by Coulomb forces and electrical thrusters. The charge product of the two-craft is illustrated in Figure 10. Comparison of the values obtained in this thesis for Coulomb forces and charge products are in agreement with those given in [45]. Reference [20] shows numerical results for along-track and orbit-normal configurations as well.

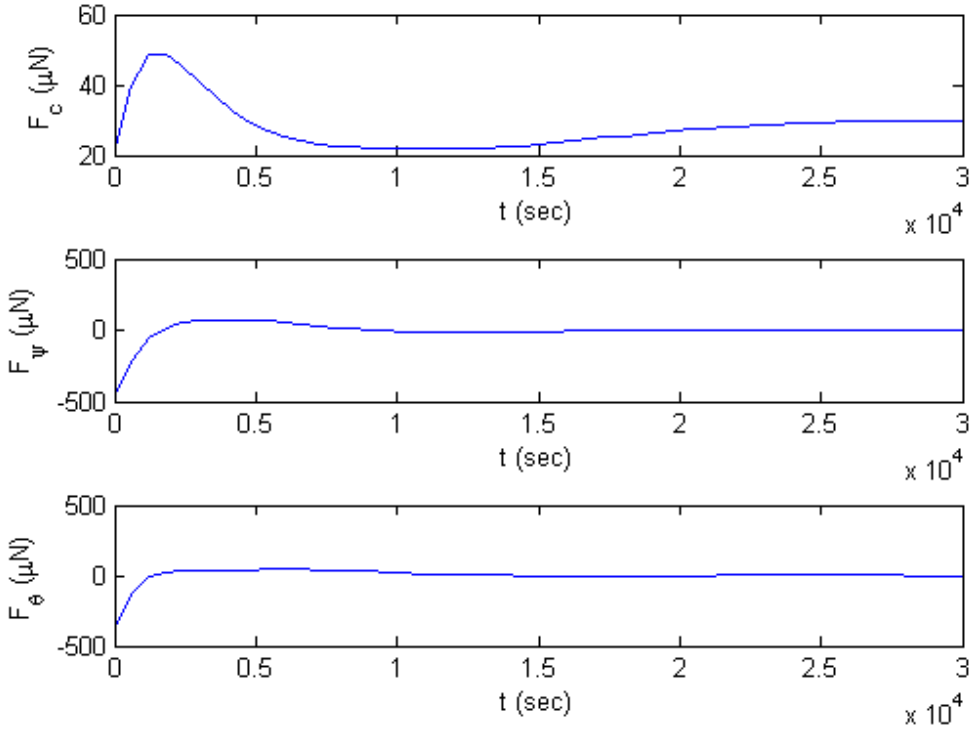

Figure 9. Coulomb force and the forces generated by the thrusters in the yaw and pitch direction using SDRE method for two-craft Earth circular orbit.

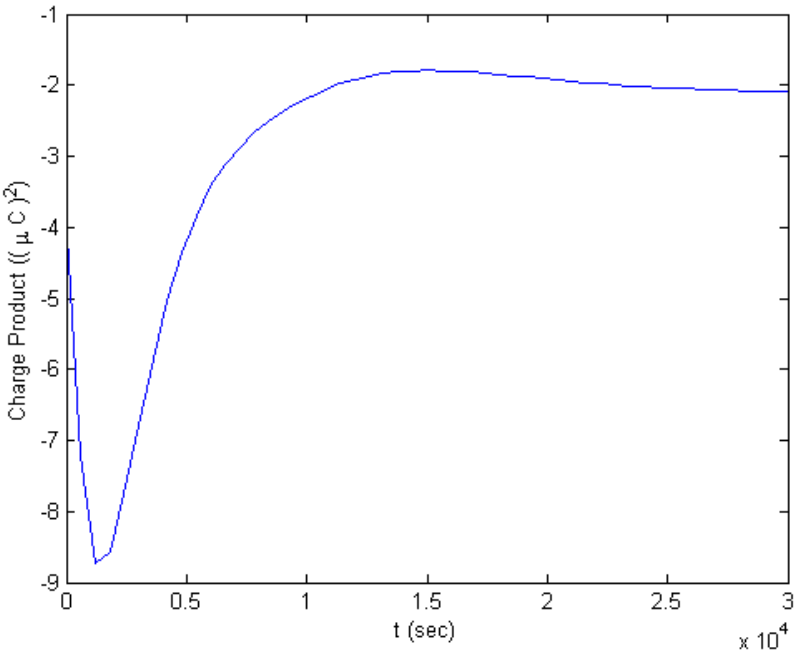

Figure 10. Charge product using SDRE method for two-craft Earth circular orbit.

6.2.2 Orbit-Radial Two-craft Coulomb Formation at Collinear Libration Points

The initial error from the nominal state variables is chosen as $L = 5\,m$, $\psi = \frac{pi}{8}\,rad$, and $\theta = \frac{pi}{8}\,rad$. The control objective is to bring the satellites $25\,m$ apart, and also bring the yaw and pitch angles to the zero. Figure 11 shows that the relative distance between the satellites settles down to desired distance, and attitudes are also stabilized and converged to zero. Therefore, the formation is brought back to the equilibrium radial configuration. A linear stability analysis at orbit radial collinear libration points was studied [8]. Also, the stabilization of the two-craft system in the presence of the solar radiation pressure using Lyapunov-based feedback control is addressed in the literature [9].

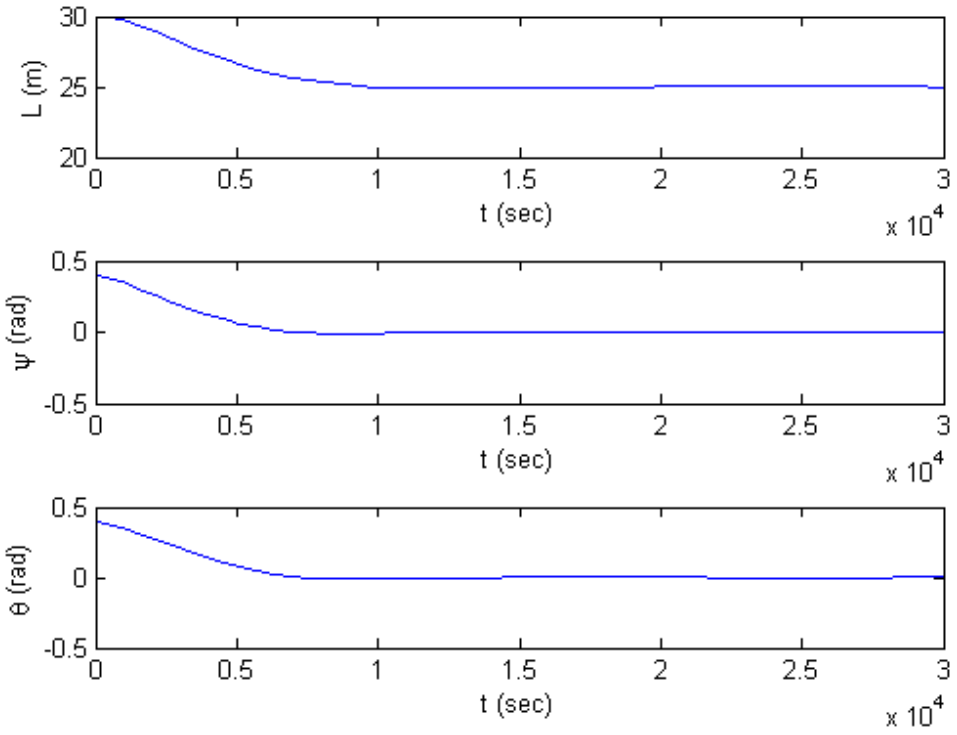

Figure 11. Separation distance, yaw angle, and pitch angle stabilizations using SDRE method for two-craft collinear libration point.

The control input histories shown in Figure 12 indicate that the requested control levels are reasonable and may be realized by Coulomb forces and electrical thrusters. The level of the forces are in agreement with those given in the literature [8, 9]. The

charge product of the two-craft is illustrated in Figure 13 that is also reasonable. The numerical simulations for along-tack and orbit-normal configurations are addressed in [26].

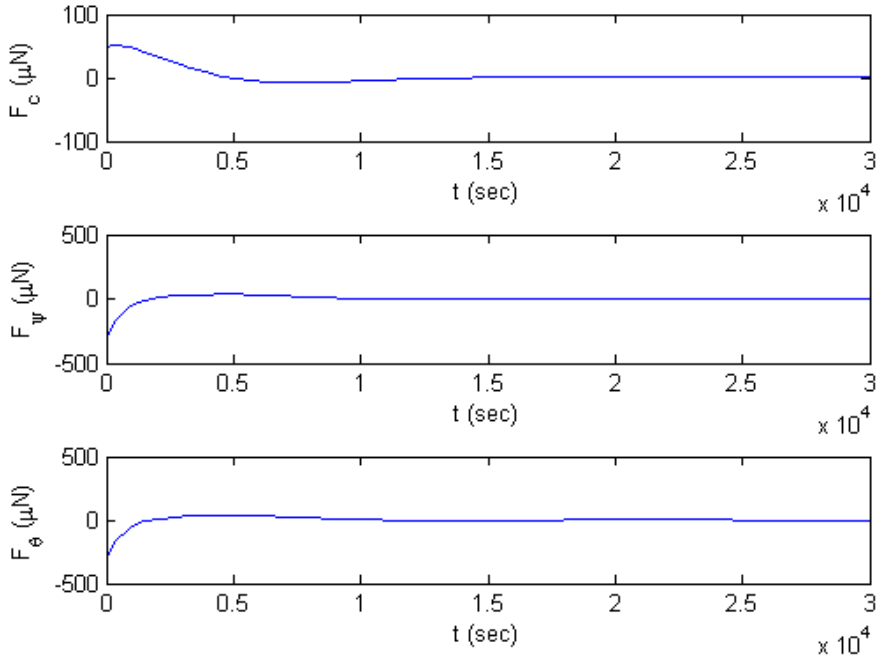

Figure 12. Coulomb force and the forces generated by the thrusters in the yaw and pitch direction using SDRE method for two-craft collinear libration point.

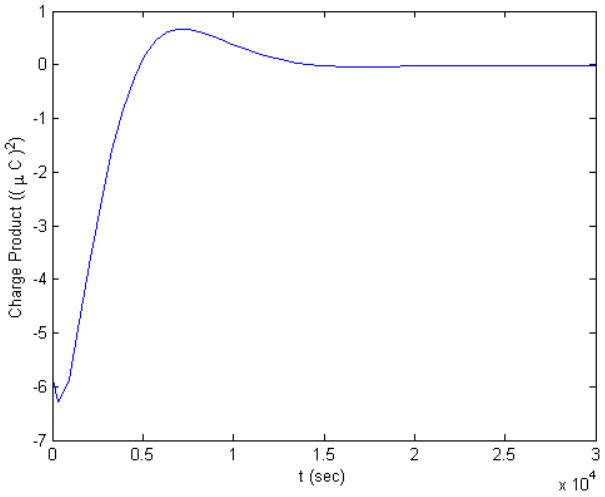

Figure 13. Charge product using SDRE method for two-craft collinear libration point.

6.2.3 Orbit-Radial Two-craft Coulomb Formation at Triangular Libration Points

The control objective is to bring the satellites $25\,m$ apart from its initial error which is $L = 5\,m$. Also, stabilize the yaw and pitch angles around zero from their initial deviations that are $\psi = \frac{pi}{8}\ rad$, and $\theta = \frac{pi}{8}\ rad$, respectively. Figure 14 shows that the relative distance between the satellites settles down to desired distance, and attitudes are also stabilized and converged to zero. Reference [8] shows the linearized dynamics and stability analysis of the two-craft at triangular libration points. The current thesis presents the first nonlinear feedback control method applied to such a system.

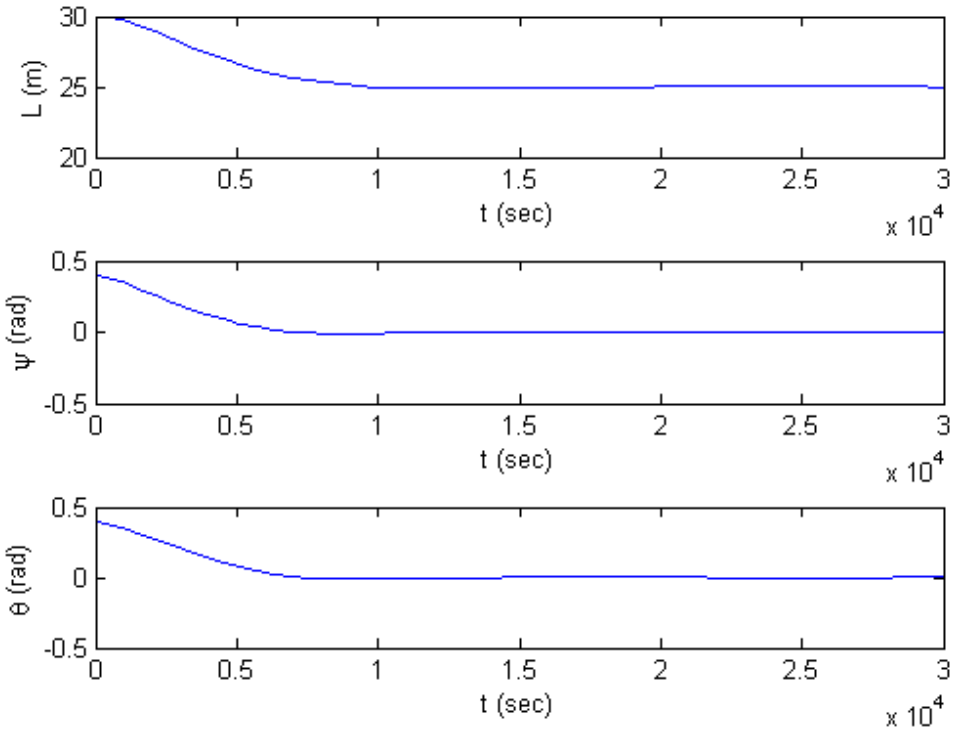

Figure 14. Separation distance, yaw angle, and pitch angle stabilizations using SDRE method for two-craft triangular libration point.

The control time histories are given in Figure 15. The charge product of the two-craft is shown in Figure 16.

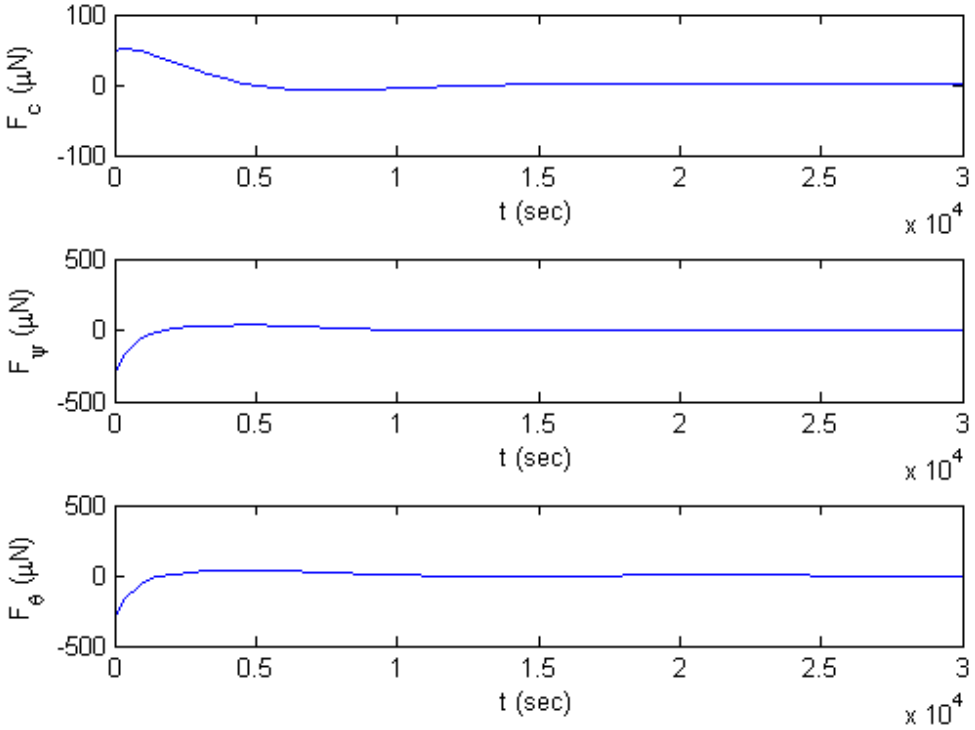

Figure 15. Coulomb force and the forces generated by the thrusters in the yaw and pitch direction using SDRE method for two-craft triangular libration point.

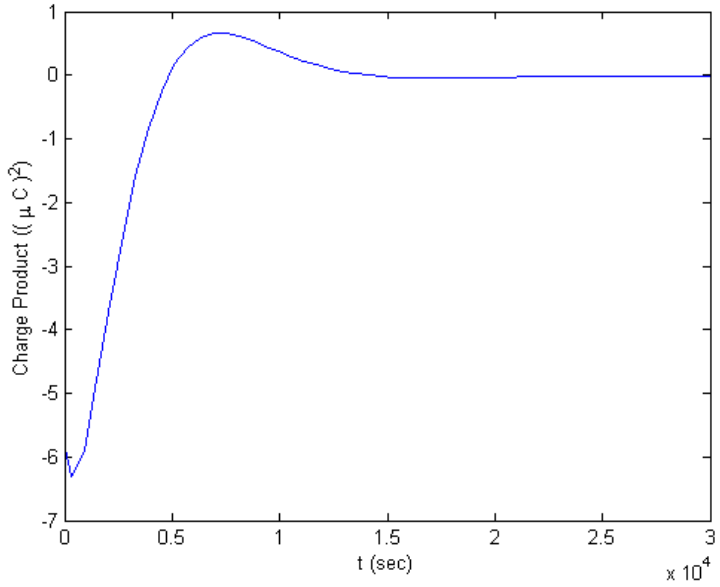

Figure 16. Charge product using SDRE method for two-craft triangular libration point.

6.2.4 Three-craft Coulomb Formation at Deep Space

Two equilibrium cases are considered. In the first one, the equilibrium is said to be marginally stable, and in the second one it is an unstable equilibrium point [12]. These equilibriums are controlled by using the SDRE control method. Simulation results of Case 1 are illustrated in the following figures. The plots in Figure 17, Figure 18, and Figure 19 give the positions of the three spacecraft from center of mass. The spacecraft all initially are away from the equilibrium condition. It may be observed that they are brought to the equilibrium.

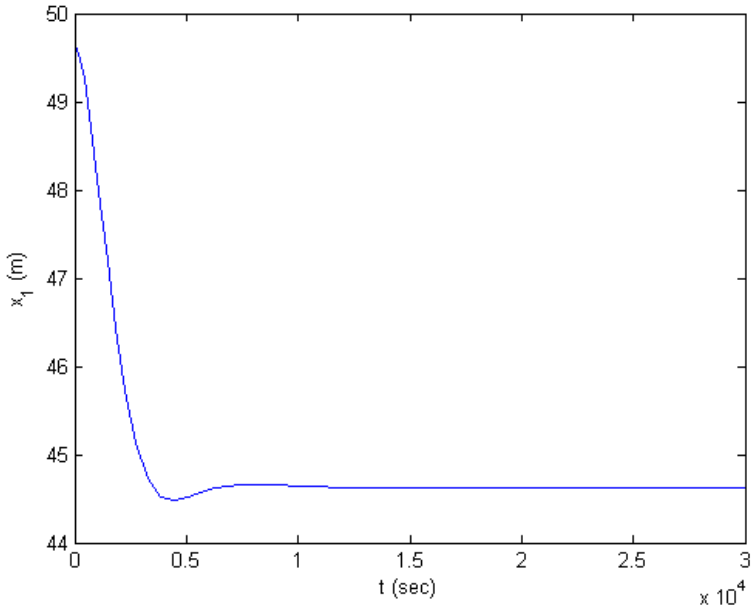

Figure 17. Position history of Craft1 for Case1.

The control forces are presented in Figure 20. It is showed that the control forces are reasonable and may be realized by coulomb forces. Angular velocity of the formation is given in Figure 21. It may be concluded that the angular velocity is also brought to the equilibrium value as well. The in-plane and out-of-plane linear stability analysis was performed in the literature [12, 46]. The three-spacecraft Coulomb formation collinear and triangular shape control problems using Lyapunov-based method is addressed [11, 47]. The results of the SDRE nonlinear feedback control method used in the current thesis are in agreement with the cited papers in the presence of very large initial position errors.

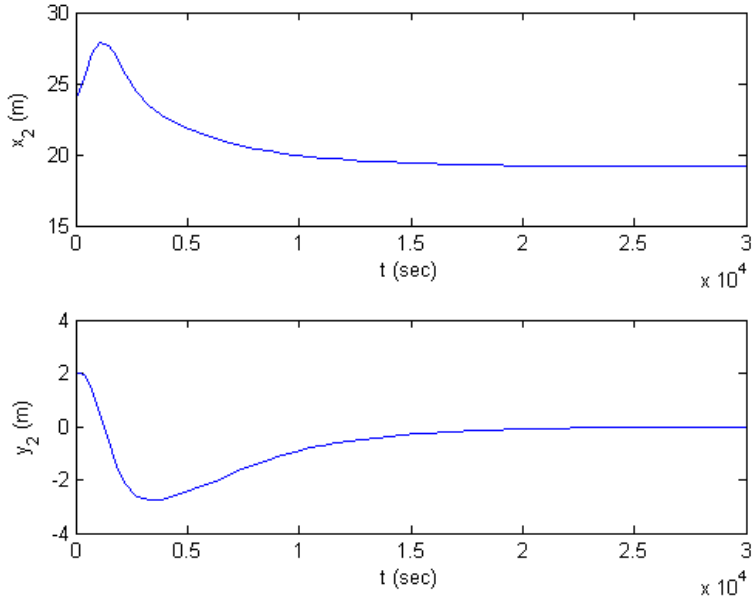

Figure 18. Position history of Craft2 for Case1.

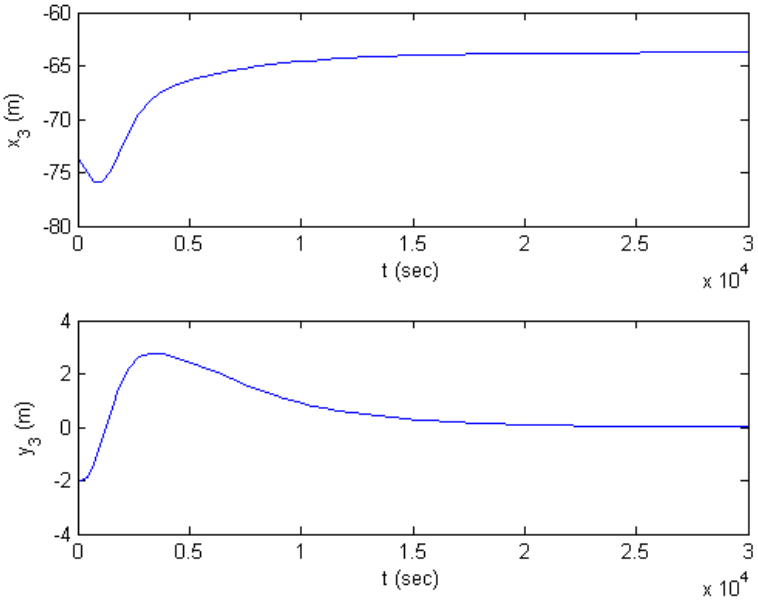

Figure 19. Position history of Craft2 for Case1.

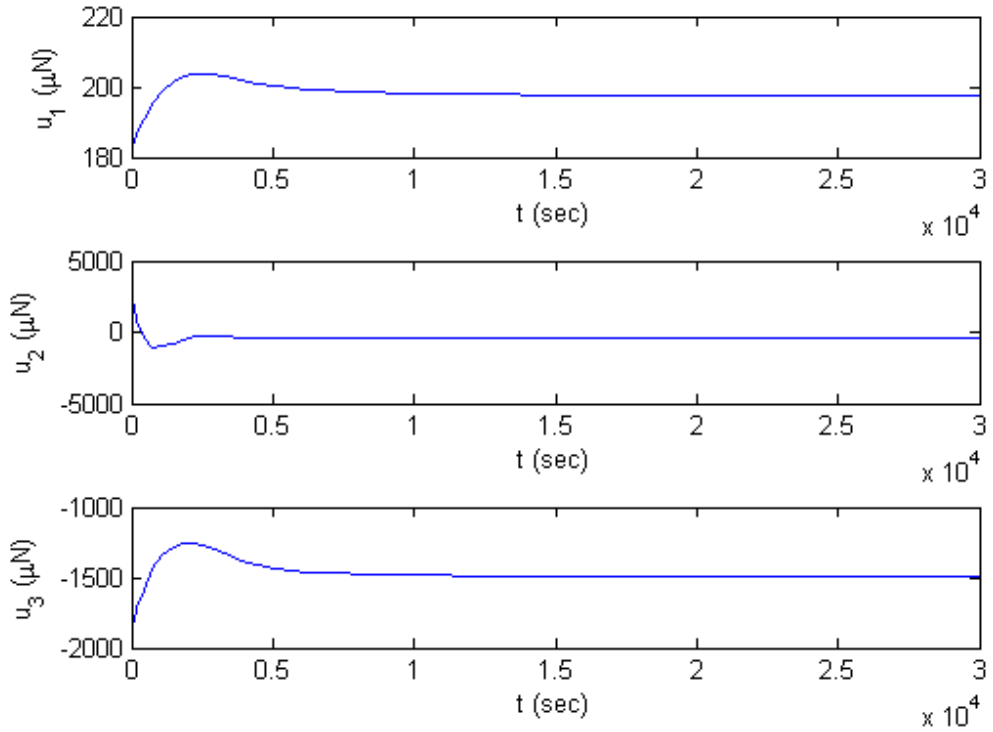

Figure 20. Control inputs for Case 1.

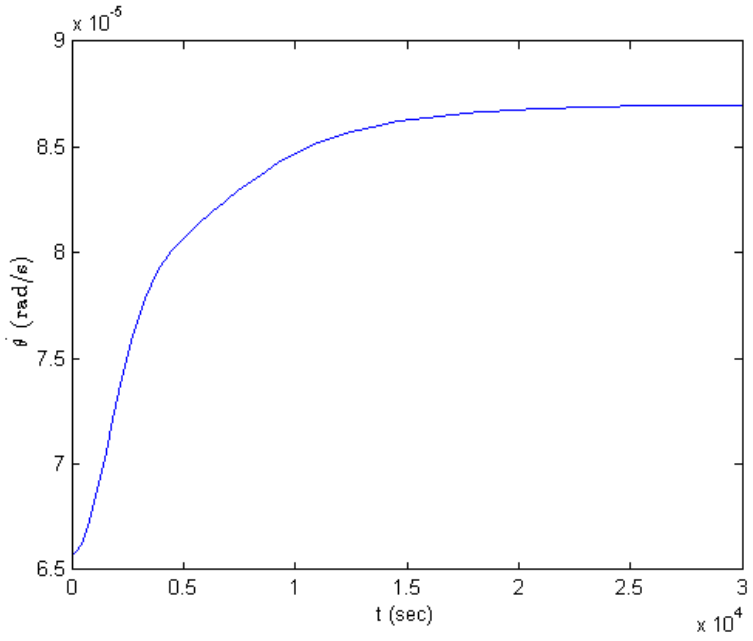

Figure 21. Formation angular velocity for Case 1.

Simulation results for Case 2 are shown below. In this case, the targeted equilibrium is unstable. The spacecraft start from arbitrary positions. From Figure 22, Figure 23, and Figure 24 it may be observed that all the three spacecraft are brought to the desire equilibrium position. The control inputs are given in Figure 25, and it is concluded from the plots that they may easily be realized with coulomb forces. Figure 26 shows the angular velocity of the formation for case 2. This shows the angular velocity reaches the desired value, as the spacecraft are brought to their equilibrium positions. The details of this part are presented in [21].

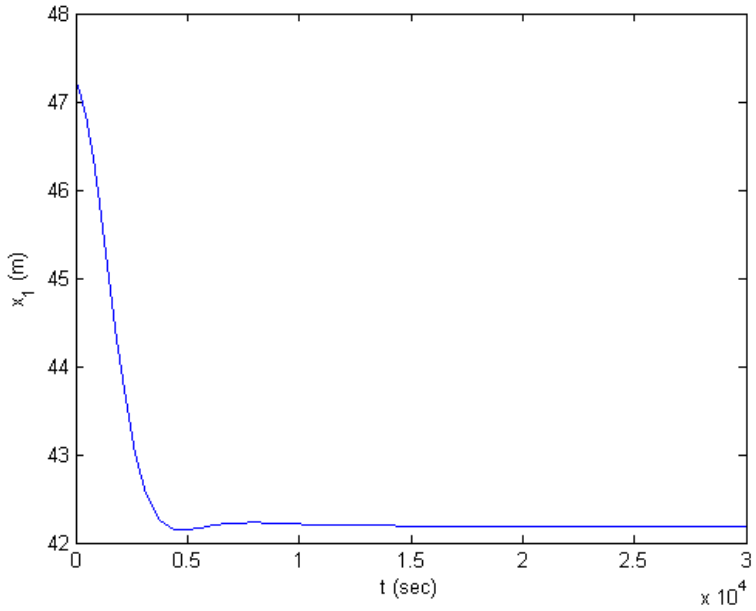

Figure 22. Position history of Craft1 for Case2.

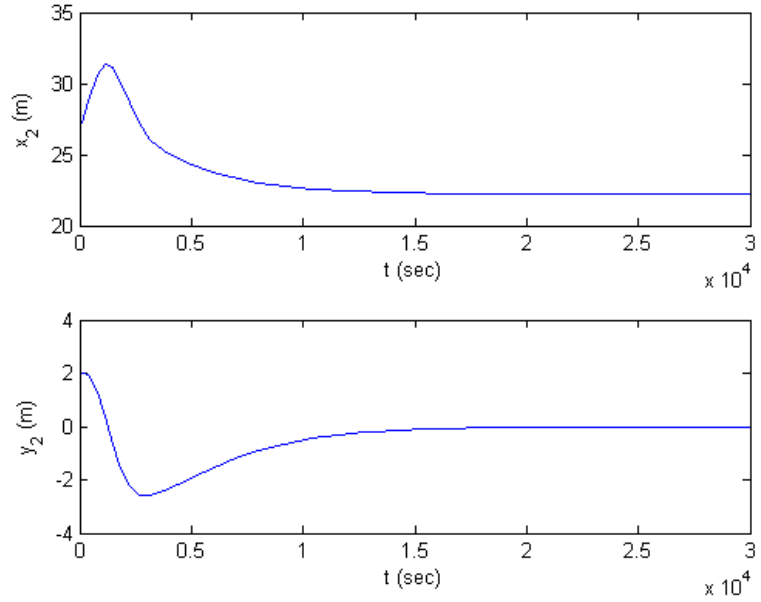

Figure 23. Position history of Craft2 for Case2.

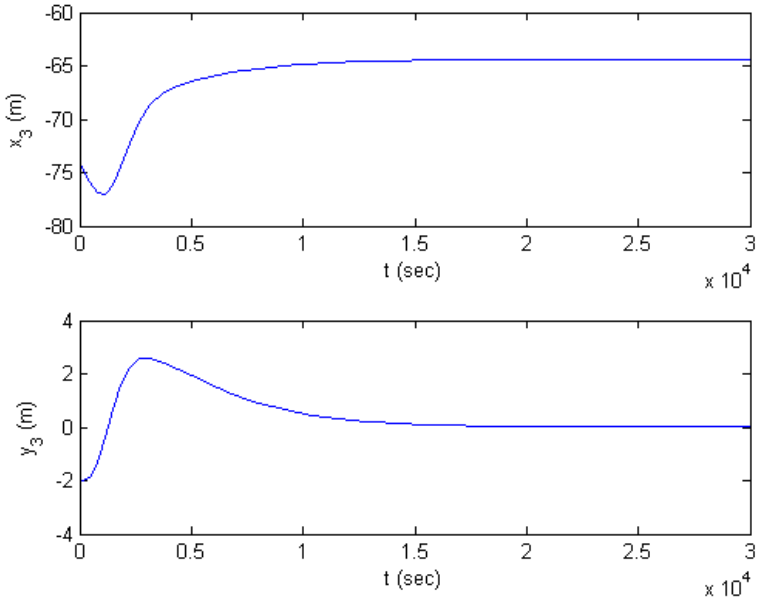

Figure 24. Position history of Craft2 for Case2.

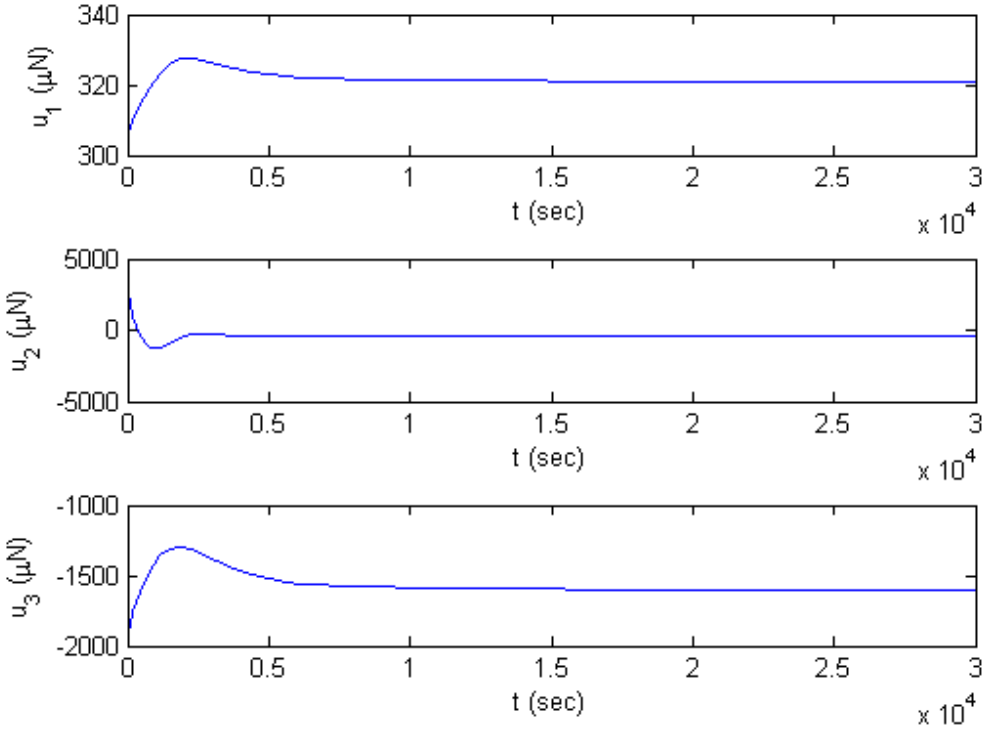

Figure 25. Control inputs for Case 2.

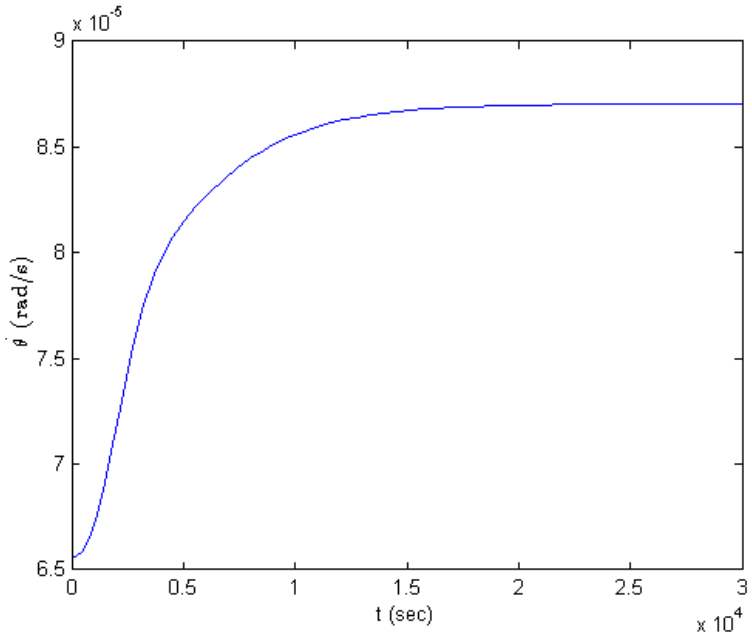

Figure 26. Formation angular velocity for Case 2.

CHAPTER 7

APPLICATION OF STATE DEPENDENT FACTORIZED OPTIMAL CONTROL METHODS TO SPACECRAFT COULOMB FORMATIONS

7.1 Numerical Simulations

In all the cases, the optimization problem represented in Eq. (5.47) is solved in Matlab using quadprog syntax with interior-point-convex algorithm with Intel Core i5 CPU 2.30 GHz. In the present implementations, the convergence is reached when

$$\varepsilon = \| \mathbf{x}^{[k+1]} - \mathbf{x}^{[k]} \|_{\infty} = \max_{t \in [t_0, t_f]} \{ | x_j^{[k+1]}(t) - x_j^{[k]}(t) |, j = 1, \ldots, n \} \leq \text{tol}$$

where ε is error and `tol' is a prescribed tolerance.

7.1.1 Orbit-Radial Two-craft Coulomb Formation at Earth Circular Orbits

Case 1. Unconstrained case is implemented here, and the results are given below. The number of iterations, error and objective function values are presented in Table 3,

Table 4, and Table 5 for the ASRE-approache1, ASRE-approach2, and SDC-Direct method, respectively. The objective function value for all the methods are in agreement with each other.

Table 3. ASRE-Approach1 iterations for two-craft Earth circular orbit Case1.

Iteration	Error	J
1	1.68E+01	3.02471E+11
2	1.71E+00	2.85011E+11
3	3.05E-01	2.82814E+11
4	2.01E-02	2.82568E+11
5	2.51E-03	2.82524E+11
6	5.81E-04	2.82519E+11
7	9.95E-05	2.82519E+11

Table 4. ASRE-Approach2 iterations for two-craft Earth circular orbit Case1.

Iteration	Error	J
1	1.68E+01	3.02472E+11
2	1.71E+00	2.85013E+11
3	3.05E-01	2.82814E+11
4	2.01E-02	2.82569E+11
5	2.51E-03	2.82524E+11
6	5.80E-04	2.82519E+11
7	9.94E-05	2.82519E+11

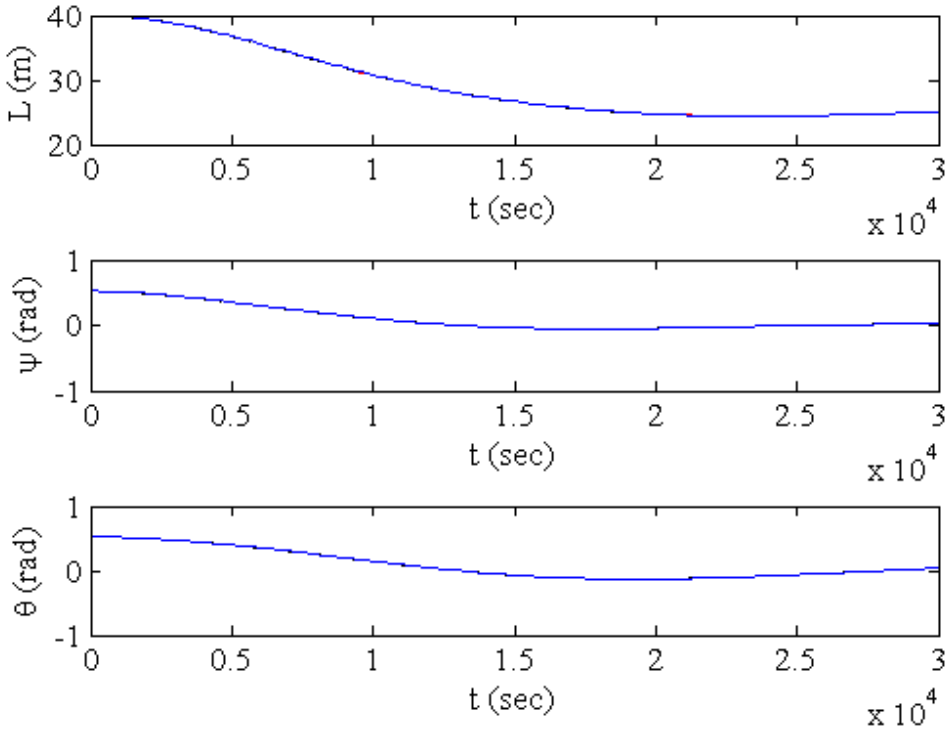

Figure 27. Approximate trajectory solutions using SDC Factorized optimal methods for two-craft Earth circular orbit Case1.

Table 5. SDC-Direct iterations for two-craft Earth circular orbit Case1.

Iteration	Error	J
1	1.68E+01	3.02432E+11
2	1.71E+00	2.84974E+11
3	3.04E-01	2.82777E+11
4	1.99E-02	2.82532E+11
5	2.64E-03	2.82487E+11
6	5.69E-04	2.82482E+11
7	1.01E-04	2.82482E+11
8	1.49E-05	2.82482E+11

The approximate trajectory and control solutions are illustrated in Figure 27 and Figure 28. These are the plots of three techniques that are approximately coincident to each other. This is a SCP in which the final states are not specified, and it is shown that the states are stabilized at the end and the formation is going to its equilibrium condition. Figure 29 shows the charge product of the two-craft.

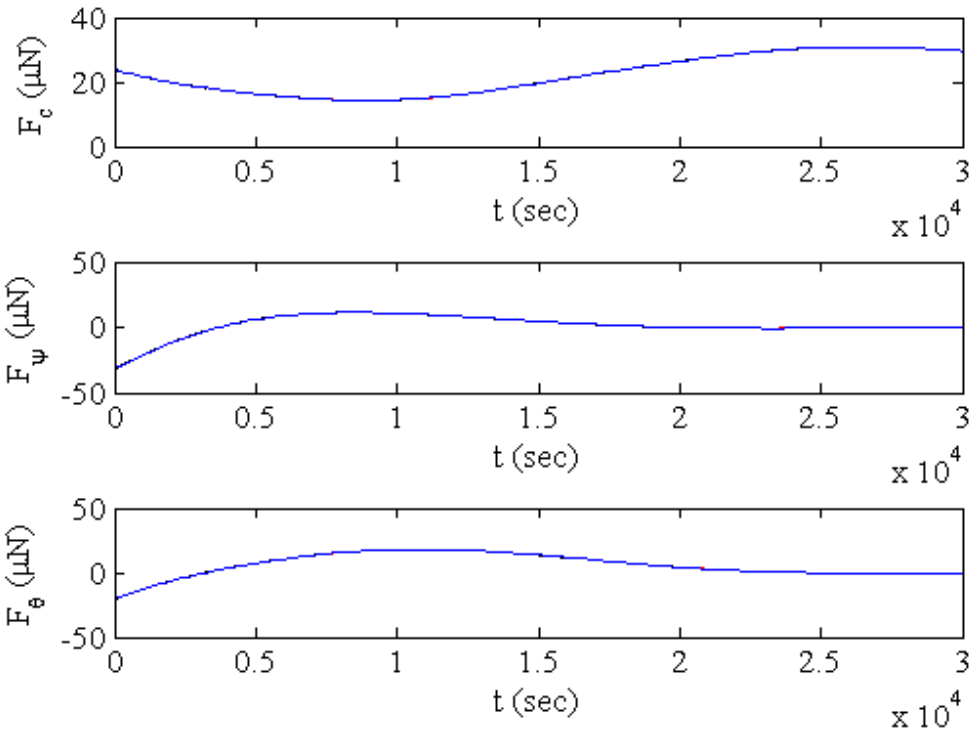

Figure 28. Approximate control solutions using SDC Factorized optimal methods for two-craft Earth circular orbit Case1.

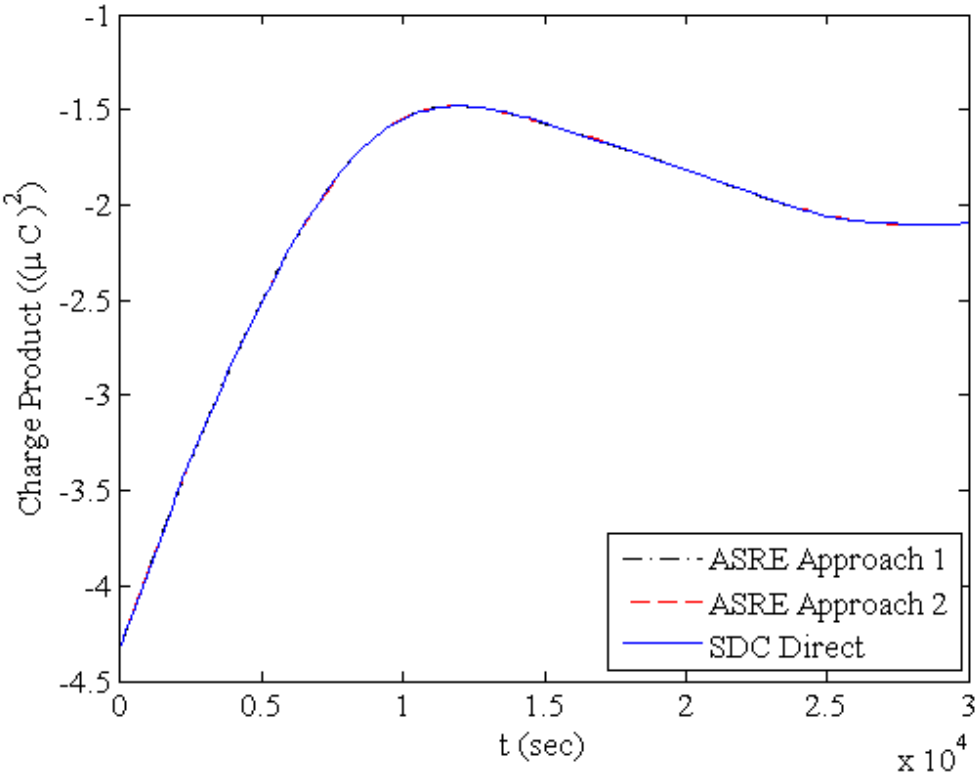

Figure 29. Charge product using SDC Factorized optimal methods for two-craft Earth circular orbit Case1.

Case 2. Here we consider that the states and inputs are constrained as

$$0 \le \psi$$
$$0 \le \theta$$
$$F_c \le 37.4\,\mu N$$
$$-30\,\mu N \le F_\psi$$
$$-30\,\mu N \le F_\theta$$

The results for the constrained case are given in Table 6. It is shown that the objective function value is increased because of the constraints. The approximate trajectory and control solutions are given in Figure 30 and Figure 31. In these figures, dashed lines show the constrained plots. Figure 32 shows the charge product of the two-craft.

Table 6. SDC-Direct iterations for two-craft Earth circular orbit Case2.

Iteration	Error	J
1	3.80E+01	6.12832E+11
2	2.18E+01	3.1057E+11
3	4.38E-01	3.05099E+11
4	4.65E-02	3.05207E+11
5	2.73E-03	3.05229E+11
6	3.79E-04	3.05233E+11
7	5.26E-05	3.05234E+11

Reference [7] addressed the in-plane optimal reconfigurations of the two-craft Coulomb formation at Earth circular orbits. In the cited paper, the two craft are reconfigured from one equilibria configuration to another one satisfying the dynamical constraints. The bounds on the inputs in [7] are the only constraints considered in that paper. In the current thesis, the SDC-Direct control approach handles the optimal control problems having bound on the inputs and states together as those given for case2. Moreover, the current work offers the in-plane and out-of-plane optimal maneuvers as is shown in Figure 30.

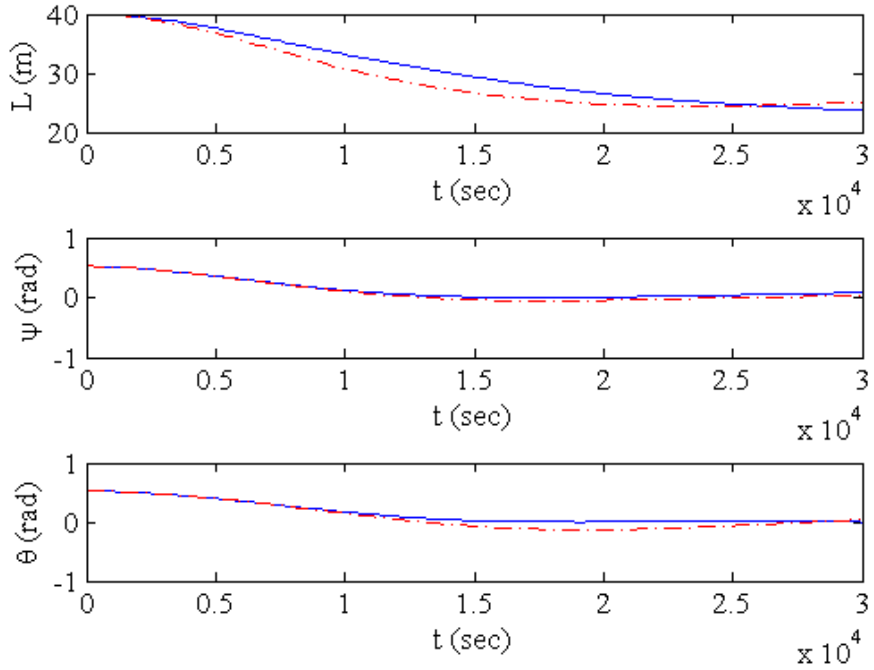

Figure 30. Approximate trajectory solutions using SDC Direct method for two-craft Earth circular orbit Case1 and Case2.

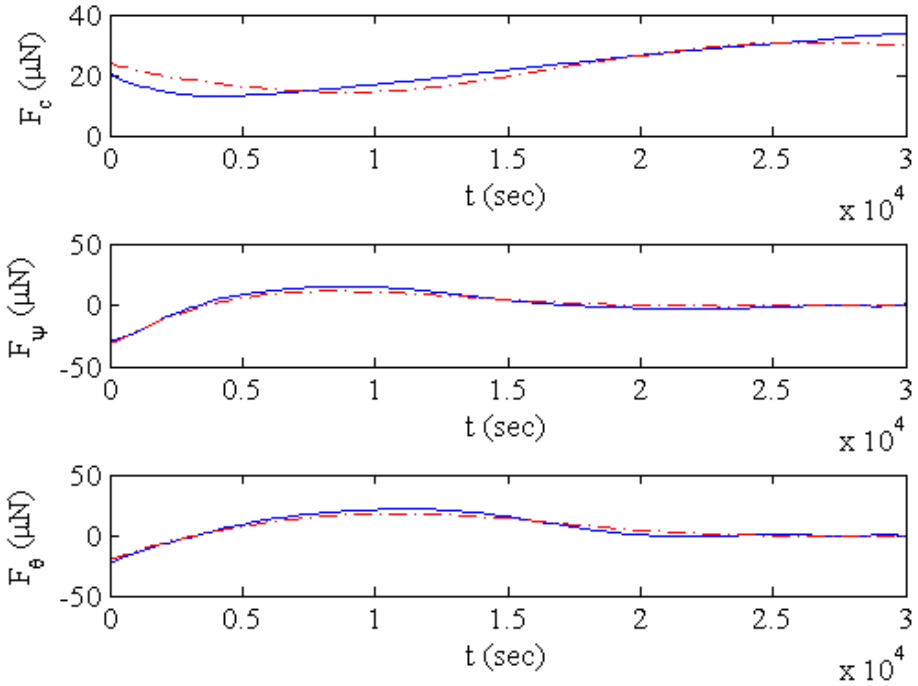

Figure 31. Approximate control solutions using SDC Direct method for two-craft Earth circular orbit Case1 and Case2.

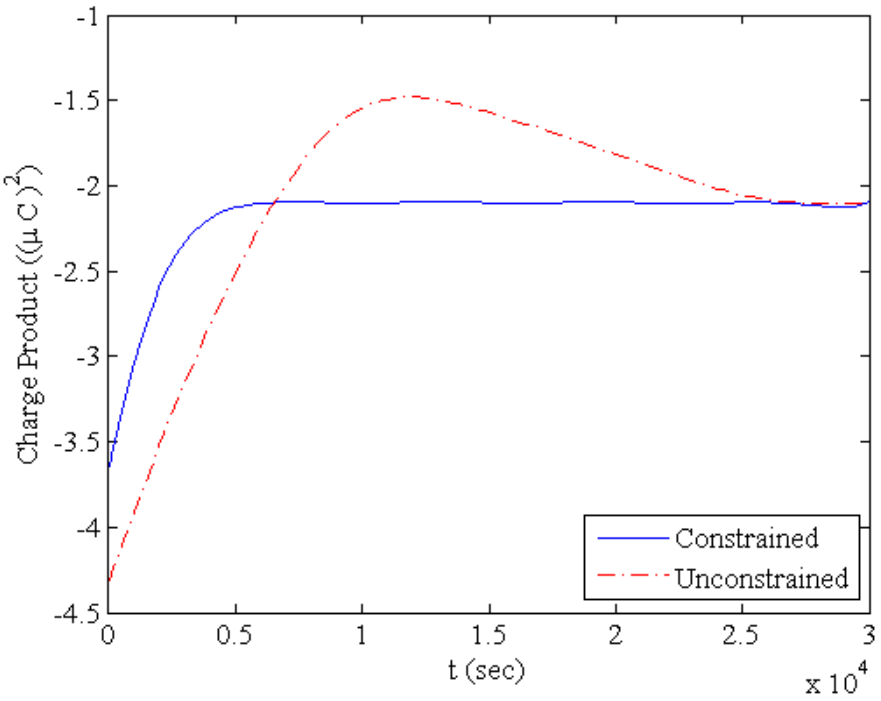

Figure 32. Charge product using SDC Direct method for two-craft Earth circular orbit Case1 and Case2.

7.1.2 Orbit-Radial Two-craft Coulomb Formation at Collinear Libration Points

The case that is simulated here is unconstrained, and the results are given below. The number of iterations, error and objective function values are presented in Table 7, Table 8, and Table 9 for the ASRE-approache1, ASRE-approach2, and SDC-Direct method, respectively. The objective function value for all the methods are in agreement with each other.

Table 7. ASRE-Approach1 iterations for two-craft collinear libration point.

Iteration	Error	J
1	1.76E+01	3.54963E+11
2	1.85E+00	3.7644E+11
3	1.87E-01	3.71765E+11
4	1.44E-02	3.7218E+11
5	3.17E-03	3.72132E+11
6	3.28E-04	3.72134E+11
7	4.78E-05	3.72134E+11

Table 8. ASRE-Approach2 iterations for two-craft collinear libration point.

Iteration	Error	J
1	1.76E+01	3.54983E+11
2	1.85E+00	3.76456E+11
3	1.87E-01	3.71781E+11
4	1.44E-02	3.72197E+11
5	3.17E-03	3.72148E+11
6	3.27E-04	3.72151E+11
7	4.77E-05	3.72151E+11

The approximate trajectory and control solutions are illustrated in Figure 33 and Figure 34. These are the plots of three techniques that are approximately coincident to each other. This is a SCP in which the final states are not specified, and it is shown that the states are stabilized at the end and the formation is going to its equilibrium condition. Figure 35 shows the charge product of the two-craft. An indirect robust control method was simulated in [48] to investigate the dynamics and reconfiguration control problem of a two-satellite Coulomb tether formation in the presence of differential solar drag near Earth–Moon libration point.

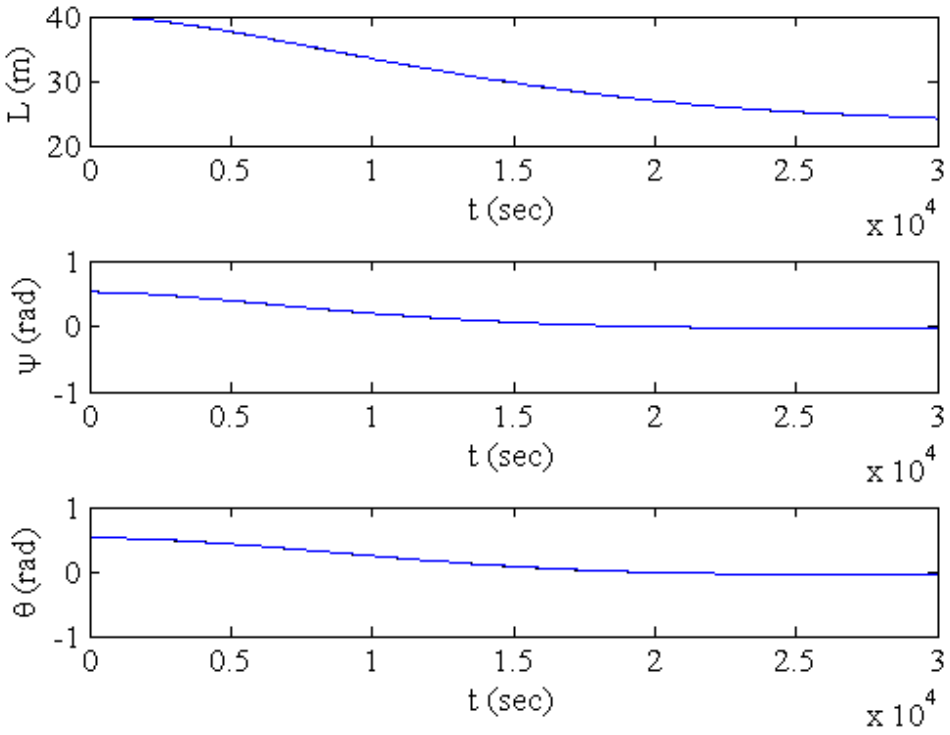

Figure 33. Approximate trajectory solutions using SDC Factorized optimal methods for two-craft collinear libration point.

Table 9. SDC-Direct iterations for two-craft collinear libration point.

Iteration	Error	J
1	1.76E+01	3.54927E+11
2	1.85E+00	3.76397E+11
3	1.87E-01	3.71723E+11
4	1.45E-02	3.72138E+11
5	3.18E-03	3.7209E+11
6	3.27E-04	3.72093E+11
7	4.76E-05	3.72093E+11

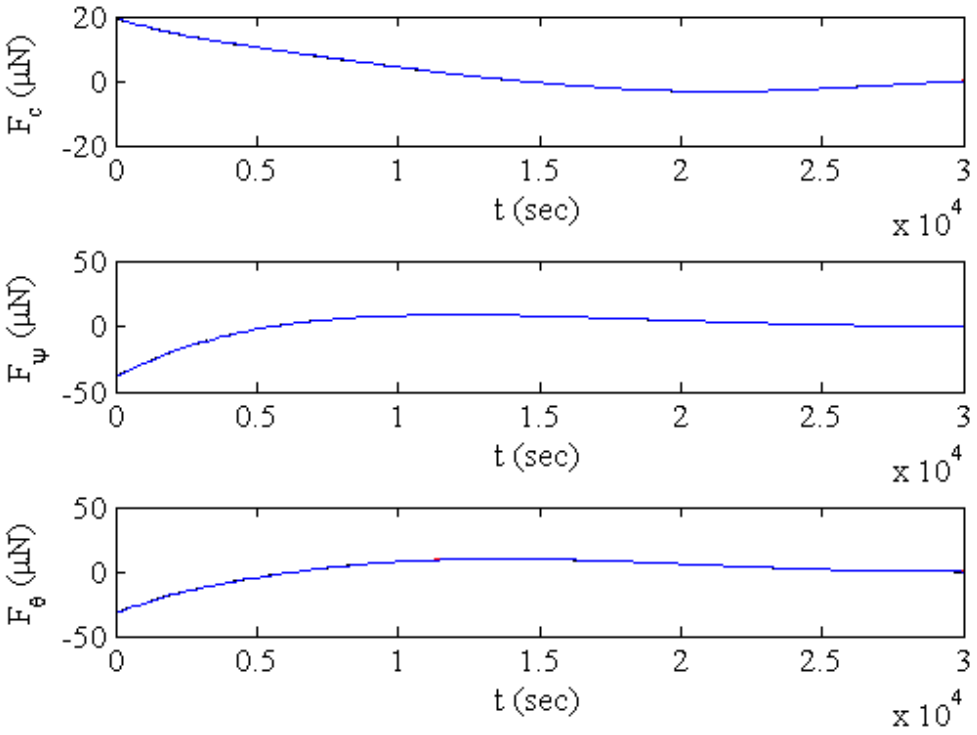

Figure 34. Approximate control solutions using SDC Factorized optimal methods for two-craft collinear libration point.

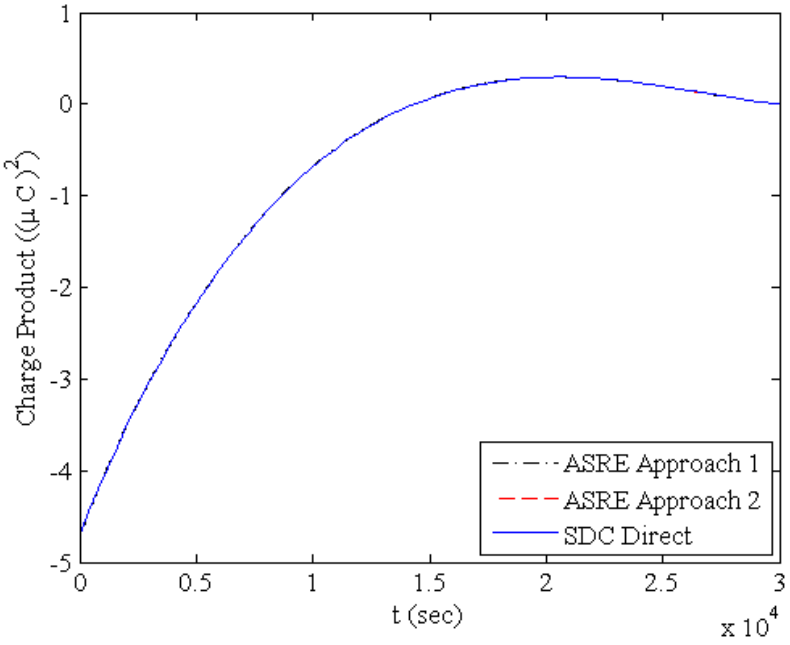

Figure 35. Charge product using SDC Factorized optimal methods for two-craft collinear libration point.

7.1.3 Orbit-Radial Two-craft Coulomb Formation at Triangular Libration Points

This is the first work showing the optimal reconfiguration of two-craft formation at triangular libration point, and no such a work is addressed in the literature. Unconstrained case is implemented here, and the results are given below. The number of iterations, error and objective function values are represented in Table 10, Table 11, and Table 12for the ASRE-approache1, ASRE-approach2, and SDC-Direct method, respectively. The objective function value for all the methods are in agreement with each other.

Table 10. ASRE-Approach1 iterations for two-craft triangular libration point.

Iteration	Error	J
1	1.76E+01	3.55272E+11
2	1.87E+00	3.75789E+11
3	2.07E-01	3.71939E+11
4	1.98E-02	3.72138E+11
5	2.11E-03	3.72158E+11
6	3.15E-04	3.72153E+11
7	4.34E-05	3.72154E+11

Table 11. ASRE-Approach2 iterations for two-craft triangular libration point.

Iteration	Error	J
1	1.76E+01	3.55292E+11
2	1.87E+00	3.75805E+11
3	2.07E-01	3.71955E+11
4	1.98E-02	3.72154E+11
5	2.10E-03	3.72174E+11
6	3.14E-04	3.72169E+11
7	4.34E-05	3.7217E+11

The approximate trajectory and control solutions are illustrated in Figure 36 and Figure 37. These are the plots of three techniques that are approximately coincident to each other. This is a SCP in which the final states are not specified, and it is shown that the states are stabilized at the end and the formation is going to its equilibrium condition. Figure 38 shows the charge product of the two-craft.

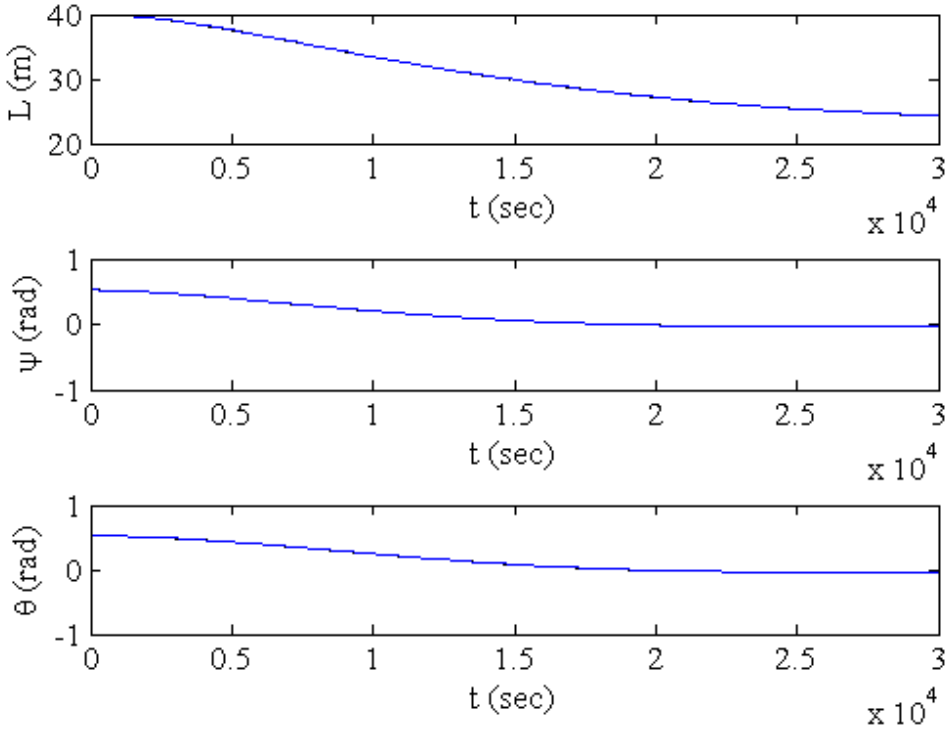

Figure 36. Approximate trajectory solutions using SDC Factorized optimal methods for two-craft triangular libration point.

Table 12. SDC-Direct iterations for two-craft triangular libration point.

Iteration	Error	J
1	1.76E+01	3.55235E+11
2	1.87E+00	3.75746E+11
3	2.07E-01	3.71898E+11
4	1.99E-02	3.72097E+11
5	2.11E-03	3.72116E+11
6	3.16E-04	3.72112E+11
7	4.33E-05	3.72112E+11

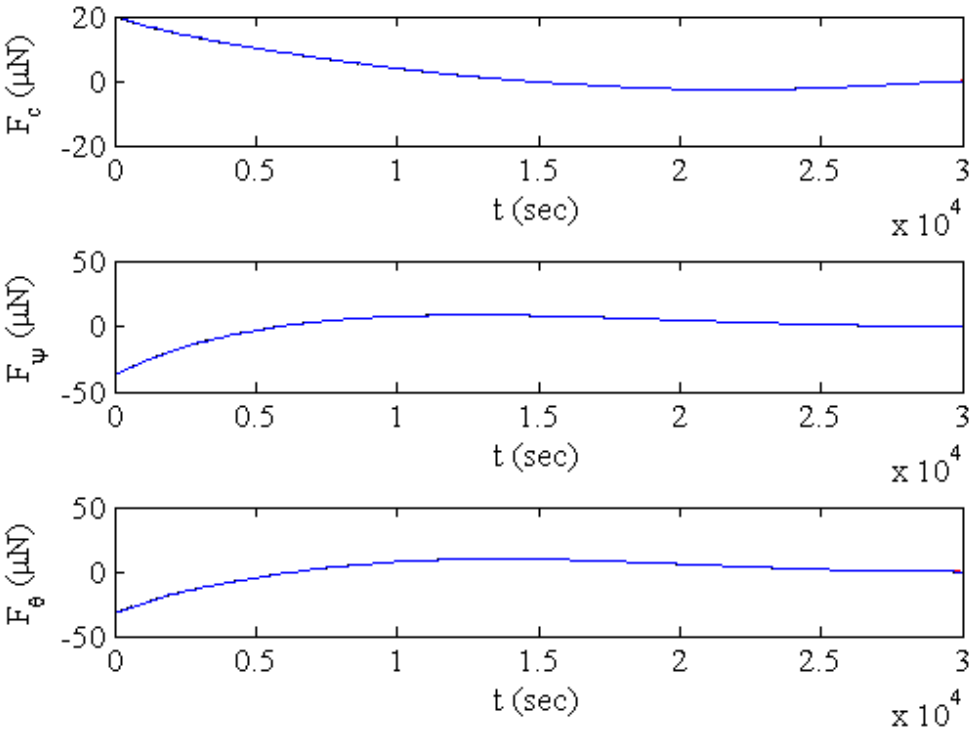

Figure 37. Approximate control solutions using SDC Factorized optimal methods for two-craft triangular libration point.

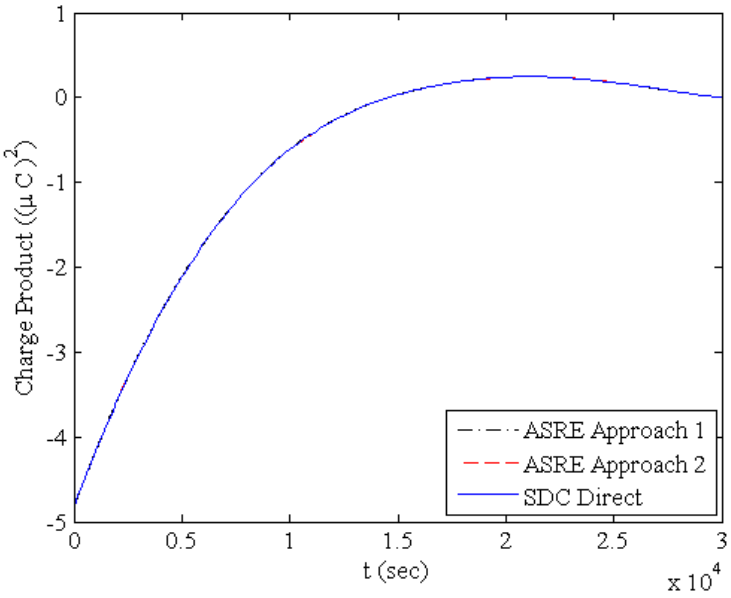

Figure 38. Charge product using SDC Factorized optimal methods for two-craft triangular libration point.

CHAPTER 8

APPLICATION OF STATE DEPENDENT FACTORIZED OPTIMAL CONTROL METHODS TO VAN DER POL OSCILLATOR AND LOW-THRUST RENDEZVOUS PROBLEMS

Two sample problems with nonlinear dynamics are considered to apply and verify the proposed SDC Direct method. In all the cases, the optimization problem represented in Eq. (5.47) is solved in Matlab using quadprog syntax with interior-point-convex algorithm with Intel Core i5 CPU 2.30 GHz. In the present implementations, the convergence is reached when

$$\varepsilon = \| \mathbf{x}^{[k+1]} - \mathbf{x}^{[k]} \|_{\infty} = \max_{t \in [t_0, t_f]} \{ | x_j^{[k+1]}(t) - x_j^{[k]}(t) |, j = 1, \ldots, n \} \leq \text{tol} \quad (8.1)$$

where ε is error and `tol' is a prescribed tolerance.

8.1 Problem 1: Van der Pol Oscillator

This problem is taken from [35, 38]. Van der Pol oscillator is a second order dynamical system

$$\dot{x}_1 = x_2$$
$$\dot{x}_2 = -(x_1^2 - 1)x_2 - x_1 + u$$

Initial states are $x_1(0) = 1$, and $x_2(0) = 0$, and the final time is defined as $t_f = 5$. The weighting matrices are $Q = I_2$ and $R = 1$, and the corresponding objective function is

$$J = \frac{1}{2}\int_0^5 \left(x_1^{\,2} + x_2^{\,2} + u^2\right)\mathrm{d}t$$

For SDC factorization the state and input matrices are chosen in the form of

$$A = \begin{bmatrix} 0 & 1 \\ -\left(1 + x_1 x_2\right) & 1 \end{bmatrix}, B = \begin{bmatrix} 0 \\ 1 \end{bmatrix}$$

In this example, the whole procedure of the proposed method will be shown step by step. Since $n > m$, the technique represented in Section 5.2.3 has to be considered. In order to use Chebyshev polynomials, the time interval $[0,5]$ is transformed to $[-1,1]$ using the transformation time $\tau = 2t/t_f - 1$. The TVLQR approximations are written as

$$\begin{aligned} \dot{x}_1^{[1]}(t) &= x_2^{[1]}(t) \\ \dot{x}_2^{[1]}(t) &= -\left(1 + x_{10}x_{20}\right)x_1^{[1]}(t) + x_2^{[1]}(t) + u^{[1]}(t) \end{aligned} \tag{8.2}$$

$$\begin{aligned} \dot{x}_1^{[k+1]}(t) &= x_2^{[k+1]}(t) \\ \dot{x}_2^{[k+1]}(t) &= -\left(1 + x_1^{[k]}(t)x_2^{[k]}(t)\right)x_1^{[k+1]}(t) + x_2^{[k+1]}(t) + u^{[k+1]}(t) \end{aligned} \tag{8.3}$$

Transforming the Eqs. (8.2)-(8.3) to Chebyshev time domain, the equations are written as

$$\begin{aligned} \dot{x}_1^{[1]}(\tau) &= \frac{t_f}{2}[x_2^{[1]}(\tau)] \\ \dot{x}_2^{[1]}(\tau) &= \frac{t_f}{2}[-\left(1 + x_{10}x_{20}\right)x_1^{[1]}(\tau) + x_2^{[1]}(\tau) + u^{[1]}(\tau)] \end{aligned} \tag{8.4}$$

$$\begin{aligned} \dot{x}_1^{[k+1]}(\tau) &= \frac{t_f}{2}[x_2^{[k+1]}(\tau)] \\ \dot{x}_2^{[k+1]}(\tau) &= \frac{t_f}{2}[-\left(1 + x_1^{[k]}(\tau)x_2^{[k]}(\tau)\right)x_1^{[k+1]}(\tau) + x_2^{[k+1]}(\tau) + u^{[k+1]}(\tau)] \end{aligned} \tag{8.5}$$

For the first iteration, the Eq. (8.4) is used, and the Eq. (8.5) is implemented for the next iterations. First, the state x_1 is approximated by Chebyshev polynomials. Second, the state x_2 will be obtained from the derivative of x_1. Third, by double differentiation of x_1, the $\dot{x}_2$ will be obtained as shown in the following

$$\dot{x}_1^{[1]}(\tau) = \frac{t_f}{2}[\dot{x}_2^{[1]}(\tau)] \tag{8.6}$$

$$\dot{x}_1^{[k+1]}(\tau) = \frac{t_f}{2}[\dot{x}_2^{[k+1]}(\tau)] \tag{8.7}$$

To this end, the input u is evaluated from the second equation of Eqs. (8.4) and (8.5). Two different subproblems are considered.

8.1.1 Soft Constrained Problem

This is a SCP in which the final states are not specified, $x_f = free$. Three different cases are solved and discussed. For case 1, both states and control are unconstrained and a solution for this case is available in [38]. Then, the input is constrained in case 2 and states are still unconstrained. Lastly, in case 3 both states and controls are constrained.

Case 1. In this case, it is assumed that there would be no constraints on the states and inputs. Table 13 represents the results for two different degrees of Chebyshev polynomials, $N = 8$ and $N = 12$. The number of iterations, the value of errors, and the objective function values are given. For both Chebyshev degree values, the optimization problem is terminated after 5 iterations and the value of the objective function is in agreement with that given in [38] which is 1.4493959719 for $N = 15$. Looking at the results in Table 13, it seems that for the unconstrained case, increasing the Chebyshev polynomial degree does not improve the objective value. Figure 39 shows the approximate trajectory and control solutions.

Table 13. SDC-Direct method iterations for Problem1-SCP-Case1.

N = 8			N = 12		
Iteration	Error	J	Iteration	Error	J
1	1.079319e+00	1.685824e+00	1	1.079237e+00	1.685822e+00
2	4.782503e-02	1.427952e+00	2	4.862783e-02	1.427863e+00
3	2.664431e-03	1.435632e+00	3	3.662316e-03	1.435654e+00
4	1.504402e-04	1.435544e+00	4	2.548840e-04	1.435615e+00
5	1.176594e-05	1.435522e+00	5	4.028370e-05	1.435570e+00

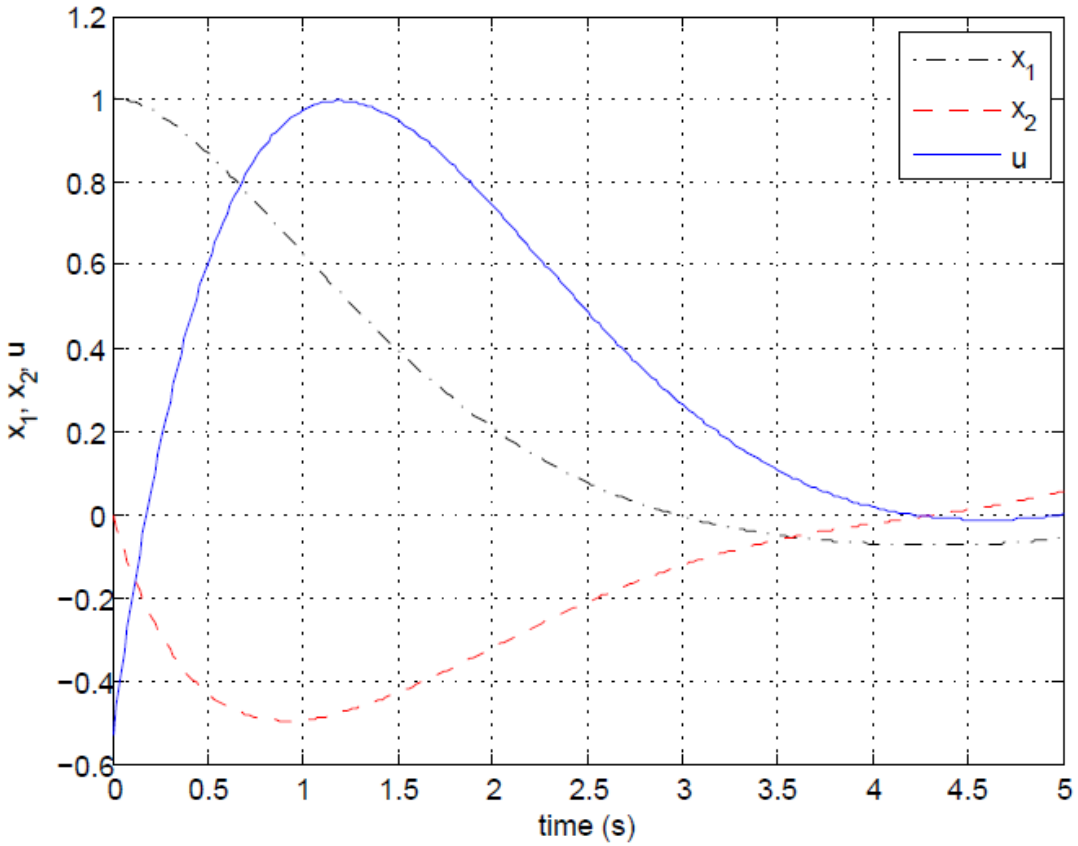

Figure 39. Problem1-SCP-Case1 (N = 12): Approximate trajectory and control solutions.

Case 2. Here we consider that the states are unconstrained and there is constraint on input which is defined as

$$0 \le u \le 0.75$$

The iterations, errors, and values of objective functions are given in Table 14. For $N = 8$, the solution is obtained after 10 iterations and for the case when $N = 12$, after 7 iterations the problem is solved. Therefore, it may be concluded that for the case with constraints on inputs, the performance of the algorithm is improved by increasing the degree of Chebyshev polynomials. Moreover, by increasing the Chebyshev polynomial degree, the value of the objective function is decreased. The optimal trajectory and control solutions are shown in Figure 40 for case 1 and case 2 together.

Table 14. SDC-Direct method iterations for Problem1-SCP-Case2.

N = 8			N = 12		
Iteration	Error	J	Iteration	Error	J
1	1.668749e+00	3.211873e+00	1	1.451901e+00	3.088773e+00
2	1.444115e+00	1.588960e+00	2	1.269662e+00	1.559349e+00
3	5.368128e-02	1.606897e+00	3	4.048383e-02	1.584761e+00
4	1.837529e-02	1.641353e+00	4	1.046905e-02	1.603692e+00
5	3.591689e-03	1.644906e+00	5	2.010635e-03	1.605551e+00
6	2.828636e-03	1.643633e+00	6	4.903323e-04	1.605002e+00
7	1.530721e-04	1.643527e+00	7	9.863860e-05	1.604865e+00
8	1.570586e-04	1.643605e+00	8		
9	1.167622e-04	1.643596e+00	9		
10	9.830951e-06	1.643612e+00	10		

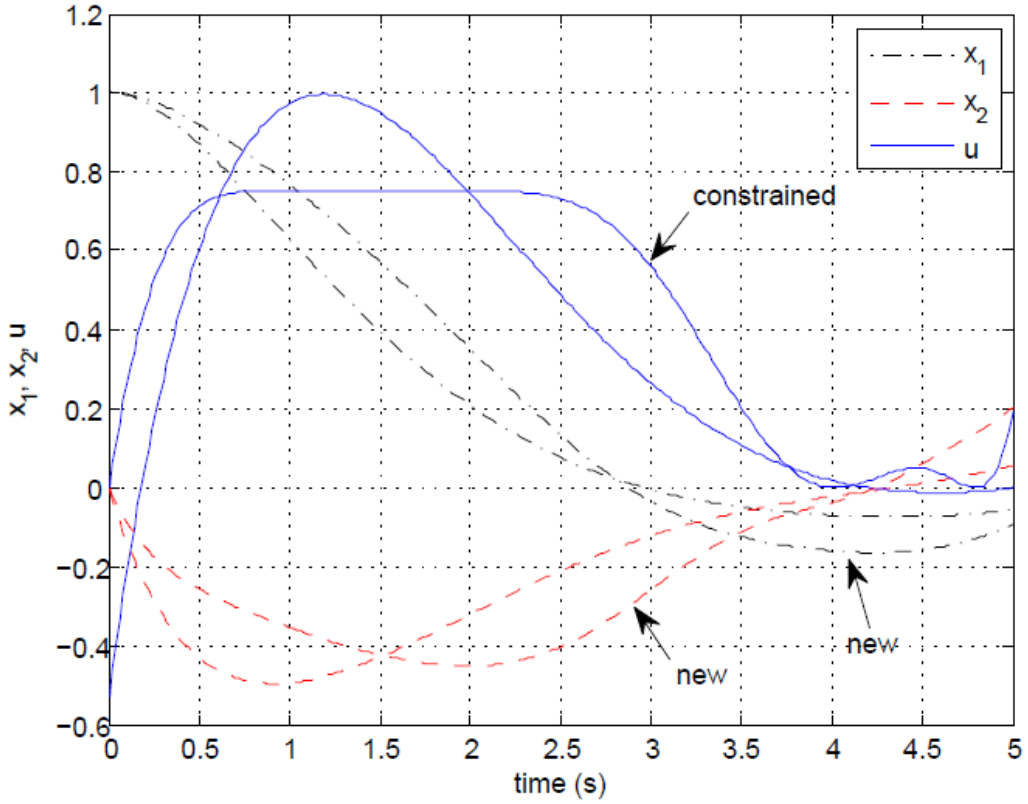

Figure 40. Problem1-SCP-Case1 (N = 12): Approximate trajectory and control solutions.

Case 3. In this case, it is considered to have constraints on both the states and the input. These constraints are defined as

$$0 \le u \le 0.75$$

$$0 \le x_1 \le 1$$

$$-0.38 \leq x_2$$

The state constraints added to the problem result in more iterations and bigger objective function value for case 3. By considering the results in Table 15, it may be again concluded that the results are improved by increasing the Chebyshev polynomial degree for constrained case.

Plots of the cases 1 and 3 are showed in Figure 41. It shows that the constraints on the states and control are satisfied and the optimal solutions are changed after applying the constraints.

Table 15. SDC-Direct method iterations for Problem1-SCP-Case3.

N = 8			N = 12		
Iteration	Error	J	Iteration	Error	J
1	1.762806e+00	5.741236e+00	1	5.878951e+00	9.450530e+01
2	1.303140e+00	2.206247e+00	2	3.879162e+00	9.934352e+00
3	4.327738e-01	1.836886e+00	3	1.987615e+00	1.756250e+00
4	7.568154e-02	1.862552e+00	4	2.819701e-02	1.786414e+00
5	8.307684e-03	1.882555e+00	5	8.817573e-03	1.801913e+00
6	2.916821e-03	1.891366e+00	6	2.809343e-03	1.808637e+00
7	6.889621e-04	1.892950e+00	7	1.023038e-03	1.810733e+00
8	1.223139e-03	1.892241e+00	8	7.394046e-04	1.811066e+00
9	6.099517e-04	1.891546e+00	9	9.837200e-05	1.811003e+00
10	5.788571e-04	1.891260e+00			
11	5.118347e-04	1.891195e+00			
12	1.621073e-04	1.891218e+00			
13	1.334805e-05	1.891245e+00			

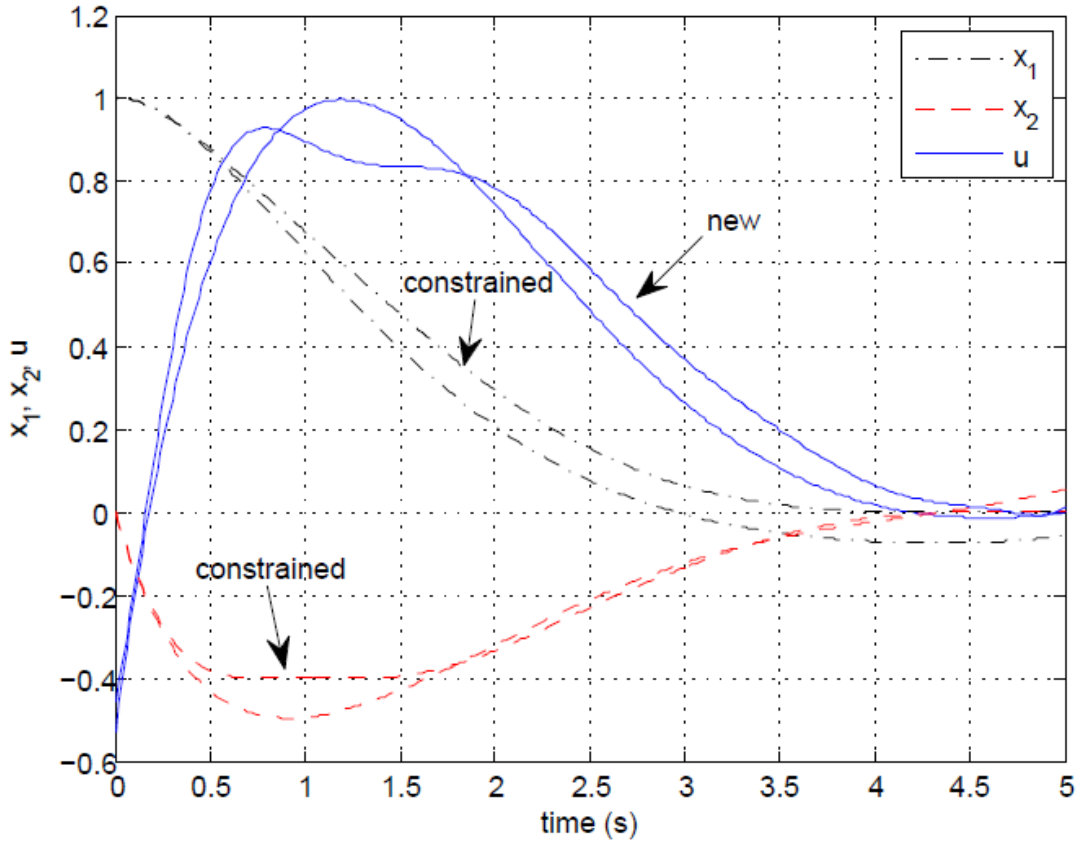

Figure 41. Problem1-SCP-Cases 1 and 3 (N =12): Approximate trajectory and control solutions.

8.1.2 Hard Constrained Problem

This is a HCP in which the final states are fully specified; $x_1(5) = -1$, and $x_2(5) = 0$. For this problem, the case with constraints on input is analyzed. Consider the constraint is defined as

$$-0.75 \le u \le 0.75$$

Figure 42 shows the approximate trajectory and control for unconstrained and constrained cases. It is shown that the initial and final state conditions are satisfied. Moreover, Figure 42 displays that the bounds on control are met, and the new state trajectories are showed after considering the input constraint. A comparison of iteration numbers and the objective function values is represented in Table 16 for different values of Chebyshev polynomial degrees. Again, it may be concluded that the results are improved by increasing the Chebyshev polynomial degree. For the

constrained case, a solution exists in [35] and the objective functions of the current paper are in agreement with that given in [35] which is 2.1389 for N = 12.

Table 16. SDC-Direct method iterations for Problem1-HCP.

N = 8			N = 12		
Iteration	Error	J	Iteration	Error	J
1	1.000000e+00	3.130124e+00	1	1.002810e+00	3.249518e+00
2	3.895121e-01	2.144377e+00	2	4.464654e-01	2.116291e+00
3	5.353388e-02	2.146860e+00	3	7.396758e-02	2.126974e+00
4	1.596711e-02	2.173787e+00	4	1.329232e-02	2.147969e+00
5	4.461313e-03	2.179621e+00	5	3.651116e-03	2.151620e+00
6	4.701491e-04	2.179486e+00	6	5.547349e-04	2.151385e+00
7	1.388092e-04	2.179309e+00	7	1.700663e-04	2.151145e+00
8	1.524415e-05	2.179304e+00	8	1.336576e-04	2.151128e+00
9	7.448995e-06	2.151141e+00			

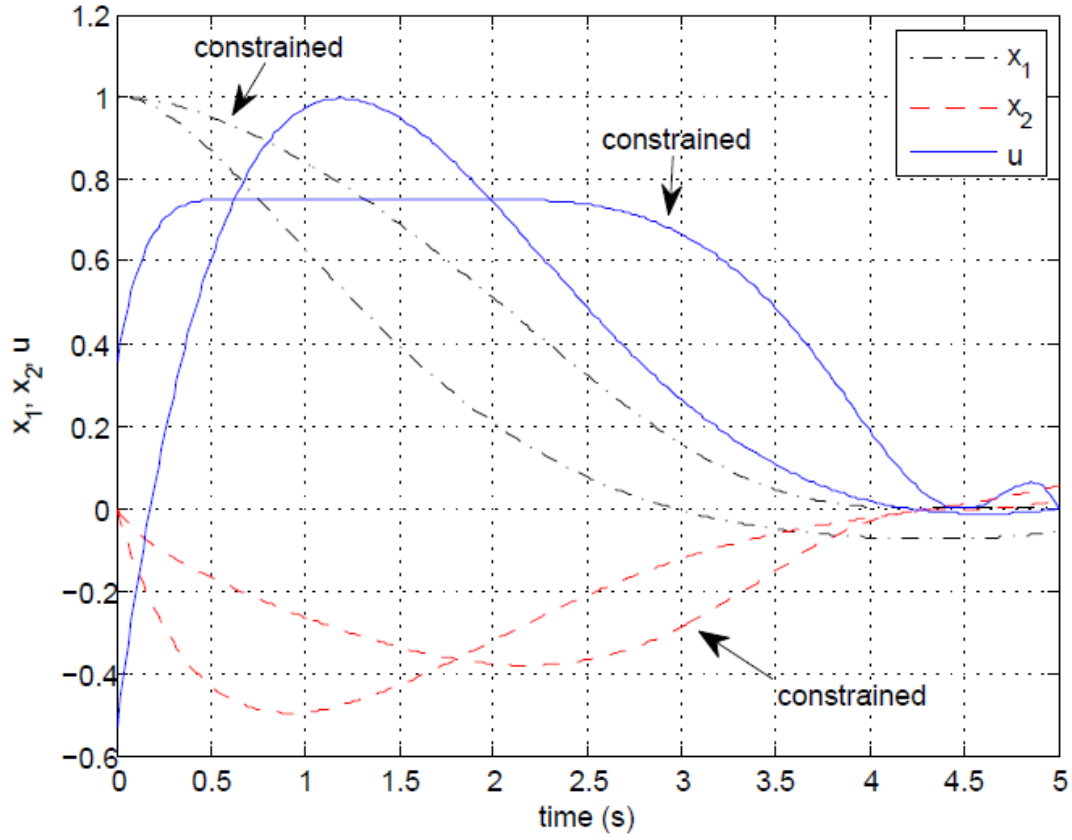

Figure 42. Problem1-HCP (N = 12): Approximate trajectory and control solutions.

8.2 Problem 2: Low-Thrust Rendezvous

This problem [28, 49], considers the planar, relative motion of two particles in a central gravity field expressed in a rotating frame with normalized units: the length unit is equal to the orbital radius, the time unit is such that the orbital period is 2π, and the gravitational parameter is equal to 1. In these dynamics, the state is $\mathbf{x} = (x_1 x_2 x_3 x_4)$; x_1 represents the radial displacement, x_2 represents the tangential displacement, x_3 represents the radial velocity deviations, and x_4 represents the tangential velocity deviations. The control $\mathbf{u} = (u_1 u_2)$, is made of by the radial and tangential accelerations, respectively. The first order system dynamics are written in the form

$$\begin{aligned}
\dot{x_1} &= x_3 \\
\dot{x_2} &= x_4 \\
\dot{x_3} &= 2x_4 + \left(1 - \frac{1}{r^3}\right)(1 + x_1) + u_1 \\
\dot{x_4} &= -2x_3 + \left(1 - \frac{1}{r^3}\right)x_2 + u_2
\end{aligned}$$

with $r = \sqrt{(x_1 + 1)^2 + x_2^2}$. The initial condition is $\mathbf{x}_0 = (0.2, 0.2, 0.1, 0.1)$, and $t_0 = 0$, $t_f = 1$. Since $n > m$, the technique introduced in Section 5.2.3 is implemented. For the SDC factorization form, the A and B matrices are chosen as

$$\mathbf{A} = \mathbf{A}(\mathbf{x}) = \begin{bmatrix} 0 & 0 & 1 & 0 \\ 0 & 0 & 0 & 1 \\ \left(1 - \frac{1}{r^3}\right)\left(\frac{1}{x_1} + 1\right) & 0 & 0 & 2 \\ 0 & \left(1 - \frac{1}{r^3}\right) & -2 & 0 \end{bmatrix}, \mathbf{B} = \begin{bmatrix} 0 & 0 \\ 0 & 0 \\ 1 & 0 \\ 0 & 1 \end{bmatrix}$$

The objective function is defined as

$$J = \frac{1}{2}\mathbf{x}^T(t_f)\mathbf{S}\mathbf{x}(t_f) + \frac{1}{2}\int_{t_0}^{t_f} \mathbf{u}^T \mathbf{u} dt$$

while weighting matrices are $\mathbf{Q} = \mathbf{0}_4$ and $\mathbf{R} = \mathbf{I}_2$. Based on the specification of final states, two different subproblems are considered.

8.2.1 Soft Constrained Problem

Here the final states are free (SCP), and the weighting matrix for final state conditions is defined as $\mathbf{S} = diag\left(25,15,10,10\right)$. Three different cases are implemented and the results are given and discussed.

Case 1. This case considers the results of the unconstrained case. Approximate trajectory and control for SDC Direct method are displayed in Figure 43 (dashed lines). The initial state conditions are satisfied and the optimal trajectories and controls are showed. The iterations and objective function values are given in Table 17 for two different degrees of Chebyshev polynomials. The objective function value is the same for both values of N, and these results are in agreement with the solution given in [28] which has the objective function of 0.5660 after 6 iterations.

Table 17. SDC-Direct method iterations for Problem2-SCP-Case1.

N = 8			N = 12		
Iteration	Error	J	Iteration	Error	J
1	3.426168e-01	5.693359e-01	1	3.426165e-01	5.693359e-01
2	1.426767e-03	5.659849e-01	2	1.425440e-03	5.659849e-01
3	1.286568e-05	5.659615e-01	3	1.284486e-05	5.659615e-01

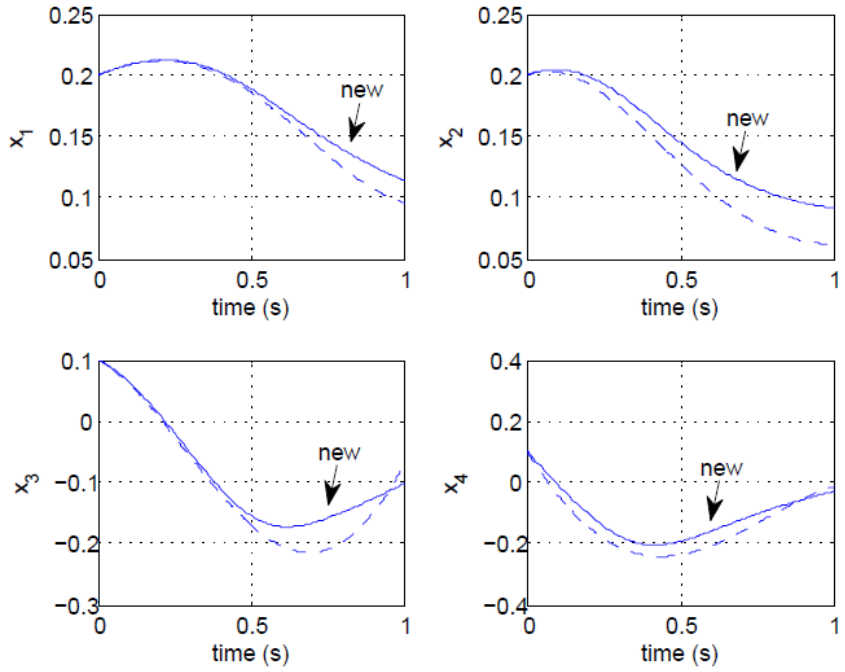

(a) Approximate trajectory.

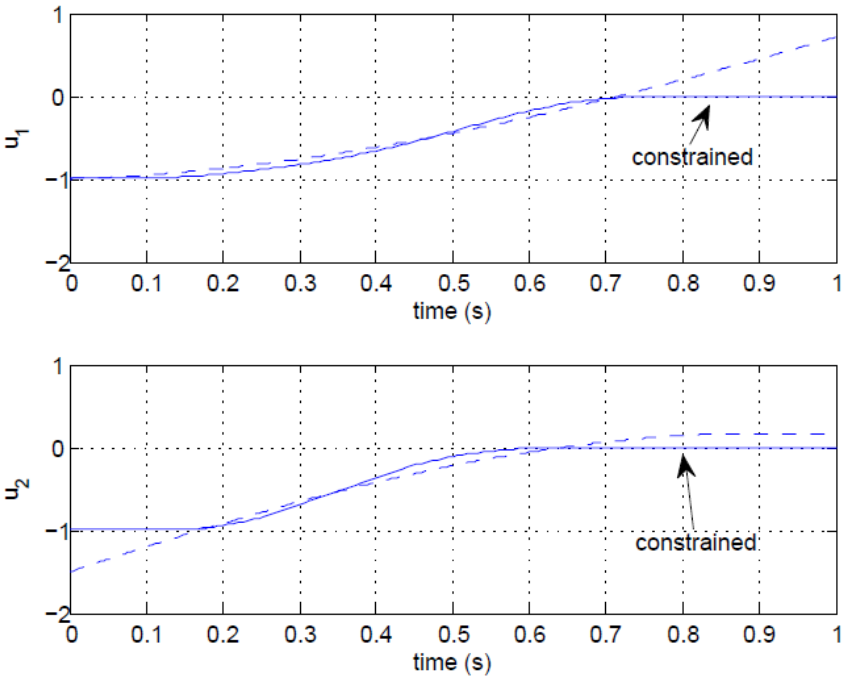

(b) Approximate control.

Figure 43. Problem2-SCP-Cases 1 and 2 (N = 12): Approximate trajectory and control solutions.

Case 2. Now for the input constrained case, the bounds on the controls are considered as

$$-1 \le u_1 \le 0, -1 \le u_2 \le 0$$

Figure 43 displays the optimal state trajectories and controls with the solid lines. It shows that the input constraints are satisfied and the new plots are the results of these constraints. Table 18 gives the error and objective function values showing an improvement by increasing the Chebyshev polynomial degree.

Table 18. SDC-Direct method iterations for Problem2-SCP-Case2.

N = 8			N = 12		
Iteration	Error	J	Iteration	Error	J
1	3.003979e-01	6.233571e-01	1	3.057933e-01	6.211742e-01
2	1.911900e-03	6.208723e-01	2	1.876686e-03	6.186383e-01
3	6.134384e-05	6.208419e-01	3	1.782679e-04	6.185371e-01
			4	4.832861e-05	6.185349e-01

Case 3. For this case, the states x_3 and x_4 and the controls are constrained as

$$-1 \le u_1 \le 0, -1 \le u_2 \le 0$$

$$-0.1 \le x_3 \le 0.1$$

$$-0.1 \le x_4 \le 0.1$$

Again, for two different Chebyshev degrees, the objective function values are given in Table 19. In addition, for this case it may be understood that the performance of the solution can be better by increasing Chebyshev degree. The state and control trajectories are shown in Figure 44 for unconstrained and constrained cases, which demonstrates that the initial state conditions and state constraints are satisfied, and the control trajectories display the justification of the constrained controls.

Table 19. SDC-Direct method iterations for Problem2-SCP-Case3

N = 8			N = 12		
Iteration	Error	J	Iteration	Error	J
1	1.999999e-01	7.224606e-01	1	2.000000e-01	7.166547e-01
2	1.701514e-03	7.197011e-01	2	1.708269e-03	7.143159e-01
3	1.045409e-04	7.196854e-01	3	3.645138e-04	7.145929e-01
	1.630952e-06	7.196859e-01	4	1.107111e-05	7.145841e-01

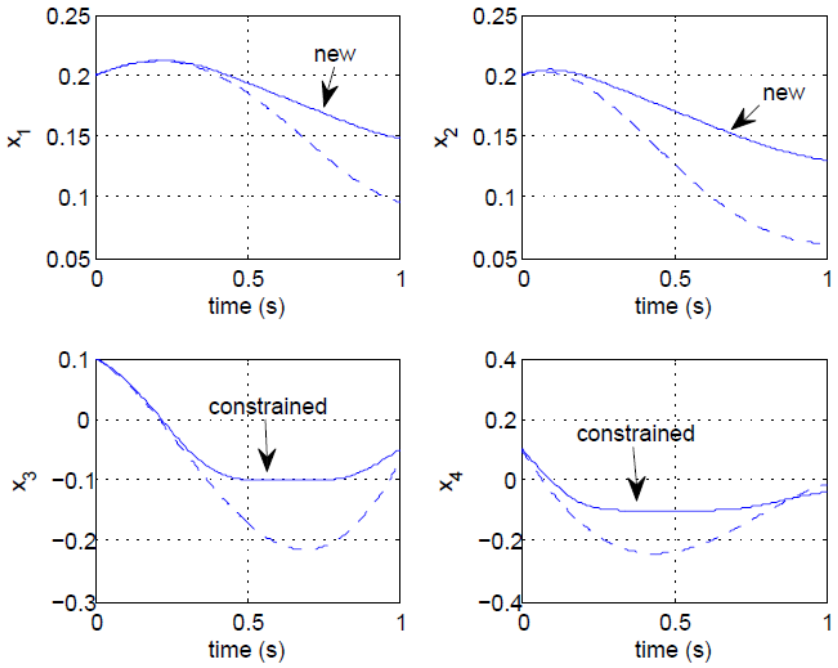

(a) Approximate trajectory.

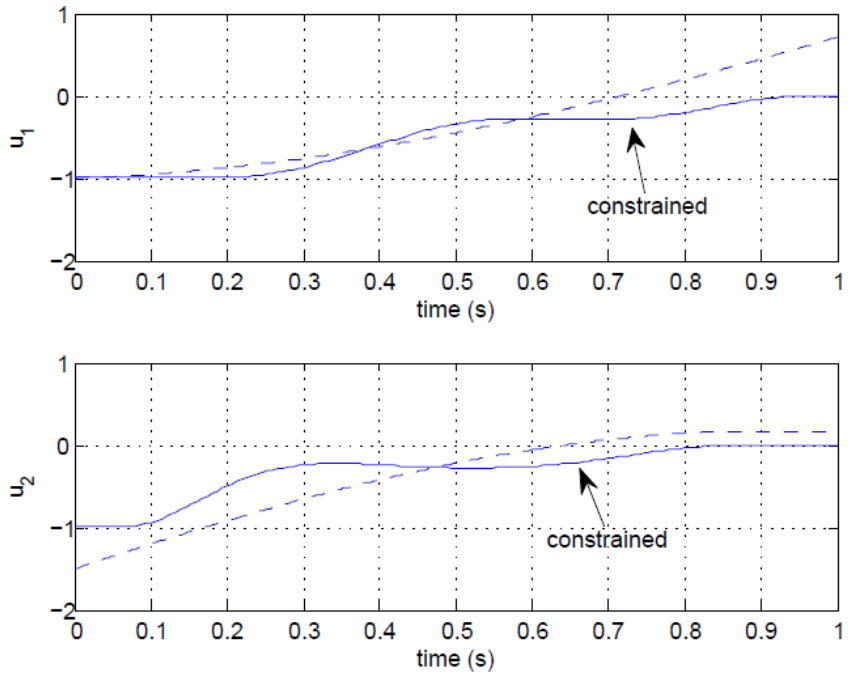

(b) Approximate control.

Figure 44. Problem2-SCP-Cases 1 and 2 (N = 12): Approximate trajectory and control solutions.

8.2.2 Hard Constrained Problem

The final states are specified for this type of problem (HCP), and those are given as $\mathbf{x}_f = (0,0,0,0)$. The weighting matrix for final state conditions is considered as $\mathbf{S} = \mathbf{0}$. The unconstrained and constrained results are discussed as following.

Case 1. Unconstrained case is implemented here, and the results are given in Table 20 and are showed with dashed lines in Figure 45. The objective function value is in agreement with that given in [28] which is 0.9586 for 5 iterations.

Table 20. SDC-Direct method iterations for Problem2-HCP-Case1.

N = 8			N = 12		
Iteration	Error	J	Iteration	Error	J
1	4.731670e-01	9.629775e-01	1	4.731672e-01	9.629775e-01
2	9.376290e-04	9.584905e-01	2	9.395097e-04	9.584905e-01
3	2.924892e-06	9.584936e-01	3	2.971336e-06	9.584936e-01

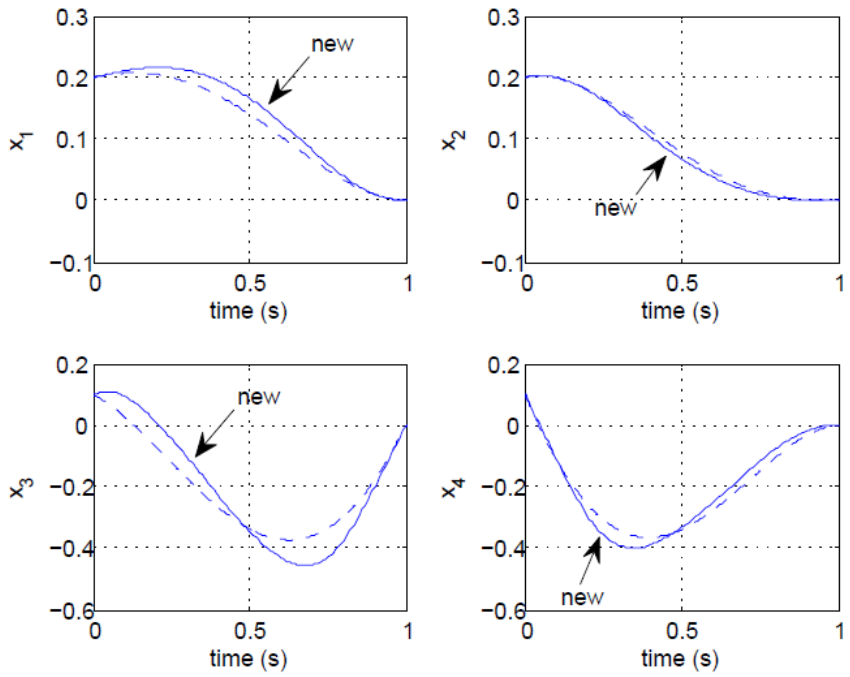

(a) Approximate trajectory.

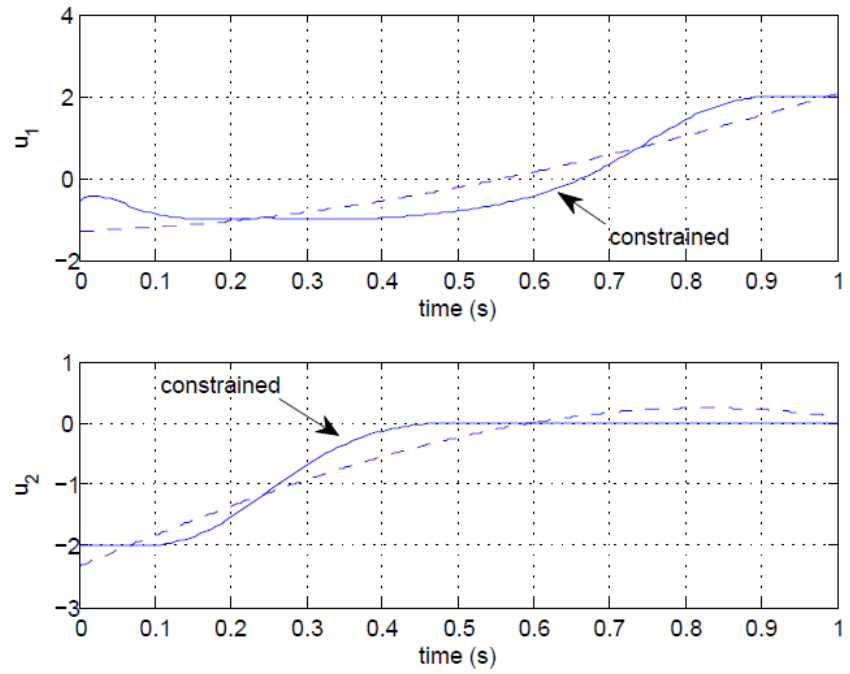

(b) Approximate control.

Figure 45. Problem2-HCP-Cases 1 and 2 (N = 12): Approximate trajectory and control solutions with SDC Direct method.

Case 2. For this case, just the inputs are constrained as

$$-1 \le u_1 \le 2, -2 \le u_2 \le 0$$

Table 21 represents the number of iterations, errors, and objective function values, and the optimal trajectories are displayed in Figure 45. Notice that for $N = 8$ no optimal solution satisfying the constraints was found.

Table 21. SDC-Direct method iterations for Problem2-HCP-Case2.

N = 12		
Iteration	Error	J
1	5.546035e-01	1.072986e+00
2	3.402995e-03	1.069829e+00
3	2.085145e-04	1.069635e+00
4	7.464199e-05	1.069662e+00

CHAPTER 9

CONCLUSION AND FUTURE WORKS

The present work introduces a method to solve constrained nonlinear optimal control problems using state dependent coefficient factorization and Chebyshev polynomials named as SDC-Direct method. In this thesis, nonlinear feedback control and optimal maneuvers of formation attitude and relative position of a two-craft and three-craft Coulomb formations utilizing coulomb forces as well as thrusters are addressed at Earth circular orbits, Earth-moon libration points, and deep space. The SDRE control method is used for nonlinear feedback control of all the cases. The nonlinear optimal control is realized using the ASRE approaches and the SDC-Direct method. The effectiveness of the approaches in reconfiguring the formation and comparison of them is demonstrated through the nonlinear simulations. For comparison of the SDC-Direct technique with the other approaches in the literature, the Van der pol oscillator and low-thrust rendezvous problem are studied and the results show that the proposed method is in agreement with those given in literature.

The future work may be extended to deriving the equations of motion of the two-craft Coulomb formation using the quaternions instead of Euler angles to describe the attitude motion of the system. Then, the nonlinear feedback control methods and SDC-factorized optimal controls may be applied to the new equations and compare the results. The proposed SDC-Direct method may be extended to the tracking optimal control problems. Moreover, the idea of the SDC-factorized optimal control methods may be combined with the Model Predictive Control (MPC) method to find some new algorithms and implementations in real-time optimal control problems.

REFERENCES

1. Berryman, J. and H. Schaub, *Static equilibrium configurations in geo coulomb spacecraft formations.* Advances in the Astronautical Sciences, 2005. **120**: p. 51-68.
2. King, L.B., et al., *Study of interspacecraft coulomb forces and implications for formation flying.* Journal of Propulsion and Power, 2003. **19**(3): p. 497-505.
3. Mullen, E., et al., *SCATHA survey of high-level spacecraft charging in sunlight.* Journal of Geophysical Research: Space Physics, 1986. **91**(A2): p. 1474-1490.
4. Schaub, H. and M. Kim. *Orbit element difference constraints for Coulomb satellite formations*. in *AIAA/AAS Astrodynamics Specialist Conference, Providence, Rhode Island*. 2004.
5. Natarajan, A. and H. Schaub, *Linear dynamics and stability analysis of a two-craft Coulomb tether formation.* Journal of Guidance Control and Dynamics, 2006. **29**(4): p. 831.
6. Natarajan, A., H. Schaub, and G.G. Parker, *Reconfiguration of a nadir-pointing 2-craft coulomb tether.* Journal of the British Interplanetary Society, 2007. **60**: p. 209-218.
7. Inampudi, R. and H. Schaub, *Optimal reconfigurations of two-craft Coulomb formation in circular orbits.* Journal of Guidance, Control and Dynamics, 2012. **35**(6): p. 1805-1815.
8. Inampudi, R. and H. Schaub, *Orbit radial dynamic analysis of two-craft Coulomb formation at libration points.* Journal of Guidance, Control, and Dynamics, 2014.
9. Inampudi, R. and H. Schaub, *Disturbance compensating control of orbit radially aligned two-craft Coulomb formation.* Celestial Mechanics and Dynamical Astronomy, 2012. **112**(4): p. 445-458.
10. Hussein, I.I. and H. Schaub, *Invariant shape solutions of the spinning three craft Coulomb tether problem.* Celestial Mechanics and Dynamical Astronomy, 2006. **96**(2): p. 137-157.
11. Wang, S. and H. Schaub, *Nonlinear charge control for a collinear fixed-shape three-craft equilibrium.* Journal of Guidance Control and Dynamics, 2011. **34**(2): p. 359.
12. Hogan, E.A. and H. Schaub, *Linear stability and shape analysis of spinning three-craft Coulomb formations.* Celestial Mechanics and Dynamical Astronomy, 2012. **112**(2): p. 131-148.
13. Cloutier, J.R., C.N. D'Souza, and C.P. Mracek. *Nonlinear regulation and nonlinear H∞ control via the state-dependent Riccati equation technique: Part 1, theory*. in *Proceedings of the First International Conference on Nonlinear Problems in Aviation and Aerospace*. 1996. Embry-Riddle Aeronautical Univ. Press Daytona Beach, FL.

14. Mracek, C.P. and J.R. Cloutier, *Control designs for the nonlinear benchmark problem via the state-dependent Riccati equation method.* International Journal of robust and nonlinear control, 1998. **8**(4-5): p. 401-433.
15. Bracci, A., M. Innocenti, and L. Pollini, *Estimation of the region of attraction for state-dependent Riccati equation controllers.* Journal of Guidance Control and Dynamics, 2006. **29**(6): p. 1427.
16. Cimen, T., *Survey of state-dependent Riccati equation in nonlinear optimal feedback control synthesis.* Journal of Guidance, Control and Dynamics, 2012. **35**(4): p. 1025-1047.
17. Harman, R.R. and I.Y. Bar-Itzhack, *Pseudolinear and state-dependent Riccati equation filters for angular rate estimation.* Journal of Guidance, Control, and Dynamics, 1999. **22**(5): p. 723-725.
18. Bogdanov, A. and E. Wan, *State-dependent Riccati equation control for small autonomous helicopters.* Journal of Guidance Control and Dynamics, 2007. **30**(1): p. 47-60.
19. Kim, C.-J., et al., *Nonlinear optimal control analysis using state-dependent matrix exponential and its integrals.* Journal of guidance, control, and dynamics, 2009. **32**(1): p. 309.
20. Gomroki, M.M. and O. Tekinalp, *Relative position control of a two-satellite formation using the SDRE control method.* Advances in the Astronautical Sciences, 2014. **152**: p. 235-254.
21. Gomroki, M.M. and O. Tekinalp, *State Dependent Riccati Equation Control of Collinear Spinning Three-Craft Coulomb Formations.* Advances in the Astronautical Sciences, 2015. **155**: p. 643-657.
22. Ratnoo, A. and D. Ghose, *State-dependent Riccati-equation-based guidance law for impact-angle-constrained trajectories.* Journal of Guidance, Control, and Dynamics, 2009. **32**(1): p. 320.
23. Çimen, T. and S.P. Banks, *Global optimal feedback control for general nonlinear systems with nonquadratic performance criteria.* Systems & Control Letters, 2004. **53**(5): p. 327-346.
24. Çimen, T. and S.P. Banks, *Nonlinear optimal tracking control with application to super-tankers for autopilot design.* Automatica, 2004. **40**(11): p. 1845-1863.
25. Gomroki, M.M. and O. Tekinalp. *Maneuvering of two-craft coulomb formation using ASRE method*. in *AIAA/AAS Astrodynamics Specialist Conference*. 2014.
26. Gomroki, M.M. and O. Tekinalp. *Nonlinear Control to Maneuver a Two-Craft Coulomb Formation at Libration Points*. in *AIAA Guidance, Navigation, and Control Conference*. 2015.
27. Topputo, F. and F. Bernelli-Zazzera, *A method to solve nonlinear optimal control problems in astrodynamics.* Advances in the Astronautical Sciences, 2012. **145**: p. 1531-1543.
28. Topputo, F. and F. Bernelli-Zazzera, *Approximate Solutions to Nonlinear Optimal Control Problems in Astrodynamics.* ISRN Aerospace Engineering, 2013. **2013**.

29. Betts, J.T., *Survey of numerical methods for trajectory optimization.* Journal of Guidance control and dynamics, 1998. **21**(2): p. 193-207.
30. Bryson, A.E., *Applied optimal control: optimization, estimation and control*. 1975: CRC Press.
31. Conway, B.A., *Spacecraft trajectory optimization*. Vol. 29. 2010: Cambridge University Press.
32. Yen, V. and M. Nagurka, *Optimal control of linearly constrained linear systems via state parametrization.* Optimal Control Applications and Methods, 1992. **13**(2): p. 155-167.
33. Teo, K. and K. Wong, *Nonlinearly constrained optimal control problems.* The ANZIAM Journal, 1992. **33**(4): p. 517-530.
34. Vlassenbroeck, J. and R. Van Dooren, *A Chebyshev technique for solving nonlinear optimal control problems.* IEEE transactions on automatic control, 1988. **33**(4): p. 333-340.
35. Jaddu, H., *Direct solution of nonlinear optimal control problems using quasilinearization and Chebyshev polynomials.* Journal of the Franklin Institute, 2002. **339**(4): p. 479-498.
36. Elnagar, G.N. and M.A. Kazemi, *Pseudospectral Chebyshev optimal control of constrained nonlinear dynamical systems.* Computational Optimization and Applications, 1998. **11**(2): p. 195-217.
37. Fahroo, F. and I.M. Ross. *Direct trajectory optimization by a Chebyshev pseudospectral method*. in *American Control Conference, 2000. Proceedings of the 2000*. 2000. IEEE.
38. Jaddu, H. and A. Majdalawi, *An iterative technique for solving a class of nonlinear quadratic optimal control problems using Chebyshev polynomials.* International Journal of Intelligent Systems and Applications, 2014. **6**(6): p. 53.
39. Clohessy, W. and R. Wiltshire, *Terminal guidance system for satellite rendezvous.* SYSTEM, 1960. **4**(1).
40. Wie, B., *Space vehicle dynamics and control*. 1998: Aiaa.
41. Schaub, H. and J.L. Junkins, *Analytical mechanics of space systems*. 2003: Aiaa.
42. Topputo, F., M. Miani, and F. Bernelli-Zazzera, *Optimal selection of the coefficient matrix in state-dependent control methods.* Journal of Guidance, Control, and Dynamics, 2014.
43. Mason, J.C. and D.C. Handscomb, *Chebyshev polynomials*. 2002: CRC Press.
44. Çimen, T., *Systematic and effective design of nonlinear feedback controllers via the state-dependent Riccati equation (SDRE) method.* Annual Reviews in Control, 2010. **34**(1): p. 32-51.
45. Wang, S. and H. Schaub, *Nonlinear feedback control of a spinning two-spacecraft coulomb virtual structure.* IEEE Transactions on Aerospace and Electronic Systems, 2011. **47**(3): p. 2055-2067.
46. Jasch, P.D., E.A. Hogan, and H. Schaub, *Out-of-plane stability analysis of collinear spinning three-craft Coulomb formations.* Acta Astronautica, 2013. **88**: p. 89-97.

47. Wang, S. and H. Schaub, *Coulomb control of nonequilibrium fixed shape triangular three-vehicle cluster.* Journal of guidance, control, and dynamics, 2011. **34**(1): p. 259.
48. Huang, J., G. Ma, and G. Liu, *Nonlinear dynamics and reconfiguration control of two-satellite Coulomb tether formation at libration points.* Aerospace Science and Technology, 2014. **39**: p. 501-512.
49. Park, C., V. Guibout, and D.J. Scheeres, *Solving optimal continuous thrust rendezvous problems with generating functions.* Journal of Guidance, Control, and Dynamics, 2006. **29**(2): p. 321-331.

CURRICULUM VITAE

PERSONAL INFORMATION

Surname, Name: Gomroki, Mohammad Mehdi
Nationality: Iranian
Date and Place of Birth: 12 April 1986, Tehran, Iran
Marital Status: Married
Phone: +90 539 406 2346
email: mohammad.gomroki@metu.edu.tr

EDUCATION

Degree	Institution	Year of Graduation
MS	Aerospace Engineering/Sharif University of Technology/ Iran	2011
BS	Aerospace Engineering/Sharif University of Technology/ Iran	2009

PROFESSIONAL EXPERIENCES

Year	Place	Enrollment
2016-Present	University of Turkish Aeronautical Association	Lecturer
February 2015	Politecnico di Milano University, Italy	Visiting Researcher
2013-2015	Middle East Technical University	European Union FP7 Marie Curie Early Stage Researcher

PUBLICATIONS

1. Gomroki, M. M., Topputo, F., Bernelli-Zazzera, F., Tekinalp, O., Solving Constrained Optimal Control Problems Using State-Dependent Factorization and Chebyshev Polynomials, Journal of Guidance, Control, and Dynamics, Ahead of Print : pp. 1-14.
2. Gomroki, M. M., Topputo, F., Tekinalp, O., Bernelli-Zazzera, F.,Two ASRE Approaches with Application to Spacecraft Coulomb Formations. In G. Gómez, J.J. Masdemont (eds.), Astrodynamics Network AstroNet-II (pp. 93–104). Astrophysics and Space Science Proceedings 44. Springer, 2016.
3. Gomroki, M.M., Tekinalp, O., State Dependent Riccati Equation Control of Spinning Three-Craft Coulomb Formation, 25th AAS/AIAA Space Flight Mechanics Meeting, Williamsburg, VA, Jan. 2015.
4. Gomroki, M.M., Tekinalp, O., Nonlinear Control to Maneuver a Two-Craft Coulomb Formation at Libration Points, AIAA Guidance, Navigation, and Control Conference, Kissimmee, Florida, January 5-9, 2015.
5. Gomroki, M.M., Tekinalp, O., Maneuvering of Two-Craft Coulomb Formation Using ASRE Metho, AIAA/AAS Astrodynamics Specialist Conference, San Diego, California, August 4-7, 2014.
6. Gomroki, M.M., Tekinalp, O., Relative Position Control of a Two-Satellite Formation Using the SDRE Control Method, 24th AAS/AIAA Space Flight Mechanics Meeting, Santa Fe, New Mexico, Jan. 2014.